TRANSPLANTATION OF DIFFERENTIATED IPSCs AS A TREATMENT STRATEGY FOR GLAUCOMA

By

Diala Walid Abu-Hassan, D.D.S

A dissertation submitted in partial fulfillment of the

requirements for the degree of

Doctor of Philosophy

in

BIOCHEMISTRY AND MOLECULAR BIOLOGY

Presented to the Department of Biochemistry & Molecular Biology

OREGON HEALTH & SCIENCE UNIVERSITY

School of Medicine

September 2013

DEPARTMENT OF BIOCHEMISTRY AND MOLECULAR BIOLOGY

SCHOOL OF MEDICINE

OREGON HEALTH & SCIENCE UNIVERSITY

CERTIFICATE OF APPROVAL

This is to certify that the Ph.D dissertation of

Diala W. Abu-Hassan

has been approved by the following:

_____

Ted Acott, Ph.D., dissertation advisor

_____

Linda Musil, Ph.D., committee co-chair

_____

Nabil Alkayed, M.D., Ph.D., committee co-chair

_____

Mary Kelley, Ph.D., co-advisor and committee member

_____

Larry David, Ph.D, exam committee member

_____

Kirsten Lampi, Ph.D., committee member

_____

Philip Streeter, Ph.D., committee member

TABLE OF CONTENTS

LIST OF TABLES

LIST OF FIGURES

LIST OF ABBREVIATIONS

α	alpha
AC	anterior chamber
AH	Aqueous humor
ALT	argon laser trabeculoplasty
AMD	age-related macular degeneration
AQP1	Aquaporin1
ASB10	Ankyrin Repeat and SOCS Box- Containing 10
BMP4	Bone morphogenetic protein 4
BMP7	Bone morphogenetic protein 7
°C	degrees Celsius
c-MYC	Myelocytomatosis Viral Oncogene
CHI3L1	Chitinase-3-like protein 1
CLANs	cross-linked actin networks
CM	conditioned medium
COPD	chronic obstructive pulmonary disease
CS	corneal stroma
CTGF	connective tissue growth factor
DF	dermal fibroblasts
DM	differentiation media
DMEM	Dulbecco's Modified Eagle's Medium
DTT	dithiothreitol
EBs	Embryoid Bodies
ECM	Extracellular matrix
ESCs	embryonic stem cells
EthD-1	Ethidium homodimer-1
Hg	Mercury

hr	hour(s)
HTM	human trabecular meshwork
HUVEC	human umbilical vein endothelial cell
IOP	intraocular pressure
iPSCs	Induced Pluripotent Stem Cells
ITS	intertrabecular spaces
JCT	Juxtacanalicular region
KLF4	Kruppel-like factor 4
µ	micro- = $1x10^{-6}$
µg	microgram (10^{-6} gram)
mg	milligram (10^{-3} gram)
MGP	Matrix Gla Protein
min	minute
µl	microliter (10^{-6} liter)
ml	milliliter (10^{-3} liter)
µM	micromolar (10^{-6} Molar)
mM	millimolar (10^{-3} Molar)
MMPs	matrix metalloproteinases
mol	mole ($6.02x10^{23}$ molecules)
mRNA	messenger ribonucleic acid
OCT3/4	Octamer- binding transcription factor 3/4
PBS	Phosphate buffered saline
PCR	polymerase chain reaction
POAG	Primary open angle glaucoma
PVDF	polyvinylidene fluoride
QDots	quantum dots
qPCR	quantitative polymerase chain reaction
RNA	ribonucleic acid

RPE	retinal pigment cells
RT-PCR	Reverse transcriptase polymerase chain reaction
SC	Schlemm's canal
SD	sheath-derived
SDS/PAGE	sodium dodecyl sulfate/ Polyacrylamide gel electrophoresis
SPARC	secreted protein, acidic, cysteine-rich
SOX2	SRY (sex determining region Y)-box 2
TGF-β2	Transforming growth factor beta-2
TM	trabecular meshwork
VCAM-1	vascular cell adhesion molecule 1
WRD36	WD repeat- containing protein 36

ACKNOWLEDGEMENTS

I first would like to extend my gratitude to Dr. Ted Acott and Dr. Mary Kelley for their support, guidance and advice in making the first steps in my scientific life. I also appreciate the help, discussions and recommendations my thesis advisory committee and exam committee- Drs. Nabil Alkayed, Linda Musil, Kirsten Lampi, Philip Streeter and Larry David- offered me. I have learned a lot from each of you both scientifically and personally.

I also want to thank all members of the Acott Laboratory, both past and present. I would like to particularly express my appreciation to Drs. Xinbo Li, Janice Vranka, Kate Keller, Mini Aga, and Yong-Feng Yang, as well as to John Bradley, Lauren Hayashi, Ying Ying Sun and Kaili Song.

Finally, I want to thank the Abu-Hassan, Ghabboun, Arrabi and Dalgamouni families for their encouragement, support and patience.

This work is dedicated…

To my family, my Mom and Dad in particular, who surrounded me with love, warmth, endless sacrifices and guidance. To the family who instilled in me the value of education and research that drove my desire and courage to excel and attend high caliber universities.

To Jordan for supporting me and providing me with a high-standard education.

To Oregon for being a nice and welcoming place to live and learn.

PEER-REVIEWED PUBLICATIONS ARISING FROM THIS DISSERTATION

Acott, T.S, Kelley, M.J, Keller K.E, Vranka J.A, **Abu-Hassan, D.W**, Li, X, Aga, M, and Bradley, J. IOP Homeostasis - Maintaining Balance in a High Pressure Environment. Journal of Ocular Pharmacology and Therapeutics. In Press.

PEER-REVIEWED PUBLICATIONS ARISING FROM THIS DISSERTATION- IN PREPARATION

Abu-Hassan, D.W, Li, X, Ryan, E, Acott, T.S & Kelley, M.J. A Novel Cell Loss Model for Primary Open Angle Glaucoma. In preparation.

Abu-Hassan, D.W, Li, X, Acott, T.S & Kelley, M.J. Use of iPS Cells to Restore Intraocular Pressure Homeostasis in a Human Model for Glaucoma. In preparation.

ABSTRACT

A compromised regulation of intraocular pressure, or IOP, is the primary risk factor for primary open angle glaucoma (POAG). A prominent feature of the disease is cellular loss. To establish a greater level of standardization of cell loss in our experimental anterior segments, we developed a cell depletion model using saponin and partially denuded trabecular meshwork (TM) areas to mimic the situation in glaucoma. With this model, we developed transplantable differentiated TM-like cells from induced pluripotent stem cells (iPSCs), and utilized these cells in an *ex vivo* perfusion system for functional testing of TM in anterior segments. This included two essential TM functional end points: 1) IOP homeostasis; and 2) phagocytosis. Subsequent to transplantation of the unique TM-like cells to denuded TM areas, we tested them for competency of function in which the modified stem cells were required to be comparable to endogenous TM cells in intact anterior segments. Our monitoring of the differentiation of iPSCs to TM-like cells was facilitated by the expression of biomarkers as well as the loss of pluripotency factors, and evaluated by confocal microscopy, Western immunoblotting and quantitative RT-PCR. The transplanted labeled TM-like cells were integrated into the TM at all levels. Transplanting these TM-like cells and subjecting them to a high pressure challenge showed the restoration of IOP homeostatic response. Additionally, a

phagocytic challenge to these TM-like cells with zymosan particles also resulted in responses comparable to those of endogenous TM cells. Establishing a connection between TM cell loss and tissue functionality is novel. In addition, replacing the lost cells in glaucomatous eyes by using iPSCs in the TM is a novel treatment strategy that has not been previously attempted in trabecular meshwork, and shows considerable promise as an alternative treatment for glaucoma.

Key words: aqueous humor, cell depletion, cell loss, development**,** differentiation, expression, glaucoma, homeostasis, homeostatic response, induced pluripotent stem cells, induction, intraocular pressure, model, markers, morphology, phagocytosis, primary open angle glaucoma, saponin, Schlemm's canal, stem cells, trabecular meshwork, transplantation.

Chapter 1

Introduction

1.1 Glaucoma and the development and physiology of the trabecular meshwork (TM).

1.1.1. Definition and statistics of glaucoma.

Glaucoma is a group of diseases in which elevations in the intraocular pressure (IOP) often damage the visual apparatus causing an irreversible blindness. This leading cause of blindness is found worldwide and affects mainly the elderly population. So far, over 67 million in the world people have been diagnosed with glaucoma and over 4 million have lost vision in both eyes [1, 2, 3, and 4]. The overall prevalence of open angle glaucoma in the US population 40 years and older is estimated to be 1.86%. Glaucoma accounts for around 25% of new blindness cases in developed countries [4, 5]. Primary open angle glaucoma (POAG) is the most common type of glaucoma and constitutes 85% of diagnosed cases. The risk factors include race (e.g. African-Americans over age 40), age (over 60 years), family history (mutations in myocilin, optineurin, WDR36 and ASB10), high eye pressure, thin corneas and abnormal optic nerve anatomy. Glaucoma is asymptomatic and is usually not detected until irreversible vision loss has taken place. The therapeutic management of glaucoma costs the United States and the United Kingdom about 2.5 billion and 216 million USD annually respectively [6, 7].

1.1.2. The development and structure of the trabecular meshwork as a part of the anterior segment.

The anterior segment is composed of the cornea, lens, iris, ciliary body and ocular drainage tissues, including the trabecular meshwork (TM) and Schlemm's canal (SC). The TM and SC are located at the angle where the iris and cornea meet, or the

iridocorneal angle [8]. In this region, the transition from cornea to sclera takes place, hence, it is called the corneoscleral transition zone [8]. The ocular drainage structures are the last to become differentiated during anterior eye development. By the 6th week of embryonic development, the rudimentary eye is composed of the bi-layered optic cup and the lens vesicle (Fig. 1.1) [9].

The optic cup is formed from forebrain neuroectoderm while the lens vesicle invaginates and separates from the overlying surface ectoderm [9, 11, 13, and 14]. At this developmental stage, mesenchymal progenitor cells encircle the developing eye, and thus are called “periocular mesenchyme”, and then migrate anteriorly [9, 11, 13, 14, 17, and 21]. The TM is derived from periocular mesenchyme that consists of neural crest and cranial paraxial mesoderm derived cells [8], whereas SC is likely derived from periocular mesenchyme and is formed as a result of vasculature remodeling in the corneoscleral transition zone [10, 11, 12, 13, and 14]. During human eye development, at the 15th to 20th week of gestation, the iridocorneal angle is occupied by a dense mass of mesenchymal cells shortly after iris elongation begins. In the following steps, these cells elongate, flatten, and become separated from each other by small fenestrations that are partially filled with extracellular fibers. Although the TM appears at the 15th to 20th week of gestation, the aqueous humor begins to be secreted by the fifth to sixth month of gestation [15, 21, and 22].

The major morphogenesis of the TM is complete around birth in humans, however, in the postnatal period, significant development of the anterior segment structures, specifically, the ocular drainage structures occurs [13, 18]. At this stage, the presumptive site of the TM at the iridocorneal angle contains a mass of packed

mesenchymal cells (Fig. 1.2 and 1.3). To allow the outflow of the aqueous humor (AH), remodeling of this mesenchymal mass and the formation of a functional TM have to occur [13]. Of the major changes that have to happen for a complete maturation of a functional trabecular meshwork are the formation of intertrabecular spaces, or fenestrations between the beams and extracellular matrix (ECM) organization into a network of beams that are covered by TM cells.

The ECM contains several structural components such as, collagen, laminin, elastin, fibronectin and vitronectin [133]. Intertrabecular spaces of the functioning meshwork allow the passage of aqueous humor to Schlemm's canal. Some of the mesenchymal cells that have a stellate phenotype remain between the trabecular lamellae and the endothelial lining of SC. These cells develop bridging contacts between the endothelial cells of SC and the TM cells on the beams, thereby forming the juxtacanalicular or cribriform layer of the trabecular meshwork where most of the resistance to aqueous humor outflow is located. The endothelial cell lining of Schlemm's canal forms drainage structures, known as giant vacuoles, that allow the flow of aqueous humor to the inside of the canal. The lumen of Schlemm's canal is connected to the venous system through collector channels. Abnormal development of ocular drainage structures at the iridocorneal angle can lead to an elevated IOP and congenital glaucoma.

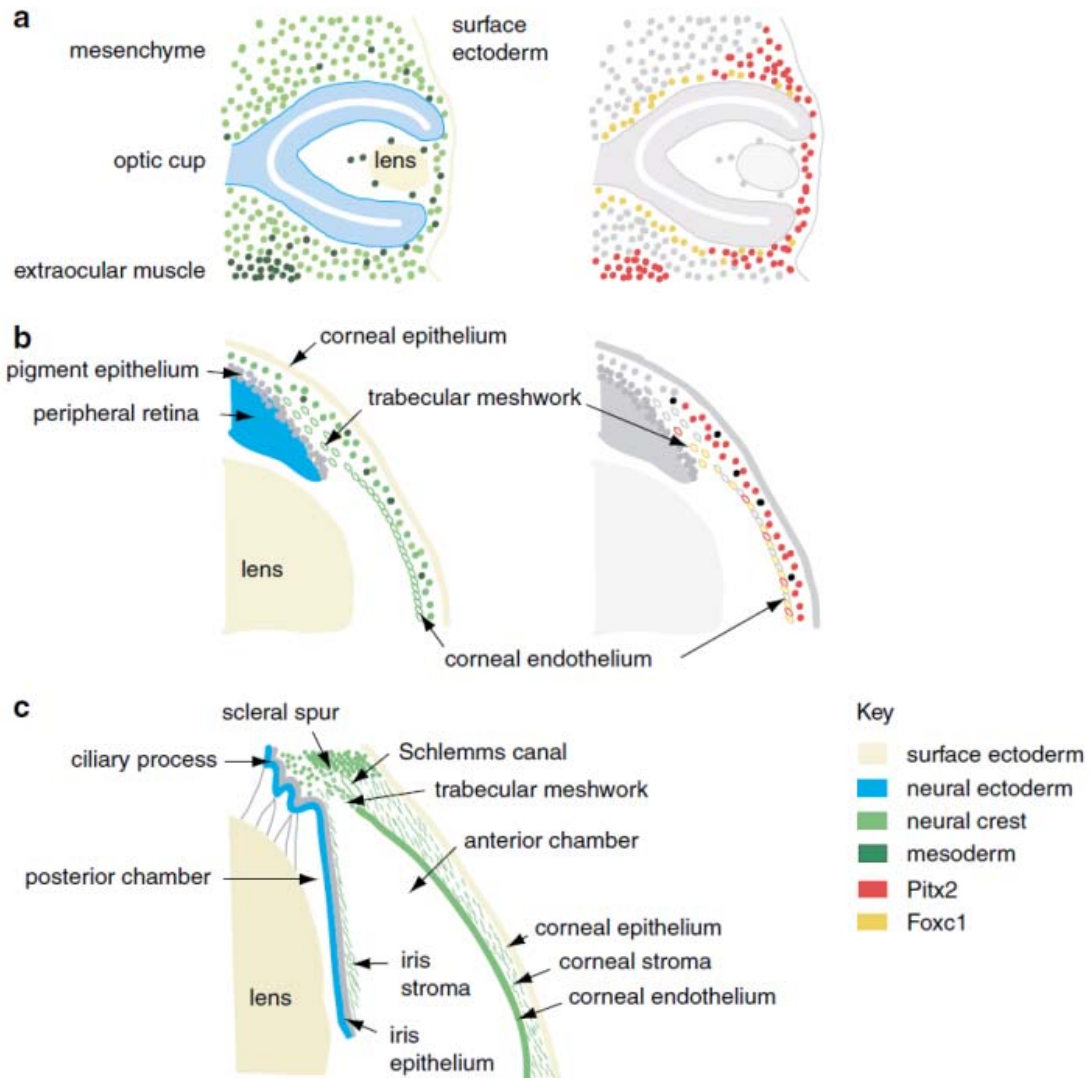

Figure 1.1: The embryonic and fetal development of the TM and SC. (A) Optic cup stage: at the 5th week of gestation, the surface ectoderm thickens and invaginates to form the lens pit and the optic vesicle forms the optic cup. **(B)** The periocular mesenchyme migrates between the surface ectoderm and lens vesicle to form corneal stroma, corneal endothelium, trabecular meshwork and Schlemm's canal at the 5th month of gestation. **(C)** Maturation of a functional TM and SC postnatally. (from J.C

Sowden, Molecular and developmental mechanisms of anterior segment dysgenesis, *Eye* (2007) 21, 1310–1318).

The TM is a tiny triangular porous structure that is composed of connective tissue beams or lamellae surrounded by endothelium. It is composed of three consecutive regions, from superficial to inner: uveal meshwork, corneoscleral meshwork and juxtacanalicular (JCT) (Fig. 1.4) [19]. The uveal meshwork consists of 3 layers of connective tissue bands covered by flat trabecular cells with irregular fenestrations in between the bands [16, 19, and 20]. These bands are known as trabecular beams or lamellae and are only found in the uveal meshwork and the next region of corneoscleral meshwork. The latter is composed of 8-15 layers of perforated sheets of fibers or beams that become smaller as they extend close to SC [16, 19, and 20]. The cells of the outer layers of the TM act primarily as pre-filters that phagocytically remove the cellular debris from AH before it moves deeper into the JCT and SC.

The JCT is the thinnest part of the TM, measuring 2-20 μm thick, and consists of 2-5 cell layers that reside in a loose connective tissue matrix directly adjacent to the inner wall endothelium of SC [16, 20]. Due to the irregular arrangement of the ECM fibers in the JCT, it was also named the cribriform region. The cells in the JCT attach to one another, to the fibrils of the ECM, and to the endothelial cell lining of SC by long cytoplasmic processes. The spaces between JCT cells and ECM fibers contain an amorphous gel-like ground substance consisting of various proteoglycans and hyaluronan and serve as an outflow pathway for AH [33, 34, and 35].

The open spaces, or fenestrations, between the lamellae are of 25-27 μm in the uveal meshwork and 2-15 μm in the corneoscleral meshwork, hence they generate a highly porous structure. The high porosity of the uveal and corneoscleral regions of the trabecular meshwork results in an insignificant resistance to aqueous humor outflow. However, the JCT is non-fenestrated and provides most of the resistance to AH flow [36,

37, 55, 56, and 57]. Evidence supporting this came from experiments where outer regions of the TM were dissected out with no resulting effect on outflow facility, and from theoretical calculations using Poiseuille's law [56, 58]. The center or stroma of the trabecular lamellae or beams contains densely packed collagen and elastic fibers, and the electron dense microfibril sheath-derived (SD) material [59, 66, 67, 68, 69, 70, and 71]. The collagen fibers are mostly type I and III [72]. The TM cells on the beams reside on a basal lamina that contains considerable amounts of collagen IV and laminin [71, 72].

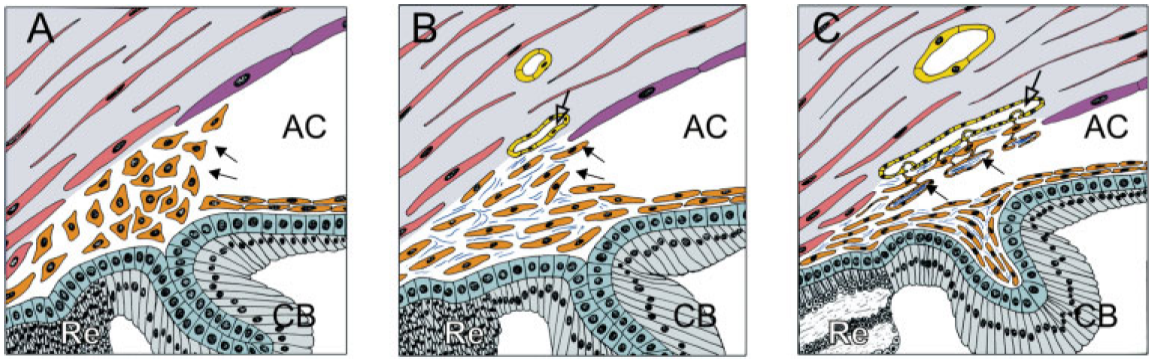

Figure 1.2: Postnatal development of the iridocorneal angle and the trabecular meshwork. The diagram shows the developmental stages of the trabecular meshwork and Schlemm's canal. **(A)** The TM appears as a condensed mesenchymal tissue (arrows). **(B)** The TM cells have differentiated and become separated from each other by small open spaces. Extracellular fibers accumulate in the intercellular spaces, whereas vessels appear in the adjacent sclera (open arrows). **(C)** The trabecular beams or lamellae have formed by reorganization of the extracellular fibers in the chamber angle but still are not fenestrated. The beams become covered by trabecular meshwork cells. The scleral vessels next to the chamber angle coalesce and fuse to SC. Anterior chamber (AC), ciliary body (CB). (from Cvekl, A. and Tamm, E. R. Anterior eye development and ocular mesenchyme: new insights from mouse models and human diseases. *BioEssays* (2004) 26, 374–386).

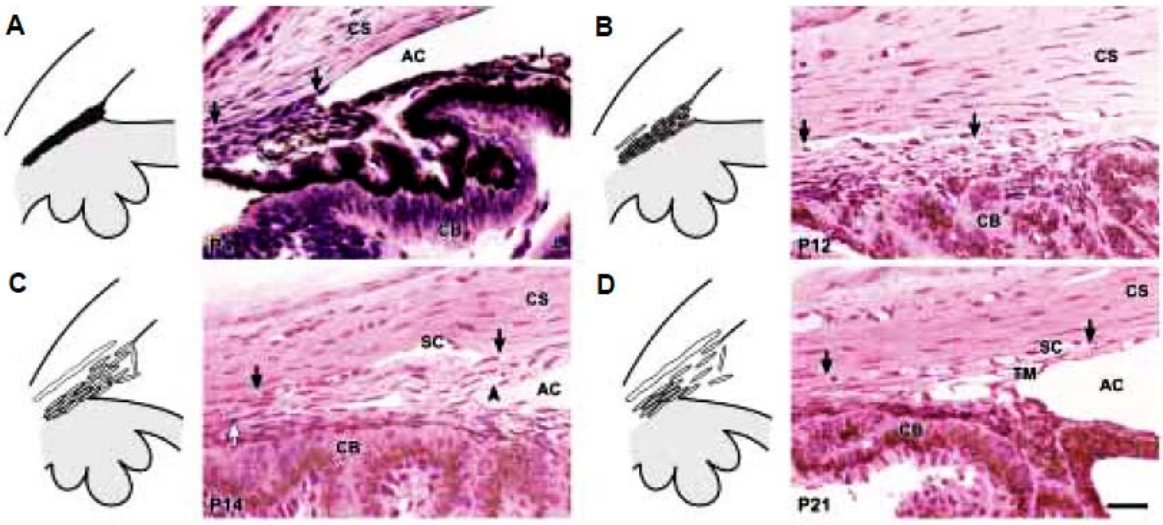

Figure 1.3: Histological postnatal development of the iridocorneal angle and the trabecular meshwork. The diagram shows the developmental stages of the trabecular meshwork and Schlemm's canal in C57BL/6J mice. **(A)** The TM is recognized as condensed mesenchymal tissue (arrows) between the corneal stroma (CS), ciliary body (CB) and anterior chamber (AC). **(B)** The TM cells have differentiated and the trabecular beams or lamellae have developed but still are not fenestrated. SC is present between (between arrows). ECM partially accumulates in the spaces. **(C)** The trabecular beams located nearest to the anterior chamber begin to separate and intertrabecular spaces appear (arrowhead), but AH entry to SC (between arrows) is still restricted. **(D)** Organization and maturation of the TM continues with enlargement of the present spaces and opening of new ones. Scale bars represent 50 μm. (from Gould, D.B. Smith, R.S. and John, S.W.M. Anterior segment development relevant to glaucoma. Int. J. Dev. Biol. (2004) 48, 000-000)

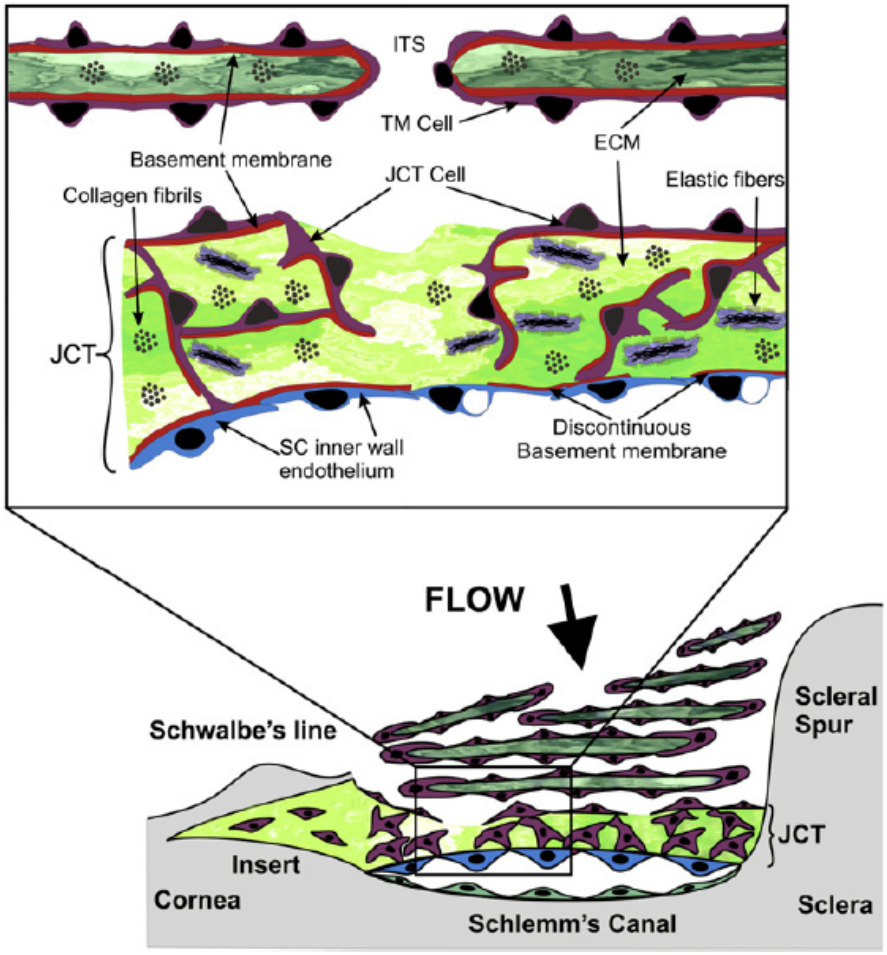

Figure 1.4: Outflow pathway through the TM and JCT. The lower portion of the figure shows a side view of the TM (radial section). The arrow indicates the direction of AH flow across the TM until it enters SC. The upper inset represents an expanded view of the JCT region. Once the AH passes through the intertrabecular spaces (ITS) of corneoscleral meshwork, it goes to the JCT region, and then through the inner wall endothelial lining of SC. (from Acott, T. S, Kelley, M. J. Extracellular matrix in the trabecular meshwork. *Exp. Eye Res.* (2008) 86, 543-561)

1.1.3. The aqueous pathway, trabecular meshwork physiology and the maintenance of the intraocular pressure (IOP).

Aqueous humor or AH, the fluid that fills the anterior and posterior chambers of the eye, is produced in the ciliary body within the posterior chamber of the eye. After it fills the posterior chamber, it moves anteriorly around the lens then exits through the pupil to the anterior part of the eye. Aqueous humor nourishes the avascular tissues of the eye, such as, lens, cornea and TM, fills the anterior and posterior chambers of the eye and aids in vision. When AH is loaded with cellular debris collected from eye tissues, it is filtered by the TM tissue located at the irido-corneal angle. The AH leaves the eye via 2 routes, a major conventional pathway through the TM and a minor nonconventional or uveoscleral pathway through the intercellular spaces of the ciliary muscle cells [52, 53, 54, 59].

Fluctuations in the IOP occur frequently as a result of many factors including the daily variation, exercise, heart rate, respiration, fluid intake, medications and alcohol consumption. In response to increases in IOP, TM cells can mount a homeostatic response to adjust the outflow resistance and restore the IOP level to physiological values [75, 77, and 78]. To measure IOP in an experimental setting, we use the commonly accepted outflow model shown in figure 1.5 [180, 181, and 182]. When the pressure in perfused anterior segment organ culture is doubled, the measured flow rate immediately doubles (Fig. 1.6). The cell surface integrins and other cell-surface receptors of the TM cells sense increases in IOP as a mechanical stretching or distortion. This stimulus implies that the outflow resistance is too high. Consequently, TM cells respond by upregulating the expression of enzymes that increase ECM turnover to reduce flow resistance. The matrix metalloproteinases (MMPs) are responsible for the

initiation of most ECM turnover, thus the expression of MMP-1, MMP-3, MMP-7, MMP-9 and MMP-14 is enhanced once the IOP is increased [77].

In addition to enhancing MMP activity, TM cells change the expression levels of other ECM components. The expression of tenascin, fibronectin, CD44, syndecan 2, SPARC, VCAM-1, Collagen XIV, Periostin, Matrix Gla protein, Link protein and MMP-2 are increased, whereas versican, syndecan 1, and thrombospondin 2 are reduced [81]. Over the next few days, the flow rate keeps increasing with time until the outflow resistance is reduced and the initial IOP is restored [83]. ECM turnover is a highly coordinated sequence of events that involves the degradation and biosynthetic replacement of specific ECM components. The aforementioned sequence of events that result in reducing outflow resistance and maintenance of the IOP at physiological levels is known as IOP homeostasis. Therefore, IOP homeostasis is maintained by ECM turnover triggered in response to pressure increases or mechanical stretch sensed by the JCT cells.

The IOP builds up in response to resistance to outflow and once it is high enough to overcome the resistance, AH flows across the TM. After AH is filtered in the TM, it leaves through Schlemm's canal to venous circulation. Fluid movement across the TM tissue takes place down a pressure gradient [86]. The IOP is dictated by the rate of AH production and the resistance to outflow. At steady-state IOP, the flow rate of AH equals its production rate by the ciliary body.

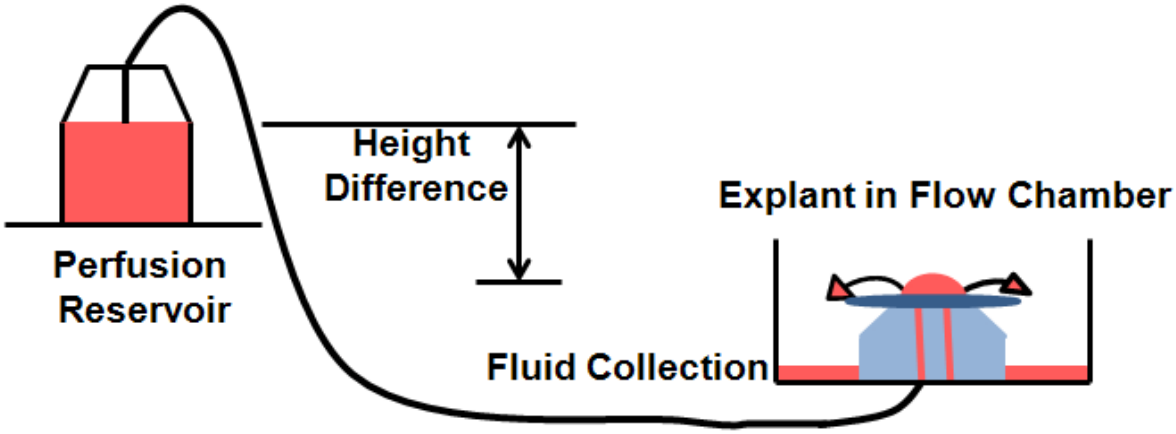

Figure 1.5: The outflow model. This figure represents the commonly accepted outflow model. In this model the anterior half of the eye explant is mounted and sealed in a chamber that is connected via tubing to a perfusion reservoir. The reservoir is placed at 8.8 mm Hg (11.5 inches) to generate normal physiological pressure, or 1x. To increase the pressure, the bottle is placed at a higher position. For instance, to increase the pressure to 17.6 mm Hg (2x), the media-filled bottle is placed at 23 inches. Once the fluid passes via tubing to the chamber, it fills the explant and passes through the TM to exit to the chamber. To measure flow rate, the fluid that leaves through the TM is measured over time.

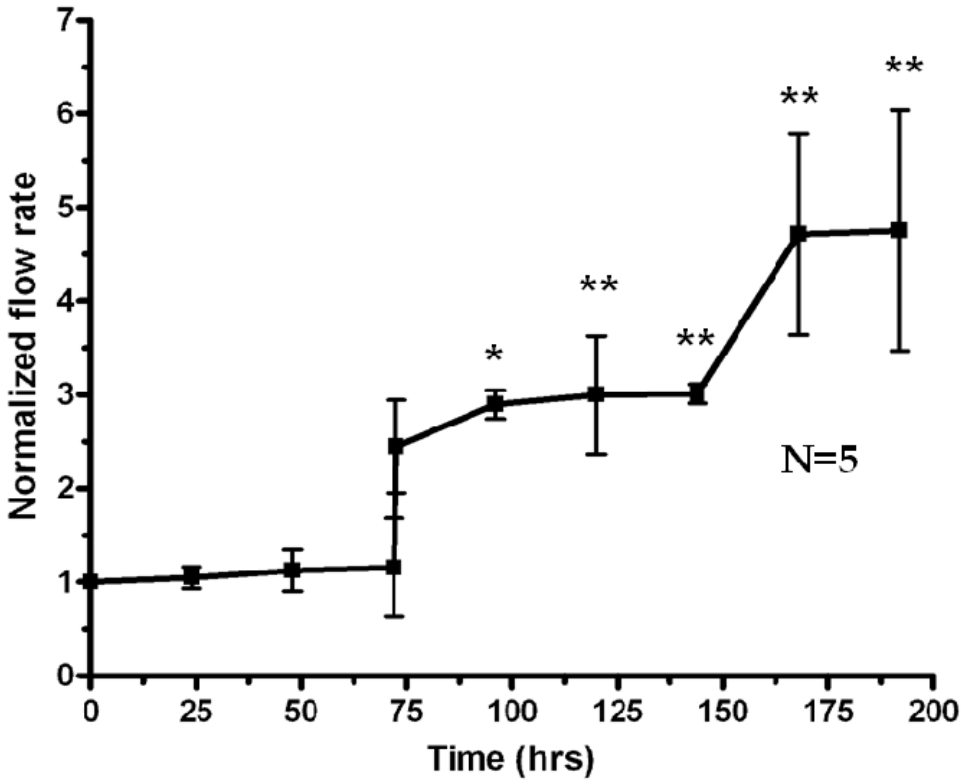

Figure 1.6: The IOP homeostatic response in cadaver human anterior segments. The fluid was flowed into the anterior segment explants at normal physiological pressure (1x), which equals 8.8 mm Hg. The measured flow rate was 2.5-3 µL/min. Afterwards, the pressure was doubled (2x) and hence, the flow rate doubled as a result of the pressure gradient that pushed the fluid across the TM. The flow rate continued to increase slowly with time over the next few days. This adaptive response to accommodate changes in pressure and maintain it at normal levels is known as the IOP homeostatic response. Error bars represent the standard error of the mean. *P<0.05, **P<0.001.

In response to the pressure gradient generated by AH flow, the SC inner wall endothelium forms cellular outpouchings, called giant vacuoles. These characteristic structures form when AH pushes against the basal side of SC cells [192]. Inner wall cells of SC rest on an incomplete basal lamina and are not supported by ECM in considerable areas of their basal cell membrane. They are in direct contact with the AH flowing in the open spaces of the JCT. The AH enters SC via 2 routes; an intracellular and paracellular. The intracellular pores have diameters from 0.1 to 2 μm and are often associated with giant vacuoles [86]. Although paracellular pores usually have diameters comparable to that of intracellular pores, they are less common in most eyes [87]. The endothelial cells that line SC are held together by tight junctions that restrict the paracellular route [90]. Microparticles of 200–500 nm in size can cross the inner wall pores [90]. Although the inner wall endothelium provides some hindrance against the outflow of AH, it does not generate more than 10% of the total TM outflow resistance [86]. The molecular mechanisms that cause the formation of intracellular pores in SC inner wall e

ndothelium are still unknown. Additionally, small diaphragmed minipores (DMPs) were identified in the inner wall of SC [91]. These minipores may represent an early stage in pore formation [92]. They are ultrastructurally similar to those forming the fenestrae of fenestrated capillaries [93]. Although DMPs are regularly found in SC inner wall endothelium, they are considerably rarer than the fenestrae in fenestrated epithelia [92, 93]. It was originally thought that the covering thin diaphragm was derived from the basal lamina in blood vessels, but the absence of a complete basal lamina in the inner wall endothelium does not support that hypothesis [92].

In glaucoma, the flow of AH is obstructed resulting in pressure elevation in the eye. The increased ocular pressure causes degenerative changes and progressive death of the retinal ganglion cells (RGCs) and damages their axons, which transfer visual information to the brain via the optic nerve. Increased IOP, which is a risk factor for POAG, is directly related to increases in outflow resistance [55, 94]. The difficulty of the passage of AH through the TM, represented by flow resistance, has been attributed mainly to the innermost region of the TM, the JCT [55, 56, and 57]. A wide variety of changes in the organization, structure and integrity of the TM tissue have been detected in glaucomatous eyes.

The most characteristic structural changes are the accumulation of ECM and banded fibrillar elements that are embedded in different glycoproteins, known as “plaque material” [95, 96, and 97]. In addition, TM cell counts were found to decrease with aging and POAG [98, 99]. The JCT specifically shows more cell loss than other layers of TM, nevertheless, the total cell number in the TM is reduced as well [98, 99]. Cellular loss in TM was also detected in congenital glaucoma and was found to be similar to the age-associated cell death [99, 100]. Mechanical stresses, oxidative damage, time, disease or other injuries also may contribute to cell loss or dysfunction. Increases in the intraocular pressure trigger a homeostatic response to reduce the IOP and maintain the health and normal function of the TM [101, 102]. With IOP elevations, mechanical stretching is sensed by TM cells and induces modifications in the composition and amount of the TM extracellular matrix. The changes in ECM decrease resistance to flow and increase outflow of AH to SC resulting in the reduction of IOP.

Many factors decrease TM cellularity, but cellularity increases in human anterior segments subjected to laser trabeculoplasty [103]. TM cell division increased by 4-fold

following laser-treatment over non-treated controls [103]. More than 60% of cell division was detected in the anterior, non-filtering region of the TM, or the insert area. In this area, the TM inserts into the cornea beneath Schwalbe's line, and ''stem-like cells'' called insert cells reside. A week after laser trabeculoplasty, 60% of tritiated thymidine labeled cells migrated out of the insert region to repopulate laser burn sites [103]. This study suggested that the insert cells might serve as TM stem cells and that the repopulation of the TM tissue by fresh healthy and functioning cells may restore the role the tissue performs in keeping eye pressure normal.

1.1.4. Molecular and biochemical mechanisms of glaucoma.

Changes in the normal structure of the TM have been detected with aging and in POAG. An increase in the thickness of the ECM in the JCT region has been observed in glaucomatous eyes compared to healthy controls [104]. Other investigations suggested the formation of deposits by the interacting ECM components, thus blocking the outflow pathway through TM. For instance, cochlin was identified by a proteomic analysis to be associated with glaucomatous TM but not in normal TM. Induced by shear stress, cochlin undergoes multimerization and forms deposits that have exclusively been found with mucopolysaccharide deposits in glaucomatous TM [105, 106]. Other changes apparent with glaucoma were trabecular thickening and fusions, hyperpigmentation of TM cells, and the loss of giant vacuoles from the inner wall of Schlemm's canal. Moreover, there is a significant increase in the amount of sheath derived (SD)-plaques in glaucomatous compared to normal eyes [107]. There is additional fibrillar material that adheres to the net of the TM resulting in an irregular thickness of the sheath. In POAG eyes, there are increased amounts of type VI collagen that surround the connecting fibrils and accumulate in advanced disease to participate in blocking the outflow pathway

[111, 112]. However, most of the exact molecular mechanisms that cause glaucoma are still unclear.

The contractility of the TM affects aqueous drainage where its increase reduces AH outflow and its relaxation upregulates AH drainage [108, 109]. Therefore, the disruption of the cytoskeleton greatly disturbs the structural integrity and functionality of the TM tissue. Among the structural changes that were observed in glaucomatous TM is the formation of cross-linked actin networks (CLANs). These polygonal structures are thought to increase the rigidity and stiffness of the TM cells rendering them more resistant to aqueous outflow [110, 111]. The formation of CLANs is also associated with cell hypotrophy and down regulation of cell migration and proliferation [119, 120, and 121].

Normally, discontinuous tight and gap junctions are commonly found between TM beam cells. However, high-resistance adherence-type junctions are formed between TM cells of glaucomatous eyes instead of lower-resistance junctions that allow more dynamic activities between cells [125, 126, and 127].

Since the JCT is the region where most of the flow resistance is located, ECM remodeling is of special importance at this particular region. Both autocrine and paracrine growth factors, such as TGF-β2, CTGF, BMP7 and BMP4, control the synthesis and degradation of ECM molecules in the JCT [128]. Moreover, glucocorticoids and prostaglandin derivatives modulate ECM turnover in the JCT [90, 149, 150, and 151]. An increase in fibrillar content in the ECM of the JCT is a prominent structural change in the eyes of patients with POAG and steroid-induced glaucoma [152]. ECM-related herniations of the JCT and the inner wall of SC have been identified but their molecular structure is still unknown. In addition, increases in the branching of

glycosaminoglycans and changes in their distribution in the JCT region have been identified in POAG [155]. Other studies have also detected an induction of calcification markers such as, matrix Gla protein and bone morphogenic protein-2 (BMP-2), thereby suggesting that calcification of the TM may contribute to the stiffness and increased flow resistance of glaucomatous tissue [132].

1.2 Treatment strategies of glaucoma and the need for novel therapies.

Since IOP is the only treatable risk factor, the current treatment strategy for glaucoma focuses on lowering eye pressure. The current treatments for glaucoma are either medical or surgical. Classes of topical glaucoma medications include beta-blockers, alpha-agonists, prostaglandin analogues, carbonic anhydrase inhibitors, cholinergic agonists, and adrenergic agonists. Often, their adverse effects, expense and multiple daily dosing contribute to the lack of patient compliance with treatment. Topical beta-blockers are the traditional therapeutic agent for glaucoma patients and have been on the market for decades. They act by reducing the production of AH from the ciliary body; hence they partially deprive the ocular tissues of the essential functions that AH performs. In addition, systemic side effects interfere with their use in patients with asthma, chronic obstructive pulmonary disease (COPD) and cardiac problems. Prostaglandin analogues shunt the outflow of AH to the alternative or uveoscleral pathway but do not affect its production; however, they do have some side effects. POAG affects primarily elderly people; as a result, the convenience of using glaucoma medications is questionable because the frequent application of medications facilitates forgetting doses and the compromised medical status of many patients contraindicates their use.

The surgical approach for treating glaucoma is also an option. A common surgery called trabeculectomy is available to relieve eye pressure. In this technique, an alternate drainage pathway is created surgically by making a tiny drainage hole in the sclera that allows fluid to flow out of the eye and reduce pressure. However, the hole tends to heal and close, thus, anti-healing agents have to be used or, alternatively, a plastic tube-shunt may be inserted into the anterior chamber to drain fluid. Surgical

procedures are not appropriate for many people because of aging and the medical condition of the patient. Additionally, cataracts or a wrinkle in the macula region of the eye may develop after surgery. Laser procedures, such as argon laser trabeculoplasty (ALT), can also help to relieve pressure. Using a laser beam in ALT, ophthalmologists induce around 50 burns in the TM. The application of the laser beam on the TM triggers a biological response in which the insert stem cells are activated to divide and migrate to the burn areas [103]. However, recurrence in 10% of laser treated patients a year in addition to failure of the treatment in some patients was detected. Moreover, medications are still needed to control eye pressure post-surgery, although with smaller doses. Overall, the currently available therapies for glaucoma cannot always prevent, and do not reverse, vision loss. Therefore, the search is continuous to find alternative preventive and therapeutic approaches for POAG.

1.3 Stem cells and the treatment of glaucoma

Current medications affect AH inflow and the alternative outflow route and do not sufficiently lower IOP in most glaucoma patients; hence, there is a need for a conventional outflow route medication. Decreasing the AH production or shunting it away from the diseased TM by the available medications starves the already compromised tissue of nutrients. Stem cell transplantation in the trabecular meshwork of the anterior chamber may provide a promising avenue for treating degenerative POAG.

Stem cells are immature and uncommitted cells that can differentiate to various cell types depending on the degree of their potency. Stem cells can replace differentiated cells lost due to pathologies or injuries, and therefore, can advance regenerative medical treatments for debilitating diseases. Tissue regeneration can take place by transplantation of embryonic or adult stem cells [196]. The stem cells can be differentiated into specialized functional cells that would serve as a replacement for dead or malfunctioning cells of different tissues.

Several sources of stem cells can be utilized for this potential novel treatment strategy, such as embryonic (ESC), umbilical cord, bone marrow and induced pluripotent stem cells. Many research groups are investigating new treatment options of glaucoma utilizing stem cells but they are mainly focusing on fixing the damage of the ocular tissues in the posterior chambers such as retina and optic nerve. Very few studies concentrate on the use of stem cells in the anterior segment, particularly the TM. Since TM is the first line of defense that maintains the IOP at normal levels, stem cells replacing the TM cells lost in glaucoma represent more of a preventive strategy than a curative one. However, the uniqueness of this potential option stems from both the use of stem cells in the TM and its preventive mode.

1.4 Induced pluripotent stem cell (IPSCs)

Ethical controversies associated with the use of ESCs and immunorejection problems are major concerns for their use. Consequently, replacing ESCs with pluripotent cells generated without sacrificing embryos is a promising alternative. Pluripotent stem cells can be generated by reprogramming adult somatic cells utilizing many methods. The induction of iPSCs from mouse fibroblasts was first demonstrated by Yamanaka *et al* (2006) [184]. Based on their investigations, four pluripotency transcription factors were established to dedifferentiate and reprogram the cells to become pluripotent. IPSCs have been generated by stably transfecting mouse and human fibroblasts with a group of transcription factors that are expressed by ESCs, those include: OCT-3/4, SOX2, KLF4, and c-MYC [183, 184]. Other research groups expressed other sets of transcription factors to generate iPSCs, such as OCT4, SOX2, KLF4 and LIN28 [194]. The transfected cells are pluripotent and can differentiate into all three germ layer-derived cells and are syngeneic [195]. Since iPSCs are derived from dermal fibroblasts, they provide an accessible non-invasive source for autologous stem cells.

Our goal is to differentiate the iPSCs into TM-like cells, and then transplant them into cell depleted cadaver human eyes to re-establish the lost function of maintaining IOP at normal levels in TM. Because the TM is partially immune-privileged, immune rejection problems are anticipated to be minimal. Ongoing research using iPSCs is underway in a wide variety of fields, yet none has been approved as a treatment. Further investigations must be performed before iPSCs become ready to move from bench to bedside. Several clinical trials using iPSCs have been started, including one from a Japanese group, the Masayo Takahashi group at the RIKEN Center for Developmental

Biology, which uses retinal pigment cells (RPE) derived from iPSCs for treating aged macular degeneration (AMD).

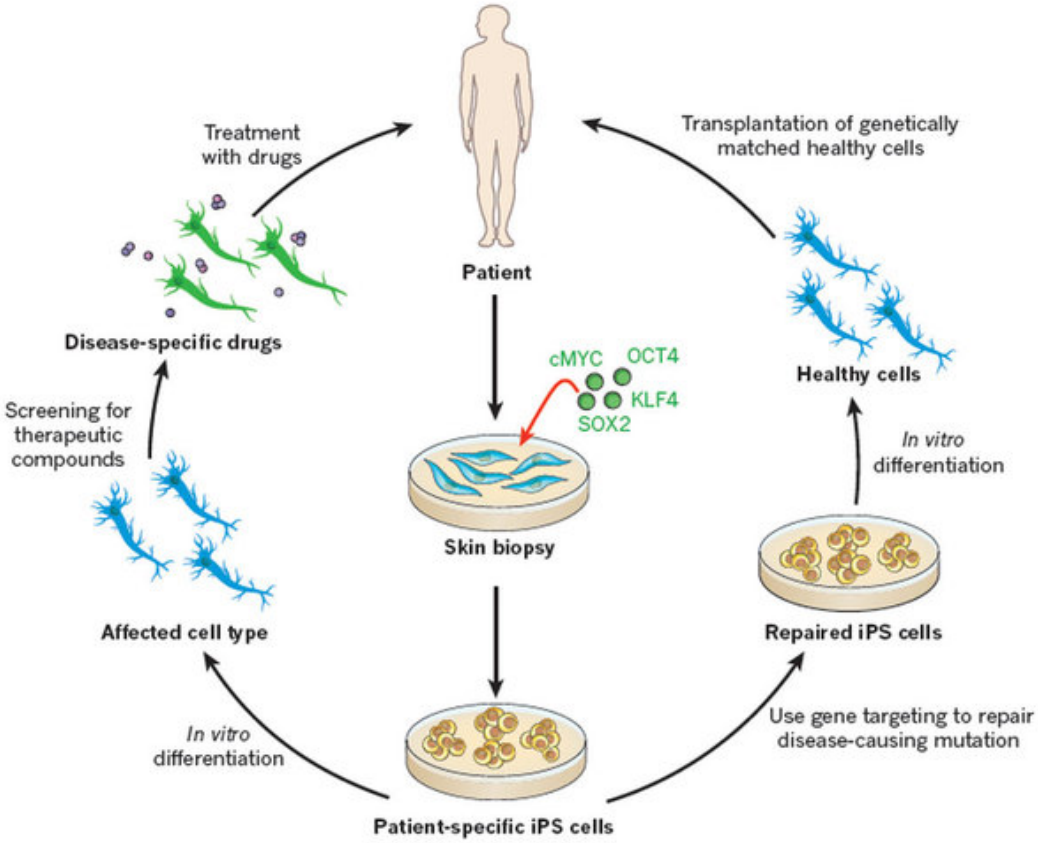

Figure 1.7: Reprogramming technology and the generation of iPS cells. Fibroblasts are obtained from a skin biopsy and dermal fibroblast cell culture is established. Following that, pluripotency transcription factors, such as KLF4, SOX2, OCT4 and c-MYC are co-expressed in the cells to dedifferentiate them. The generated patient-specific iPS cells can be used to model and treat human disease. In this example, the patient has a neurodegenerative disorder. The genetic problem can be corrected (right side) and then the cells can be differentiated into the cells of interest, such as neurons in this example. The corrected differentiated patient-specific iPS cells can be tranplanted back into the tissue and start functioning normally to restore the lost function. Alternatively, directed differentiation of the patient-specific iPS cells into the cells of interest (left side) allows *in vitro* modeling of patient's disease, and screening

potential drugs, thus, aiding in the discovery of novel therapeutic compounds. (from Robinton, D.A and Daley G.Q. The promise of induced pluripotent stem cells in research and therapy. *Nature* (2012) 481, 295-305)

(This page was intentionally left blank)

Chapter 2

A Novel Cell Loss Model for Primary Open Angle Glaucoma

The majority of the research in this chapter is in preparation for submission for publication as:

Abu-Hassan, D. W, Li, X, Ryan, E, Acott, T. S & Kelley, M. J. A Novel Cell Loss Model for Primary Open Angle Glaucoma.

2.1 Abstract

Purpose: Elevated intraocular pressure, or IOP, is the primary risk factor for primary open angle glaucoma (POAG). Trabecular meshwork (TM) cell loss is associated with POAG and likely exacerbates other aspects of the disease. To facilitate cellular replacement studies to ameliorate glaucoma, a TM cell loss model system was developed utilizing perfused human and porcine anterior segment organ culture.

Methods: Human or porcine anterior segments in perfusion culture were subjected to saponin exposure for various times to diminish cellularity. Effects of saponin treatment on cellular vitality and density were assessed using confocal microscopy with a cellular Live/Dead assay. Effects on outflow and on IOP homeostatic capacity were evaluated by perfusion at standard pressure (1x) and after pressure elevation (2x). Cultured human TM cells were labeled with quantum dots (QDots) and transplanted onto anterior segments. Efficacy of cellular replacement was assessed by evaluating the impact on IOP homeostatic capacity.

Results: Saponin treatment induced partial TM cell loss in human cell and anterior segment organ culture. The partial cellular denuding from saponin treatment did not significantly affect outflow, but did reduce the capacity for IOP homeostatic response when challenged with 2x pressure. Transplanted labeled TM cells were integrated into the TM and restored IOP homeostatic capability.

Conclusions: This is the first experimental demonstration of a relationship between cell loss and loss of function. The saponin model of controlled cell loss provides a means to functionally assess and correlate TM cell deficit with loss of IOP homeostasis. Additionally, this model shows that TM can be repopulated successfully with

transplanted TM cells, and illustrates the feasibility of using transplantation of stem cells in trabecular meshwork to restore normal IOP homeostasis in glaucomatous eyes.

2.2 Introduction

Glaucoma, an optic neuropathy, is the second leading cause of blindness worldwide [1, 3, and 156]. Increased intraocular pressure (IOP) is often associated with glaucomatous axonal damage at the optic nerve head and is a major risk factor for glaucoma progression [55, 94]. The elevated IOP is directly associated with abnormally increased resistance to aqueous humor outflow [28, 29, 30, 55, 56, 57 and 94]. The majority of aqueous humor exits the eye via the conventional outflow pathway through the TM [158, 159]. In normal eyes, an IOP homeostatic response, i.e., a corrective reduction in outflow resistance, is induced by increases in IOP [55, 199]. The TM responds to IOP elevation with a compensatory reduction in the outflow resistance, which occurs over several days [55, 159, 199, and 200].

A significant reduction in TM cellularity is a common consequence of primary open-angle glaucoma (POAG) and is apparently caused by a number of genetic and possibly environmental factors [98, 99, 162, 163, and 164]. TM cell loss is more severe in POAG than in normal aged eyes and is thought to be an earlier event in POAG [98, 99, 162, and 163]. Between ages 20 and 80, as much as 50% of cells are lost and for POAG patients, the loss is even greater [98, 162]. The loss of cellularity occurs in a gradient-like manner where the inner zones are the most affected and the outermost tissues are the least affected [162]. Whatever the direct causes and other consequences of POAG, this reduction in TM cell density will clearly exacerbate the ability of the TM to maintain IOP homeostasis. One approach to counter this cell loss is to use cellular replacement as a therapeutic strategy [167].

Studies were thus undertaken to develop a model system for use in testing and analyzing the efficacy and feasibility of the proposed cellular replacement therapy.

Glaucomatous eyes for such studies are in limited supply and exhibit considerable variability in cellularity, cellular viability and degree of IOP homeostatic capability. Thus, a model with manageable and uniform degree of cell loss is advantageous. Most available animal models have limitations in terms of similarity to the human outflow pathway, expense, size of the eyes or ease of triggering and assessing the IOP homeostatic response across the appropriate time frame. Since the primary model system for aqueous outflow pathway studies and for testing the degree of IOP homeostatic responsiveness is perfused anterior segment organ culture [180, 181, and 182], we chose to develop a method of producing relatively consistent cell loss in this model system.

2.3 Materials and Methods

2.3.1 Materials

Saponin detergent was purchased from Sigma Life Sciences (Saint Louis MO). Live/Dead Viability/Cytotoxicity Kit for mammalian cells was obtained from Molecular Probes/ Invitrogen (Eugene, OR).

2.3.2 Cells

TM cells were extracted from porcine (PTM) and human eyes (HTM) as described before [173, 174, 175, 176, 177, and 178] and maintained in medium glucose Dulbecco's Modified Eagle Medium (DMEM) supplemented with 10% HyClone fetal bovine serum (Thermo Scientific, South Logan, Utah) and 1% Antibiotic-Antimycotic 100X (Life Technologies, Grand Island, NY).

2.3.3 Saponin Treatment of Trabecular Meshwork Cells in Tissue Culture

Porcine TM cells were grown on glass chamber slides for 48 hours until confluent. In each chamber the cells were washed with PBS, and then subjected to several concentrations of saponin detergent (0.001%, 0.01%, 0.025%, 0.05% or 0.1%) dissolved in serum free medium glucose DMEM for 5 minutes. The saponin was then removed and the cells were rinsed gently with phosphate buffered saline (PBS). *Slow Fade* Gold Antifade reagent with DAPI (Molecular Probes/ Invitrogen) was applied to prepare the slides for confocal microscopy analysis.

2.3.4 Perfused Human or Porcine Anterior Segment Organ Culture and Saponin Treatment of Trabecular Meshwork.

Human and porcine perfused anterior segment organ cultures were used as described previously [176, 177, 178, 179, 180, 181, and 182] and perfused at constant pressure (8.8 mm Hg) (1x) to generate an average flow rate of 1-7 μL/min for humans

and 2 to 8 µL/min for porcine eyes. Human donor eye pairs were acquired from Lions Vision Gift (Portland, OR). Human donor tissue protocols were approved by the Oregon Health & Science University Institutional Review Board and were conducted in accordance with the tenets of the Declaration of Helsinki.

Saponin was dissolved in serum-free medium glucose DMEM to 0.01% concentration then injected into the perfusion chamber after human and porcine eyes had been subjected to flow for 48 hours. The flow was stopped and the human and porcine anterior segment explants in the ocular perfusion system were treated with saponin for 7 or 10 minutes, respectively. They were thoroughly rinsed afterwards with serum-free medium glucose DMEM. The flow baseline was re-established for 24 hours, and the pressure was doubled to 17.6 mm Hg (2x) to produce an IOP homeostatic pressure challenge over the next few days. Outflow rates were measured gravimetrically.

2.3.5 Live/Dead Staining Assay

The Live/Dead Viability/Cytotoxicity Assay Kit provides a two-color fluorescence cell viability assay in which two probes, calcein AM and ethidium homodimer (EthD-1), indicate cellular viability and plasma membrane integrity. Porcine TM cells cultured on chamber slides were washed with sterile PBS, incubated in Live/Dead solution for 30 minutes at 37°C, and then the nuclei were stained with DAPI. The stained cells were examined afterwards by confocal microscopy. Porcine and human anterior segments perfused subsequent to saponin treatment were washed with sterile PBS, soaked in Live/Dead solution and incubated for 30-45 minutes at 37°C. At the end of the incubation period, the cells and anterior segments were washed with PBS and visualized by confocal microscopy.

2.3.6 Examination of Cell Viability by Confocal Microscopy

The stained Live/Dead TM cells and radial sections from anterior segment explants were viewed on confocal microscopy. Twenty images were captured for porcine TM cells treated for 7 min with each concentration of saponin (0, 0.001, 0.01, 0.025, 0.05 or 0.1%). The percentage of dead cells out of the total cell number of cells per field was calculated. Eight radial wedges were prepared from each eye and frontal sections were generated for analysis. The Live/Dead kit was used to stain TM tissue for live (green) cells and dead (red) cells. Several images were taken per section to examine live and dead cells in all areas of the TM tissue by confocal microscopy. Equal numbers of eyes were either treated or untreated with saponin.

2.3.7 Transplantation of Cultured TM Cells into Saponin-denuded Eyes

Primary cell cultures of TM cells were harvested by trypsin treatment, cells were rinsed thoroughly and labeled with 3 µL of Qtracker 655 nanoparticles Cell Labeling Kit (Life Technologies, Eugene, OR) prior to transplantation. To label the TM cells, they were incubated with these nanoparticles for an hour at 37°C, and then washed thoroughly to eliminate residual particles that had not been taken up. The HTM cells were visualized on the confocal microscope to verify their uptake of nanoparticles.

Human anterior segments were mounted in the flow chamber for 48 hours, and then treated with saponin. After 24 hours, the pressure was increased to 2x for 48 hours to assess cell pre-treatment IOP homeostatic capability following saponin treatment but prior to transplantation. Subsequently, cellular transplant with the labeled TM cells was performed using 0.3 million cells/TM. The replacement cells were injected into the flow chamber in an upside-down position and flowed in at 0.5x pressure for 2 hours, followed by an overnight incubation at 37°C with the flow stopped. On the subsequent day, the

flow was resumed for 24 hours at physiological pressure (1x), and then doubled for 96 hours. During the steps preceding and subsequent to the pressure challenge, the flow rate was assessed.

2.3.8 Statistical Analysis

One-way ANOVA with Dunnett's Multiple Testing Correction or unpaired t-tests were used to determine statistical significance.

2.4 Results

2.4.1 Cellular loss is greater in glaucomatous eyes.

Previous studies by Alvarado *et al* showed that TMs of eyes from persons with glaucoma exhibited reduced cell density compared to normal aged eyes [98, 99]. Using Live/Dead staining to compare glaucomatous and normal anterior segment cell density, we confirmed these results although our sample size was not as large as theirs (Fig. 2.1). Frontal sections of glaucomatous eyes, examined by confocal microscopy, have less live cells than normal (Fig. 2.1E). Additionally, the TM of the affected eyes shows more dead cells (Fig. 2.1F).

2.4.2 Saponin treatment triggers TM cell death and sloughing in both cell culture and human eyes.

To create more uniform and controlled cell death in the TM of normal aged eyes, we treated anterior segments with the detergent saponin [168, 169]. Initially, saponin was applied to cultured TM cells at different concentrations: 0% (vehicle control), 0.001%, 0.01%, 0.025%, 0.05% and 0.1%, with all in serum-free DMEM.

Saponin treatment produced death of the TM cells with stronger effects occurring at higher concentrations (Fig. 2.2A). At 0.025% saponin and higher, nearly all of the cells were killed and much more sloughing of TM cells was observed (Fig. 2.2A-B). When saponin was applied in 0.01% concentration, it induced death in 36% $\pm$ 9 of TM cells, whereas 0.001% killed 20% $\pm$ 3 of cells (Fig. 2.2B). Consequently, we chose 0.01% saponin for 7 minutes for induction of TM cell death in human anterior segments to simulate the approximate level of cell loss detected in glaucomatous eyes [98].

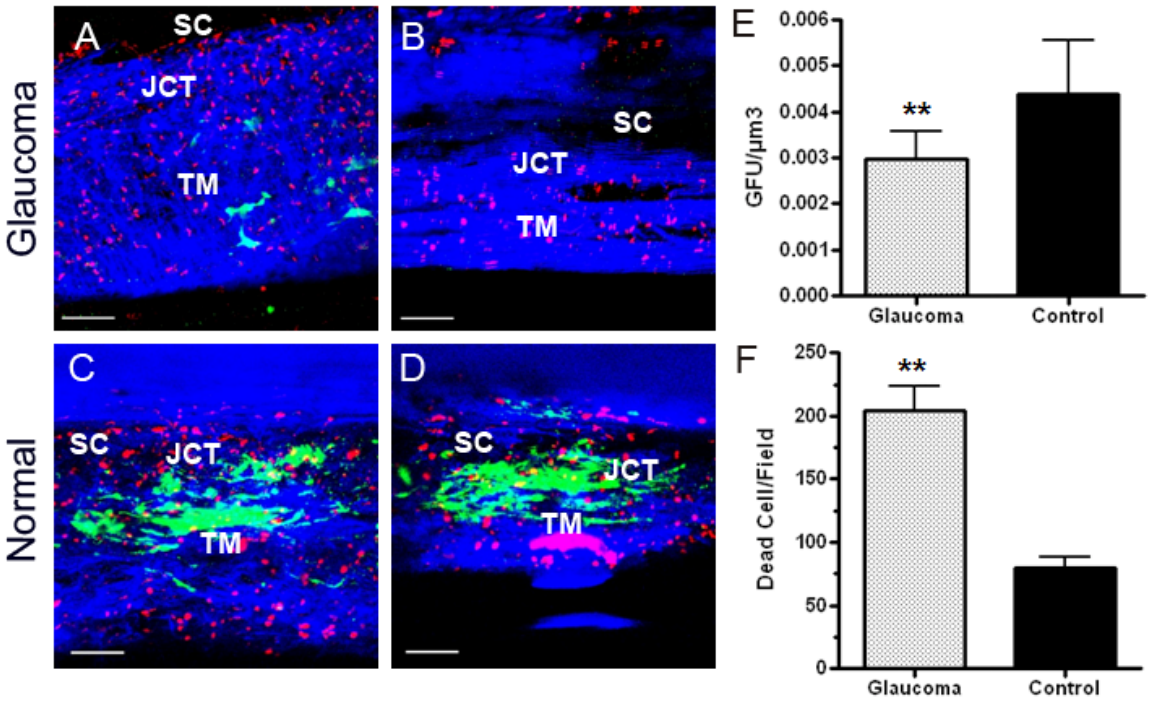

Figure 2.1: Glaucomatous eyes show more dead cells and less live cells in the TM. Frontal sections were generated and examined by confocal microscopy after human **(A, B)** glaucomatous eyes and **(C, D)** normal aged eyes were perfused for 48 hours and stained with calcein AM (green) to label live cells and ethidium homodimer (EthD-1; red) to mark dead cells. Notice the presence of more live cells in normal eyes. **(A)** and **(B)** are different fields of the same glaucoma eye. **(C)** and **(D)** are different fields of the same normal eye. Scale bars represent 100 µm. **(E)** The live cell volume, represented by green fluorescent unit (GFU) volume, relative to beam volume was measured using ImageJ. **(F)** The average number of dead cells per field was quantified in glaucomatous eyes and compared to normal eyes. A significant increase in cell death was detected in glaucomatous eyes. **(E)** and **(F)** are averages of 40 images captured for 5 glaucomatous and 5 control eyes. Error bars represent the standard error of the mean. P values are less than 0.001.

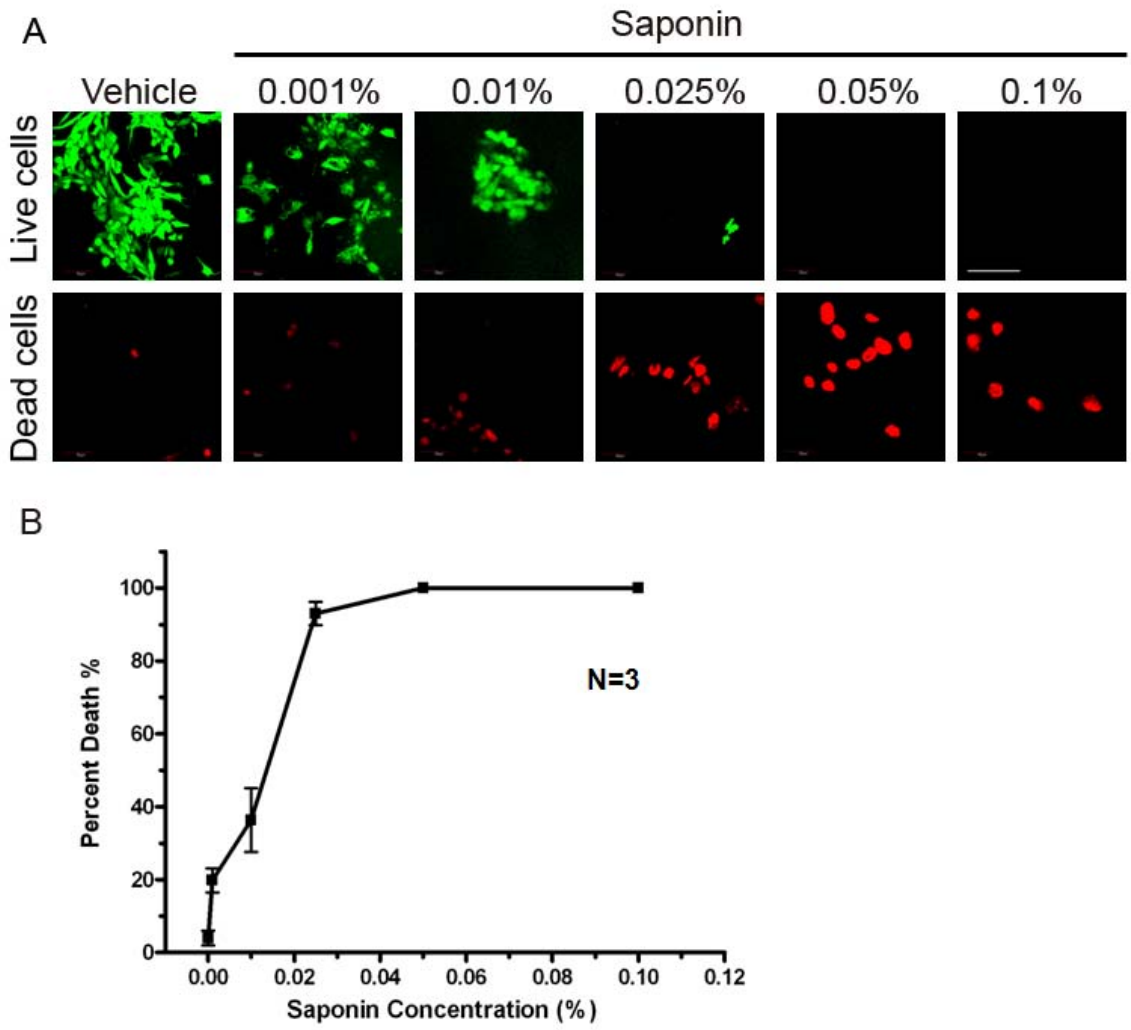

Figure 2.2: Dose-response effect of saponin on TM cells. Porcine TM cells (PTM) were grown on chamber slides, and then treated with several concentrations of saponin for 5 minutes. The concentration of saponin is shown above each image. Subsequently, the saponin was washed off the cells with PBS. TM cells were stained with Live/Dead staining with calcein AM (green) and Eth-1 (red). **(A)** Twenty images of cells exposed to each concentration were captured by confocal microscopy from 3 independent experiments. Higher concentrations of saponin increase cell death and sloughing. The

scale bar represents 100 μm. In **(B)** cell death=% of dead cells out of the total number of cells in the field. Error bars represent the standard error of the mean.

2.4.3 TM tissue shows basal cellular death preceding any treatment.

The delayed acquisition (up to 48 hours postmortem), normal restoration process (around 5 days in stationary culture) and significant effects of natural aging on human eyes can be expected to result in reduced cellularity and cell death prior to saponin treatment [99,162, 196]. Some loss may also be observed in porcine TMs.

In order to determine the extent of the baseline cell loss, we examined the viability of TM cells in fresh porcine eyes and compared them to their saponin-treated counterparts. Dead cells were detected in untreated porcine anterior segments (Fig. 2.3 D'-E'). However, saponin induced significant cell death (Fig. 2.3F). Moreover, higher counts of live PTM cells were detected when compared to untreated HTM cells (Fig. 2.3G and Fig. 2.4B-E, 4I). Porcine eyes are from a much younger population compared to most donor human eyes (average age around 74). As a result, we detected more dead cells in human untreated eyes than in porcine eyes. We also noticed variability of total cell counts across the TM of the same eye (Fig. 2.3 B-E and B'-E').

2.4.4 Saponin treatment significantly increased the number of dead cells in anterior segments.

The chosen concentration of saponin, 0.01%, was injected into the flow line of human anterior segments mounted in the ocular perfusion system and incubated in the TM for 7 minutes before being washed out. The Live/Dead assay was used to determine whether saponin affected the viability of human TM cells in frontal sections of anterior segments (Fig. 2.4A-E). Saponin treated anterior segments contained more dead TM cells than vehicle treated anterior segments (Fig. 2.4F). Saponin treatment induced cell death although more live than dead cells still populated the TM, indicating that saponin's effect was partial (Fig. 2.4F-G).

Additionally, saponin was able to penetrate deeply into the TM and kill cells in all zones of the TM down to the juxtacanalicular region (JCT) (Fig. 2.4B-E). Moreover, comparing the percentage of live cells in glaucomatous and saponin-treated eyes relative to normal eyes revealed very close amounts of live cells, 67.42% and 66.42% respectively (Fig. 2.4H). The previous comparison suggests that saponin treatment induced changes in cell counts that approximate those found in glaucoma.

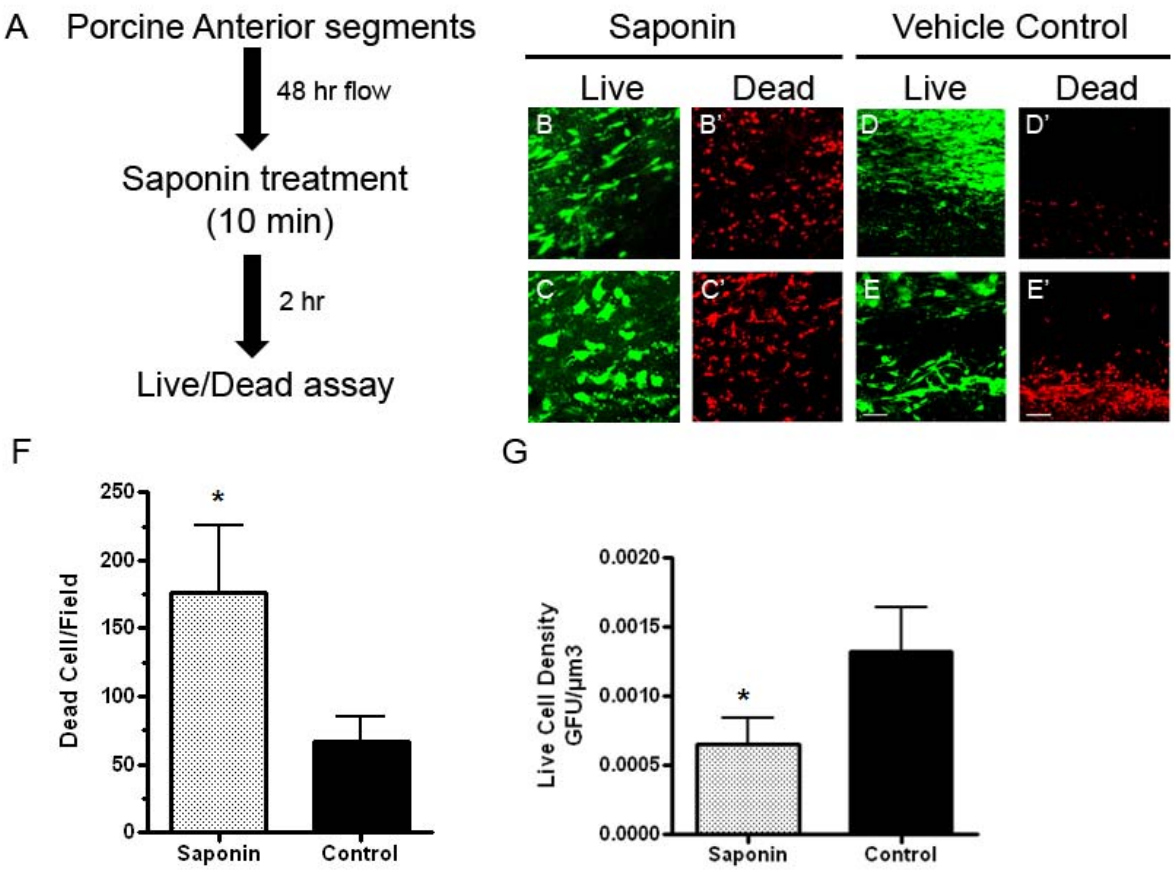

Figure 2.3*:* **Basal death of TM cells in fresh porcine eyes. Basal death of TM cells in fresh porcine anterior segments. (A)** A schematic diagram of the experiment. **(B-E, B'-E')** Fresh porcine anterior segments were perfused for 48 hours, and then treated with 0.01% saponin for 10 minutes or with the vehicle alone. The porcine anterior segments were stained with live (green) and dead (red) stain and were cut into wedges. These were imaged *en Face* by confocal microscopy and **(B-E)** show live (green) and **(B'-E')** show dead (red) channels. The majority of cells are alive in untreated sections, although some cellular death was detected **(D'-E')**. However, control eyes show considerably less dead cells and more live cells **(F-G)**. Notice total cell count variability in different fields of view across the TM**. (B-C)** and **(D-E)** are different fields in the same

porcine anterior segments. Primed images represent the same fields as their unprimed counterparts. Scale bars represent 100 μm. **(F)** Average number of dead cells per field was counted and significant increase in cell death was detected with saponin treatment. In addition, death was detected in the absence of any treatment indicating the presence of basal cell death. **(G)** Live cell volume per unit volume (μm^3) of the TM tissue was quantified using ImageJ software. The green fluorescent unit volume was compared in saponin-treated and control anterior segments. The results in **(F)** and **(G)** represent the average of three porcine eye pairs Error bars represent the standard error of the mean. P values are less than 0.05.

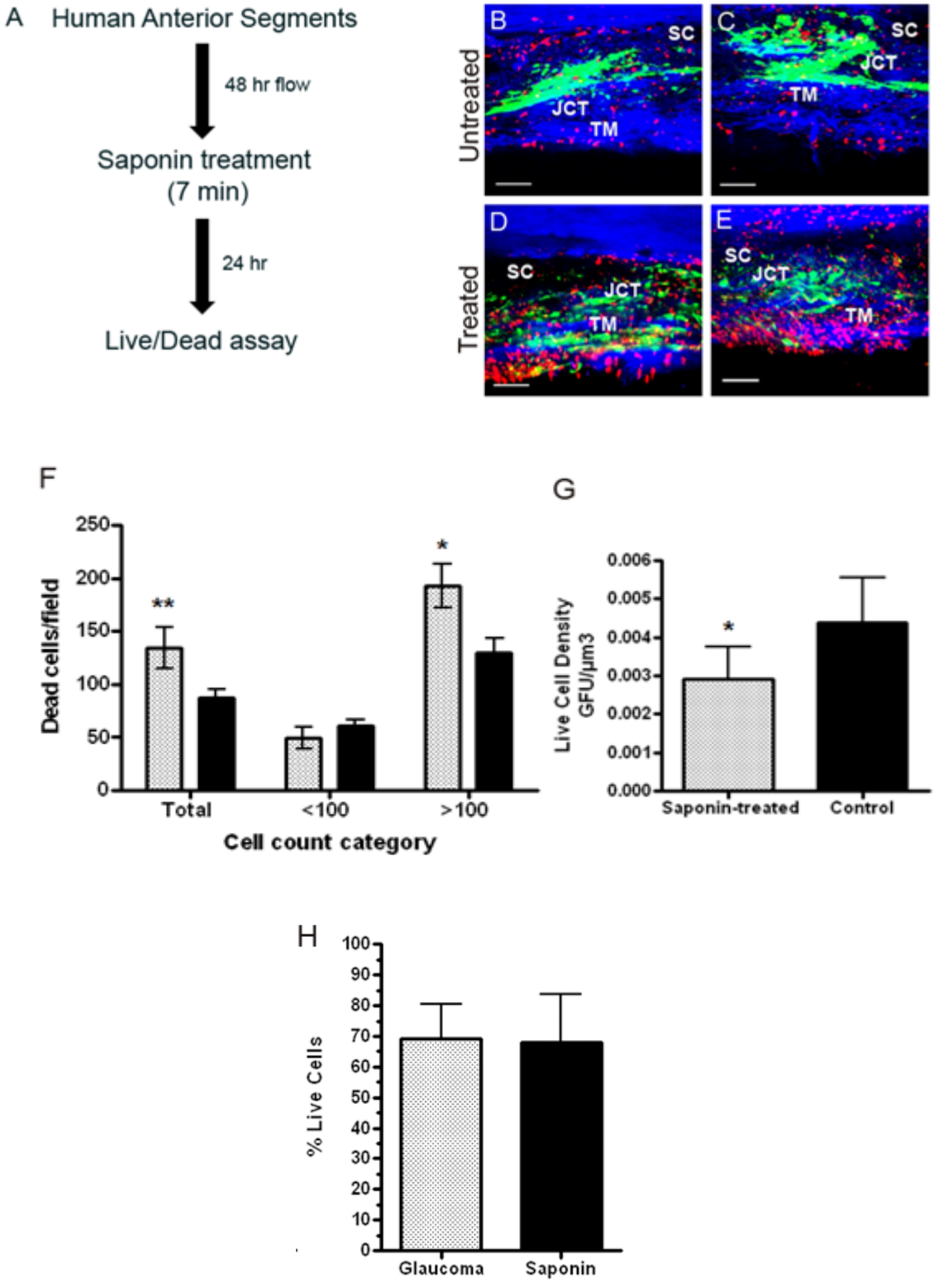
A
Human Anterior Segments
48 hr flow
Saponin treatment
(7 min)
24 hr
Live/Dead assay
B
C
D
E
Untreated
Treated
SC
JCT
TM
F
Dead cells/field
250
200
150
100
50
0
**
*
Total
<100
>100
Cell count category
G
Live Cell Density
GFU/µm3
0.006
0.005
0.004
0.003
0.002
0.001
0.000
*
Saponin-treated
Control
H
% Live Cells
100
90
80
70
60
50
40
30
20
10
0
Glaucoma
Saponin

Figure 2.4: Saponin treatment produces cell death in perfused human anterior segment explants. (A) A schematic of the experiments done in this figure. After the flow was stopped, saponin (0.01%) was applied to perfused human anterior segments for 7 minutes by injection through the flow line. **(B-E)** Frontal sections of human anterior segments show the induction of cellular death in saponin-treated TM. Cellular death was detected by red staining with EthD-1, whereas, live cells uptake calcein AM and stain green. The TM beams autofluoresce and are shown in blue color in the images. Saponin produced death at all TM levels including JCT in several fields of the same eye. Scale bars represent 100 μm. Notice the greater numbers of dead cells in **(D-E)** saponin treated eyes. However, more live cells are apparent in **(B-C)** the controls (untreated eyes). **(B)** and **(C)** represent different fields of the same eye, whereas **(D)** and **(E)** represent different fields of the contralateral eye. **(F)** The cell death produced was quantified by counting the total number of dead cells per field. Saponin significantly produced death in treated anterior segments (total columns, **P<0.001, 30 fields were counted). Regions of the TM that have more cellular content (>100 columns) show a significant increase in cellular death with saponin (*P<0.05, 10-13 fields were counted) while the low cellularity areas do not. **(G)** Live cell volume per unit volume (μm^3) of the TM tissue was quantified using ImageJ software. The green fluorescent unit volume was compared in saponin-treated and control human anterior segments. P values are less than 0.05. **(H)** The remaining live cells in glaucomatous eyes in Fig. 1 and in anterior segments exposed to saponin relative to the average live cell volume in normal anterior segments were calculated and compared. The columns show very similar amounts of live cells indicating that the effect of saponin on tissue cellularity simulates what is found

in glaucoma. The results in **(F), (G)** and **(H)** represent the average of three human eye pairs. Error bars represent the standard error of the mean.

2.4.5 Saponin treatment reduces the capability of TM for the IOP homeostatic response when challenged with high pressure.

To examine the influence of saponin treatment on the ability of TM to respond to IOP and trigger the normal homeostatic response, we measured the effects of exposure to 0.01% saponin on this process (Fig. 2.5B). Anterior segments were perfused at normal 1x physiologic perfusion pressure (8.8 mm Hg) until the flow had stabilized.

One anterior segment from paired human eyes was then exposed to saponin and the other exposed to vehicle both for 7 min. Saponin or vehicle was washed out and perfusion was restarted at 1x perfusion pressure. After 24 hours, perfusion pressures were increased to 2x (17.6 mm Hg). Flow rates doubled immediately after pressure was elevated to 2x in both treatment and control anterior segments. Over several days, the TM cells of the vehicle-treated anterior segments slowly reduced the outflow resistance resulting in a gradual and significant increase in outflow rate (Fig. 2.5B-black line). The saponin-treated anterior segment did not show this gradual increase in flow, i.e. the IOP homeostatic response, but instead remained at approximately the 2x flow rate without triggering changes in the outflow resistance (Fig. 2.5B-dashed line).

2.4.6 Transplanted HTM cells integrated into the TM of saponin-treated anterior segments and restored the IOP homeostatic response.

Anterior segments that were exposed to saponin and lost the ability to adjust the outflow resistance when subjected to a 2x pressure challenge, regained this capability after HTM cells were added back and allowed to integrate into the explants (Fig. 2.6C). After the saponin-treatment and assessment of response to 2x pressure challenge, QDot-labeled HTM cells were injected into the perfusion line, allowed to flow into the TM at 0.5x pressure for 2 hrs, and then the pressure was reduced to 0 mm Hg for 24 hrs to

facilitate attachment to the saponin-denuded areas of the anterior segments. Perfusion pressure was then reinitiated and maintained at 1x to reestablish the baseline flow, and then increased to 2x and the flow measured for several days (Fig 2.6D).

When examined by confocal microscopy (Fig. 2.6B-C), QDot-labeled transplanted TM cells were observed throughout the TM. The transplanted cells appeared to have attached to the structural beams of the TM and to inner layers of TM including the JCT (Fig. 2.6B-C). Although the IOP homeostatic response to 2x pressure was lost after saponin treatment, it was regained after the TM cells were added back (Fig. 2.6D).

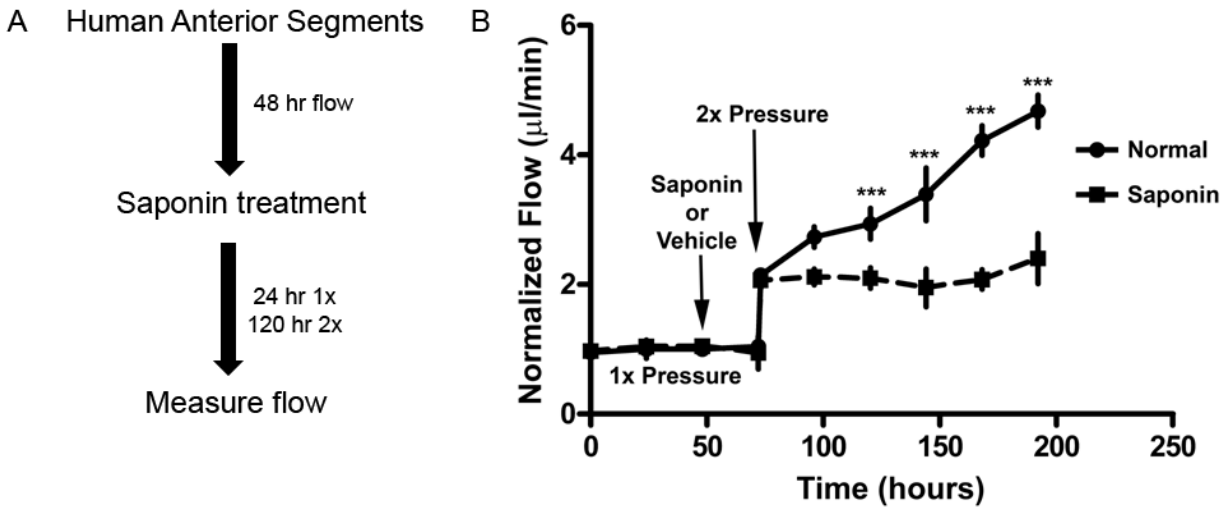

Figure 2.5: Saponin treatment reduces the IOP homeostatic response in human anterior segments. (A) A schematic of the experiments performed in this figure. After human anterior segments were perfused for 48 hrs, they were treated with 0.01% saponin for 7 minutes. After 24 hrs at 1x, the pressure was doubled (2x) and the flow was measured for 5 days. **(B)** The flow rate of the saponin treated anterior segments (dashed line) was calculated and compared to the untreated human anterior segments (vehicle control; black line). The gradual increase in flow beyond the initial doubling shown in the control represents the normal IOP homeostatic response, whereas saponin treated eyes do not show increased flow rate with time, beyond the initial doubling when pressure was increased. The results were reproduced in human anterior segments, where n=8 for normal controls and n=17 for saponin treated eyes. Values are the mean and error bars represent the standard error of the mean with significance by one-way ANOVA where ***$P<0.001$.

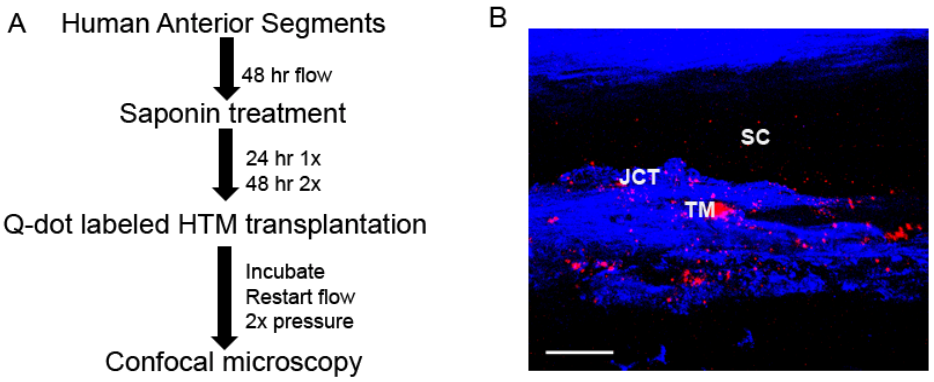
A
Human Anterior Segments
48 hr flow
Saponin treatment
24 hr 1x
48 hr 2x
Q-dot labeled HTM transplantation
Incubate
Restart flow
2x pressure
Confocal microscopy
B
SC
JCT
TM

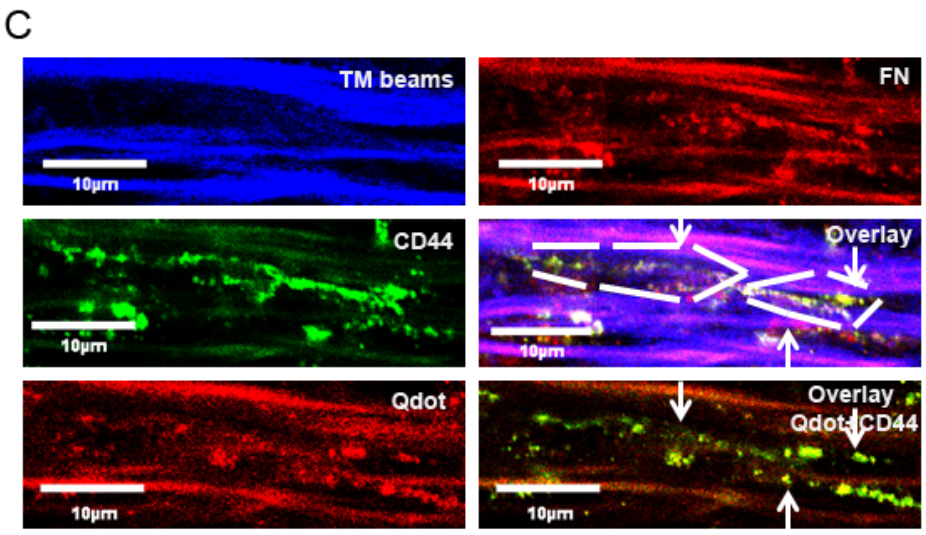
C
TM beams
FN
CD44
Overlay
Qdot
Overlay
Qdot-CD44
10μm

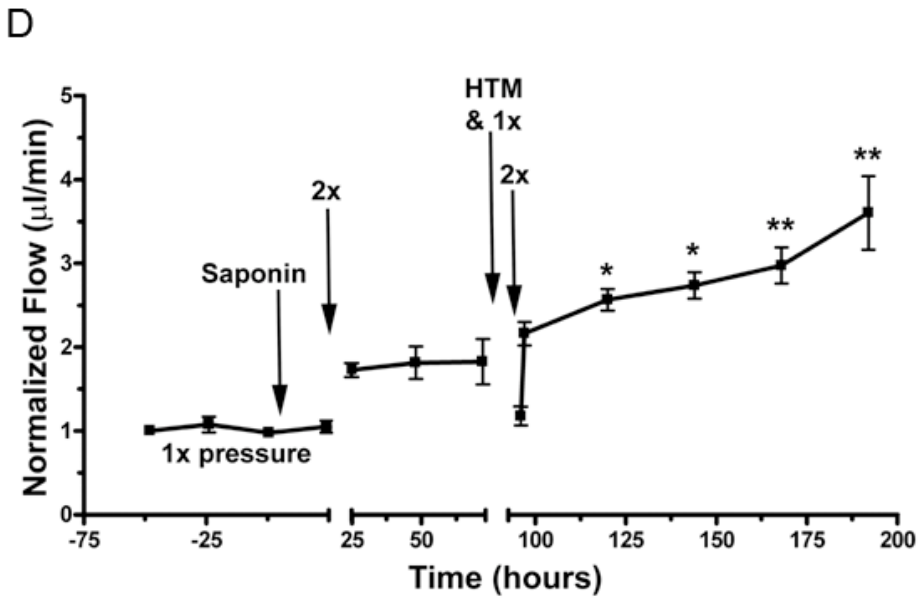
D
Normalized Flow (μl/min)
Time (hours)
Saponin
2x
HTM
& 1x
2x
1x pressure
*
*
**
**
0
1
2
3
4
5
-75
-25
25
50
100
125
150
175
200

Figure 2.6: Replacement TM cells restore the IOP homeostatic response in saponin treated human anterior segments. (A) Experimental scheme illustrating step by step the experiments done in this figure. Human anterior segments were perfused for 48 hours then treated with 0.01% saponin for 7 minutes. The flow was resumed after saponin was rinsed thoroughly with serum free medium glucose DMEM. After 24 hours, HTM cells that had been labeled with Q-dots (red) were injected into the flow line to the perfused anterior segment explants. The cells were allowed to attach overnight, and then flow was restarted at physiological pressure (1x). The pressure was doubled (2x) 24 hours later and the flow was measured for 5 days. **(B)** Frontal sections of fixed eyes were generated and examined for nanoparticle-labeled (red) transplanted TM cells. Labeled transplanted cells integrated deep into the TM tissue reaching the JCT. Blue label shows collagen and elastin autofluorescence from the TM beams. Scale bars represent 100 μm. **(C)** The transplanted HTM cells labeled with Q-dots were stained for CD44 to demarcate their outline (green, dashed line) and fibronectin (FN) (red) was stained as a component of the ECM that covers the TM beams. The HTM cells (arrows, 2 cells) integrated into the TM tissue and attached to the TM beam surface (blue autofluoresence). Scale bar represents 10 μm**. (D)** Transplanted replacement TM cells are able to restore IOP homeostatic response when the pressure is elevated to 2x. Line shows mean for 6 experiments and error bars represent the standard error of the mean with significance by one-way ANOVA where *$P<0.05$ and **$P<0.001$.

2.5 Discussion

The gradual loss of TM cells with aging and the larger loss in glaucoma seem almost certain to exacerbate the effects of other factors involved in triggering this disease [1, 94, and 156]. Although the exact extent of this TM cellular loss is somewhat variable between individuals, it is thought to be a linear progression with estimated losses approximating 0.58% of TM cells per year from birth to 81 years of age [156]. Glaucoma is primarily an aging disease with strong genetic contributions and possibly some environmental components. The primary function of the TM is thought to be the maintenance of IOP homeostasis [55, 56]. Since elevated IOP is the primary risk factor for glaucomatous optic nerve damage, this trabecular IOP homeostatic process is very likely the key reason that most people do not develop glaucoma [55, 57].

No clear relationship between any specific glaucoma causal agents and the well-documented glaucoma-associated cell loss has been previously established [97, 98, 99, and 100]. Although it has long been assumed that loss of TM cells would exacerbate IOP regulation, the studies presented herein provide the first direct experimental evidence that TM cell loss has any effect on IOP regulation [97, 98, 99, and 100]. We show that TM cellular reduction, which has minimal direct effect on outflow facility, significantly reduces the IOP homeostatic response to pressure elevation. We initially verified the prior reports of TM cell loss with glaucoma (Fig. 2.1) using confocal microscopy. After testing various conditions and doses, we found that 0.01% saponin for 7 minutes produced a relatively consistent level of cell loss. This loss approximated that of POAG and was sufficient to compromise the IOP homeostatic response in perfused human anterior segment organ culture.

This is the first direct model for IOP homeostatic response capability providing a potential system to study cell replacement therapy for glaucoma. In order to test the potential of this model system to facilitate assessment of the potential efficacy of stem cell repopulation studies, we added back cultured TM cells. These cells were able to restore the lost IOP homeostatic response. Although some other stem cell therapy approaches have been proposed for TM cell replacement, none of these studies had any way to assess efficacy of replacements. This is the first model system that will provide both endpoints for effective TM cell loss and for cell restoration efficacy. The saponin model for TM cell depletion is thus ideal to facilitate studies of the potential of autologous stem cells to restore IOP homeostatic function to glaucomatous eyes [197].

2.6 Acknowledgments

The authors thank Ruth Phinney (Lions Vision Gift, Portland, Oregon) for facilitating the procurement of human donor eyes.

Supported by NIH grants EY021800 (MJK), EY003279 (TSA), EY008247 (TSA), and EY010572 (TSA), an unrestricted grant to the Casey Eye Institute from Research to Prevent Blindness, New York, New York, and the University of Jordan.

Disclosure: **D. W. Abu-Hassan**, None; **X. Li**, None; **E. Ryan**, None; **T.S. Acott**, None; **M.J. Kelley**, None

(This page was intentionally left blank)

Chapter 3

Use of iPS Cells to Restore Intraocular Pressure Homeostasis in a Human Model for Glaucoma

The majority of the research in this chapter is in preparation for submission for publication as

Abu-Hassan, D. W, Li, X, Acott, T. S & Kelley, M. J. Use of iPS Cells to Restore Intraocular Pressure Homeostasis in a Human Model for Glaucoma.

3.1 Abstract

Purpose: Elevated intraocular pressure, or IOP, is the primary risk factor for primary open angle glaucoma (POAG). Cellular loss within the tissue which regulates IOP, the trabecular meshwork or TM, is a notable feature of glaucoma. We used a saponin TM cell depletion model to mimic the cell loss associated with glaucoma, and then repopulated with TM-like cells differentiated from induced pluripotent stem cells (iPSCs). To determine the feasibility of this prospective treatment, we assessed the major functions of the TM, IOP homeostasis and phagocytosis of debris.

Methods: iPSCs were differentiated to TM-like cells using previously determined combinations of TM growth medium, TM cell conditioned medium (CM) and TM cell extracellular matrix (ECM). Differentiation was evaluated by comparing marker expression by the TM-like cells with both TM and iPS cells using immunohistochemistry, Western blotting and quantitative RT-PCR. Restoration of IOP homeostatic capability following saponin treatment and TM-like cell replacement was assessed in perfused human anterior segment organ culture. Pre-labeled TM-like cells were examined by immunohistochemistry and confocal microscopy after transplantation. An established assay for phagocytosis was used to investigate phagocytosis of zymosan particles by the TM-like cells, and this was compared to human trabecular meshwork cells (HTM) and iPSCs.

Results: The differentiated TM-like cells expressed the same biomarkers as TM cells, but not those of stem cell pluripotency factors seen with iPSCs. Upon transplantation into saponin denuded anterior segments, labeled TM-like cells attached tightly in all levels of the TM. TM-like cells transplanted into the saponin cell depletion model

restored IOP homeostatic capability when challenged with pressure elevation, and were capable of phagocytosis of debris in culture, while iPSCs were not.

Conclusions: Differentiated TM-like cells transplanted onto partially denuded TM in the saponin cellular depletion model were able to repopulate the TM, and to restore IOP homeostatic capability. The phagocytosis assay showed that the differentiated TM-like cells phagocytosed debris like TM cells, unlike cultured iPSCs. This is the first report of successful restoration of function after transplantation of differentiated iPSCs into TM. IPSCs, as patient-specific cells hold high promise as a treatment option in glaucoma.

3.2 Introduction

Glaucoma is a relatively common optic neuropathy affecting over 67 million persons worldwide [1, 94, and 156]. Elevated intraocular pressure (IOP) is a primary risk factor and lowering IOP remains the only viable treatment for all forms of glaucoma [156]. The trabecular meshwork (TM) is a small filtration tissue surrounding the inner circumference of the cornea [42, 67]. It provides the resistance to the outflow of aqueous humor from the anterior portion of the eye and is thus responsible for regulating IOP [43, 57, 92, and 198].

There are several distinct forms of glaucoma, of which primary open-angle glaucoma (POAG) is the most common [67]. Numerous genetic loci for glaucoma have been mapped and several glaucoma genes have been identified [201]. There are also likely to be environmental factors involved. No single genetic locus or environmental source accounts for more than a minor portion of glaucoma and cohesive common pathway involvements remain elusive. Currently, several treatments are used to reduce or control IOP, initiating with several classes of medications, and progressing to laser treatments and several surgeries [55, 67, 199, and 200]. Most medications either reduce inflow of aqueous humor (AH) or divert outflow through the unconventional route via the ciliary muscle. Several recent medications actually increase outflow through the conventional pathway, i.e. through the TM. All require frequent treatments with eye drops, often multiple times per day. Compliance remains highly problematic and significant side effects are not uncommon. Consequently, more innovative alternative long-term therapies are being explored.

The most well-established system to study IOP regulation is perfused human anterior segment organ culture [75, 77,180, and 181]. The anterior portion of the eye is

mounted in an *ex vivo* perfusion culture system and effects of treatments on outflow can be assessed. In normal eyes, pressure elevations trigger homeostatic responses that maintain IOP within narrow physiologic ranges [77, 198]. IOP homeostasis is the primary function of the outflow pathway and loss of this capability can thus be considered a hallmark for glaucoma.

It has long been known that TM cellularity declines progressively with ageing and even more aggressively in glaucoma [94, 98, and 99]. Although this cell loss seems likely to compromise IOP regulation, the association between TM cell loss and outflow regulation has only been correlative [98]. We have recently shown experimentally that controlled TM cell reduction diminishes the ability of this tissue to maintain IOP homeostasis (paper in chapter 2). Furthermore, repopulation of the original depleted TM cells with cultured TM cells from another individual restores IOP homeostatic capability.

It thus becomes conceptually feasible to use autologous stem cells to repopulate the outflow pathway as a means of restoring cellular function and IOP homeostatic capability to glaucoma patients with reduced cellularity [167]. Consequently, we used this human cell depletion model system to study the feasibility of restoration of IOP homeostatic function by addition of differentiated induced pluripotent stem cells (iPSCs).

3.3 Materials and Methods

3.3.1 Materials

Live/Dead Viability/Cytotoxicity Kit for mammalian cells and zymosan particles for phagocytosis assay were obtained from Molecular Probes/Invitrogen (Eugene, OR). Saponin detergent was purchased from SIGMA Life Sciences (Saint Louis, MO). Aqueous humor (AH) was collected from porcine eyes by inserting a 27 gauge needle through the cornea into the anterior chamber and removing 100-150 µL/eye. The AH was then stored at -20°C until used

3.3.2 Cells

Human iPSCs (DF6-9-9T.B), derived from dermal foreskin fibroblasts, were purchased from WiCell Laboratories (Madison, WI), grown, and maintained according to the company's instructions. Normal adult human dermal fibroblasts (DF) were purchased from American Type Culture Collection **(**Manassas, Virginia) and cultured according to their instructions. Human umbilical vein endothelial cell line (HUVEC) were a gift from Dr. Nabil Alkayed, Department of Anesthesiology and Perioperative Medicine, Oregon Health and Science University, Portland, OR), and were cultured according to the supplier's instructions (Life Technologies Corporation, Carlsbad, CA). Primary human TM cells were cultured as previously detailed [173, 174, 175, 176, 177, and 178] in TM culture medium (a 1:1 mix of high- and low-glucose Dulbecco's Modified Eagle Medium (DMEM) supplemented with 10% HyClone fetal bovine serum (Thermo Scientific, South Logan, Utah) and 1% Antibiotic-Antimycotic 100X (Life Technologies). TM cells were used from passages 2 to 5.

3.3.3 Generation of Embryoid Bodies (EBs)

To generate uniform small size EBs on a large scale, medium sized undifferentiated iPS cell colonies were detached from 6 well plate surfaces by treatment with Accutase enzyme (Innovative Cell Technologies, San Diego, CA). Cells were transferred to AggreWell plates (Stem Cell Technologies, Vancouver, B.C., Canada) and incubated in AggreWell medium (Stem Cell Technologies) for 24 hours. The next day, the formed EBs were harvested from the AggreWell plate and transferred to 6-well plates where differentiation was begun as described in the next section of methods.

3.3.4 Differentiation of iPS cells

The generated EBs were cultured on ECM derived from cultured porcine TM cells in a mixture of TM cell growth medium and AggreWell medium from Stem Cell Technologies and conditioned medium (CM) (25%, 50% and 25% respectively). We designated the previous mixture DiffMedium. The CM was collected after 48 hours of serum starvation of HTM cells. The EBs were grown in DiffMedium and maintained in culture for 30 days. After 30 days, the differentiated cells were cultured in TM growth medium (10% fetal bovine serum in medium glucose DMEM) and passaged with trypsin like TM cells for at least 7 passages, at which point the cellular growth slowed.

3.3.5 Immunoblotting

HTM, iPS and TM-like cells were grown on 6-well plates until they reached confluence. Cell lysates were collected using a RIPA buffer mixed with a protease inhibitor cocktail (Sigma-Aldrich). Protein concentrations were measured using a BCA kit from Pierce Biotechnology (Thermo Scientific). Loading buffer with 0.1 M dithiothreitol (DTT) was added to the lysates and samples were boiled for 15 minutes. Equal amounts of protein (20 µg) were loaded per lane in SDS/PAGE gels. Gels were run at 120 volts

for 90 minutes and wet transferred at 4°C to polyvinylidene fluoride (PVDF) membranes. Non-fat dry milk (5%) was used as a blocking buffer. Primary antibodies for immunoblotting were used at a 1:1000 dilution in phosphate buffered saline (PBS) and 0.05% Tween and incubated at 4°C overnight, Table 3.1. Secondary antibodies, both rabbit and mouse, were purchased from Rockland Immunochemicals (Gilbertsville, PA), diluted in PBS and incubated for 1 hour at room temperature.

TABLE 3.1. Primary Antibodies Used for Immunostaining and Western Blotting

Antibody	Type	Source	Catalog Number
AQP1	Rabbit polyclonal	Santa Cruz Biotechnology (Santa Cruz, CA)	sc-20810
CHI3L1	Rabbit polyclonal	Abcam (Cambridge, MA)	ab88847
Integrin α3	Rabbit polyclonal	Novus Biologicals (Littleton, CO)	NBP1-19724
KLF4	Rabbit polyclonal	Abcam	ab72543
NANOG	Rabbit polyclonal	Santa Cruz Biotechnology	sc-33759
LAMP1	Mouse monoclonal	Abcam	ab25630
OCT3/4	Mouse monoclonal	Santa Cruz Biotechnology	sc-5279
SOX2	Rabbit polyclonal	Santa Cruz Biotechnology	sc-20088
α-Tubulin	Rabbit monoclonal	Millipore (Temecula, CA)	04-1117
Wnt1	Rabbit polyclonal	Abcam	ab15251

3.3.6 Immunohistochemistry

HTM, iPS and TM-like cells were grown on glass chamber slides until 60-80% confluent. They were fixed with 4% paraformaldehyde and permeabilized with 0.3% Triton X100 in PBS. Slides were blocked in 5% normal goat serum in PBS, and then primary antibodies for the cell markers (Table 3.1) were added at a 1:200 dilution. Alexa Fluor 488- and 595-conjugated secondary antibodies (Molecular Probes/Invitrogen) were used at 1:500 dilutions.

3.3.7 Real-Time Quantitative PCR

HTM, iPS and TM-like cells were grown on 6 well plates until confluent. Cells were harvested by Trizol (Life Technologies) and RNA was extracted using the manufacturer's protocol. Reverse transcription was performed using SuperScript III First Strand Synthesis System (Invitrogen, Carlsbad, CA) following the manufacturer's procedure. Primers for Wnt1, CHI3L1, integrin β1, AQP1, KLF4, NANOG, SOX2 and OCT3/4 were designed using the integrated DNA Technologies website (www.idtdna.com). Primer sequences are listed in Table 3.2. Ribosomal (18S) RNA was used as a housekeeping gene. DNA Engine quantitative RT-PCR machine and RT^2 SYBR Green qPCR mastermixes (Qiagen, Germantown, MD) were used for real-time PCR according to the manufacturer's protocol. The threshold cycle (C_t) was determined for each sample and used to quantify the relative mRNA levels standardized to the measured iPSC counts.

TABLE 3.2. Primer Sequences Used in Quantitative RT-PCR

Gene Name	DNA Sequence
AQP1	Forward: CTCCTGGCTATTGACTACACTG Reverse: GAAGTCGTAGATGAGTACAGCC
CHI3L1	Forward: TGTCCAAGCAGTCAAGAGAAG Reverse: CACATGAGAATTCCTGGGAGAG
Integrin α3	Forward: CATGGAGAGAAGCTGGGACTG Reverse: GGTTGTAAGCAAAGCACAGC
KLF4	Forward: ACCTACACAAAGAGTTCCCATC Reverse: TGTGTTTACGGTAGTGCCTG
NANOG	Forward: GAAATACCTCAGCCTCCAGC Reverse: GCGTCACACCATTGCTATTC
OCT3/4	Forward: GTGAAGCTGGAGAAGGAGAAG Reverse: TGGTTCGCTTTCTCTTTCGG
SOX2	Forward: TCTTCGCCTGATTTTCCTCG Reverse: GTTCTCCTGGGCCATCTTG
Wnt1	Forward: CTGGCTGGGTTTCTGCTACGC Reverse: TATCAGACGCCGCTGTTTGCGGC
18S Ribosomal RNA	Forward: TGTCCTCATGCCTTGGTGCT Reverse: AGAGATCAAGGGACTTGCTT

3.3.8 Saponin Treatment of Trabecular Meshwork in Perfused Human Anterior Segment Culture.

For perfusion culture, human anterior segments were prepared as described previously [176, 177, 178, 179, 180, 181, and 182] and perfused at 1x constant pressure (8.8 mm Hg) to generate an average flow rate of 1-7 µL/min. Perfusion medium was the same as TM culture medium (detailed above), except that it was serum-free. Paired human donor eyes were acquired from Lions Eye Bank of Oregon (Portland, OR). Human donor tissue protocols were approved by the Oregon Health and Science University Institutional Review Board and were conducted in accordance with the tenets of the Declaration of Helsinki.

Saponin was diluted in perfusion medium to 0.01% and injected into the perfusion chamber after human eyes were stabilized in flow for 48 hours. The flow was stopped during saponin treatment for 7 minutes, then the anterior eye segments were washed thoroughly with perfusion medium. The flow was resumed for 24 hours at 1x to stabilize the baseline, and then the perfusion pressure was doubled (2x) to trigger the IOP homeostatic response. The eyes were exposed to 2x pressure for 5 days. During perfusion, the flow through the TM was measured gravimetrically.

3.3.9 Transplantation of differentiated TM-like iPSCs, EB 5% AH, DF and/or HUVEC cells into saponin-denuded human anterior segments.

TM-like iPSCs, DF and HUVEC cells grown on plates were harvested by trypsin treatment. Cells were rinsed thoroughly and labeled with 3 µL of Qtracker 655 Cell Labeling Kit (Life Technologies, Eugene, OR) prior to transplantation. For labeling, cells were incubated with Qtracker 655 for an hour at 37°C, and then washed thoroughly to eliminate residual particles. The labeled cells were visualized on the confocal

microscope to verify their uptake of Qtracker 655 nanoparticles. Human eyes were placed in the flow chamber for 48 hours, and then treated with saponin. After 24 hours, the pressure was increased to 2x for 48 hours.

Subsequently, cellular transplant with the labeled TM cells was performed using 300,000 cells. The replacement cells were injected into the flow chamber which was in an upside-down position to let the cells home to the TM tissue. Following cell injection, the anterior segments were exposed to 0.5x pressure for 2 hours followed by an overnight incubation at 37°C with the flow stopped. On the subsequent day, the flow was resumed for 24 hours at 1x pressure, then raised to 2x pressure for 96 hours. During the steps preceding and subsequent to the pressure challenge, the flow rate was measured gravimetrically.

3.3.10 Phagocytosis assay in TM-like iPSCs, iPSCs and HTM cells.

Zymosan bioparticles and opsonizing reagent were purchased from (Invitrogen/Molecular Probes). All cell types (TM-like iPSCs, iPS and HTM cells) were cultured on chamber slides until they were 60% confluent. Zymosan particles were opsonized according to the manufacturer's instructions and then incubated with each of the above mentioned cell types for an hour at 37°C. The cells were then fixed in 4% paraformaldehyde, perforated with 0.3% triton X100 and stained for LAMP1, a lysosomal marker (1:500 dilution) to establish internalization. Using confocal microscopy, the co-localization of zymosan particles with LAMP1 antibody in Q-dot labeled cells was visualized.

3.4 Results

3.4.1 EBs differentiate to become morphologically similar to human TM cells.

The EBs that were developed from iPSCs became differentiated or more "TM-like" in appearance in the presence of ECM and CM from cultured primary porcine TM cells. Various other treatment combinations, including aqueous humor (AH) separately or with other components, were less effective or even ineffectual. These TM-like iPSCs resembled human TM cells (Fig. 3.1), which have a relatively distinctive morphology.

3.4.2 TM-like iPSCs express TM cell markers and have diminished expression of iPSC markers.

To assess the differentiation of EBs to TM-like cells at a molecular level, we compared expression of several TM cell markers in TM-like iPSCs, iPSCs and human TM (HTM) cells. Although there is no specific cell marker for TM cells, CHI3L1, Wnt1, integrin α3 and AQP1 are expressed by TM but are not expressed or only lightly expressed by iPSCs. The TM-like iPSC expression pattern resembled HTM cells much more than iPSCs. This was assessed by confocal immunohistochemistry (Fig. 3.2), Western immunoblot (Fig. 3.3) and quantitative RT-PCR (Fig. 3.4). Although the expression patterns are not absolutely present or absent, their expression similarities are strong and clear. On the other hand, TM-like iPSCs exhibited reduced expression of several iPS cell markers, such as NANOG, SOX2, OCT3/4 and KLF4 compared to undifferentiated iPSCs (Figs. 3.2, 3.3 and 3.4). Here also, the expression patterns in TM-like iPSCs and HTM cells are severely diminished from iPSCs, but clearly do distinguish the iPS pattern from either HTM or TM-like iPSCs.

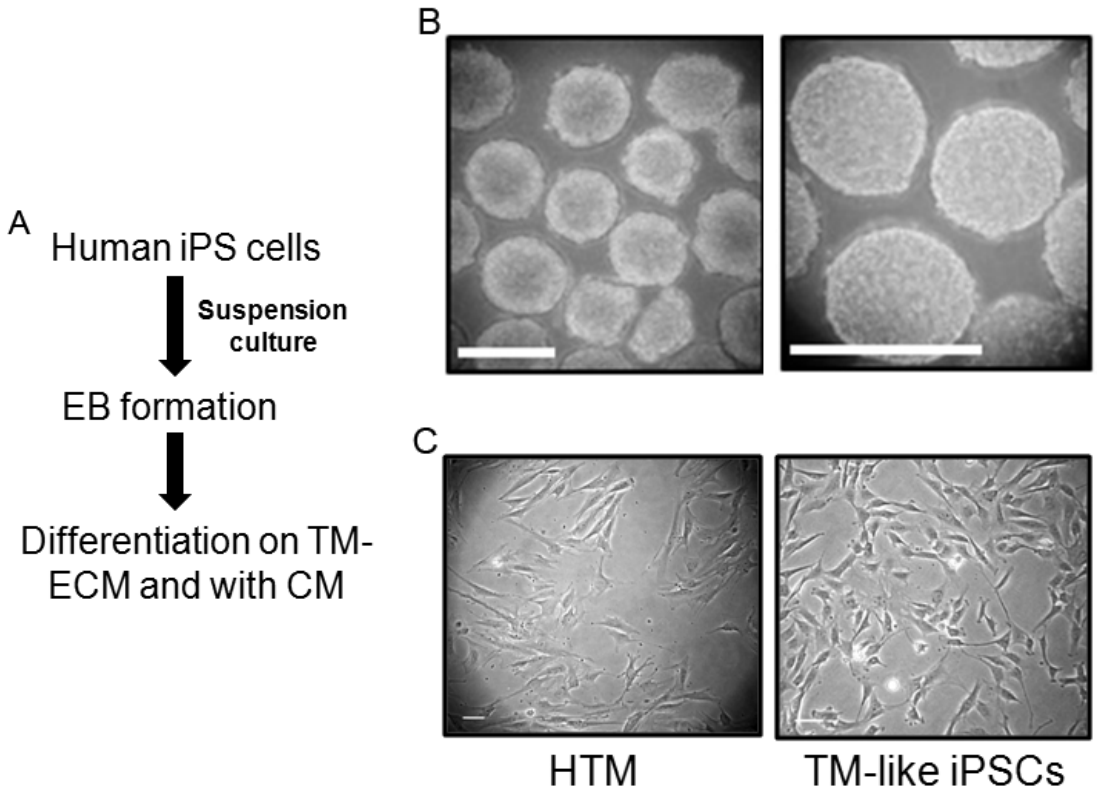

Figure 3.1: Embryoid body (EB) formation and differentiation into TM-like cells or TM-like iPSCs. (A) An experimental scheme of the EB formation and differentiation into TM-like cells. **(B)** EBs were generated using Aggrewell plates and images show EBs after they attached to the ECM of the TM. Scale bars are 50 μm. In **(C),** EBs were differentiated on TM-ECM and in the presence of DiffMedium. The TM-like iPSCs show a similar morphology to human TM cells (HTM). Scale bars represent 100 μm.

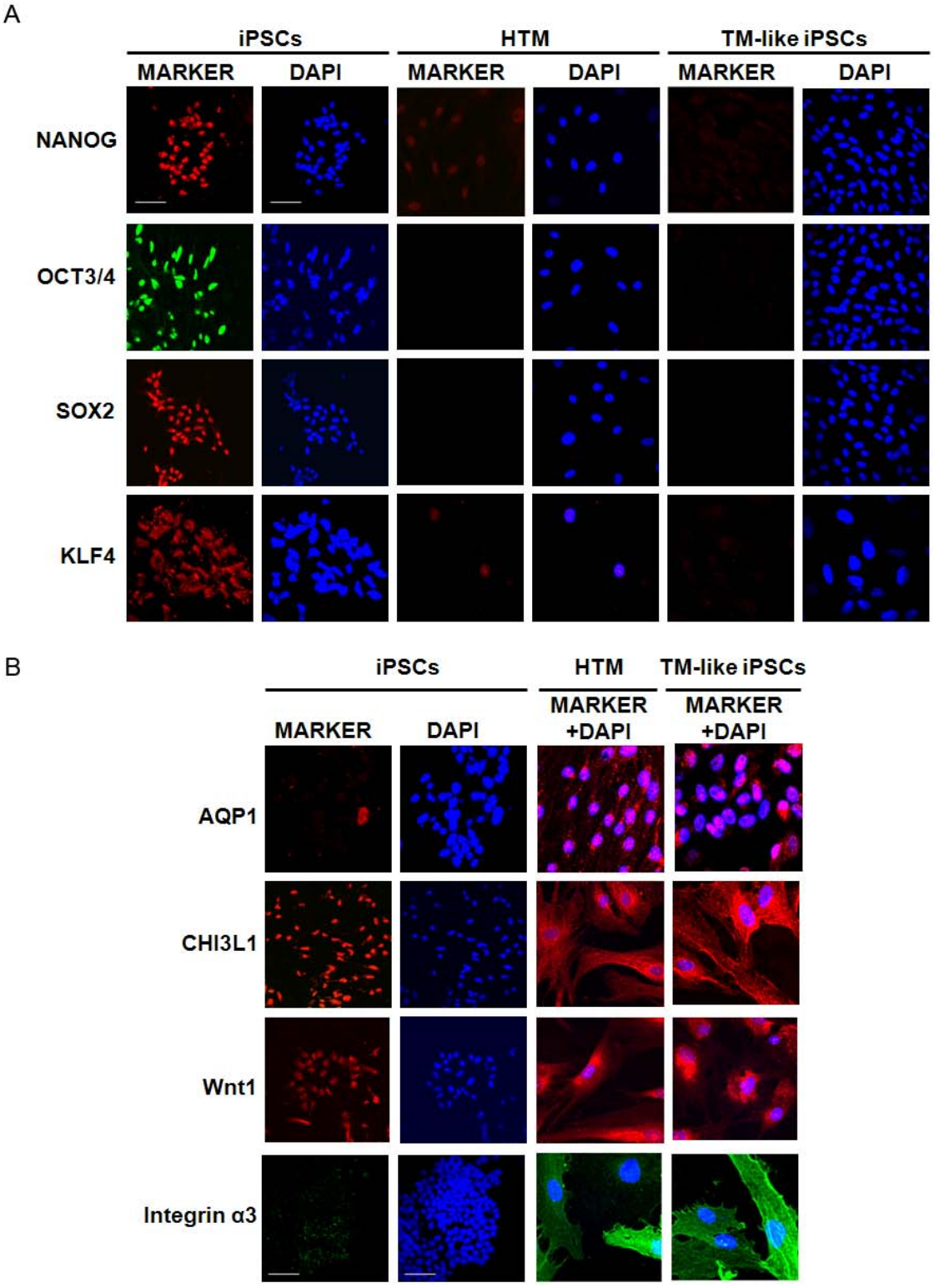
A
iPSCs
HTM
TM-like iPSCs
MARKER
DAPI
MARKER
DAPI
MARKER
DAPI
NANOG
OCT3/4
SOX2
KLF4
B
iPSCs
HTM
TM-like iPSCs
MARKER
DAPI
MARKER +DAPI
MARKER +DAPI
AQP1
CHI3L1
Wnt1
Integrin α3

Figure 3.2: TM-like iPSCs express TM markers and inhibit iPS marker expression. Human TM cells, human iPS cells and TM-like iPSCs were grown on chamber slides then fixed by 4% para-formaldehyde. The fixed cells were immunostained for **(A)** several iPS cell markers and **(B)** several TM cell markers. Marker columns show only the marker and DAPI columns show only the blue nuclei channel, while two of the columns show the merge of the two channels. Images were taken with confocal microscopy. Scale bar represent 50 μm.

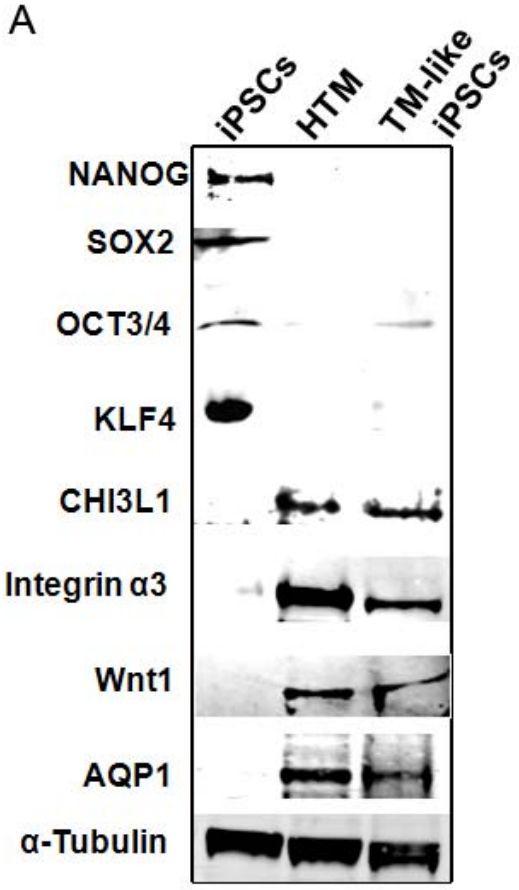
A
iPSCs
HTM
TM-like iPSCs
NANOG
SOX2
OCT3/4
KLF4
CHI3L1
Integrin α3
Wnt1
AQP1
α-Tubulin

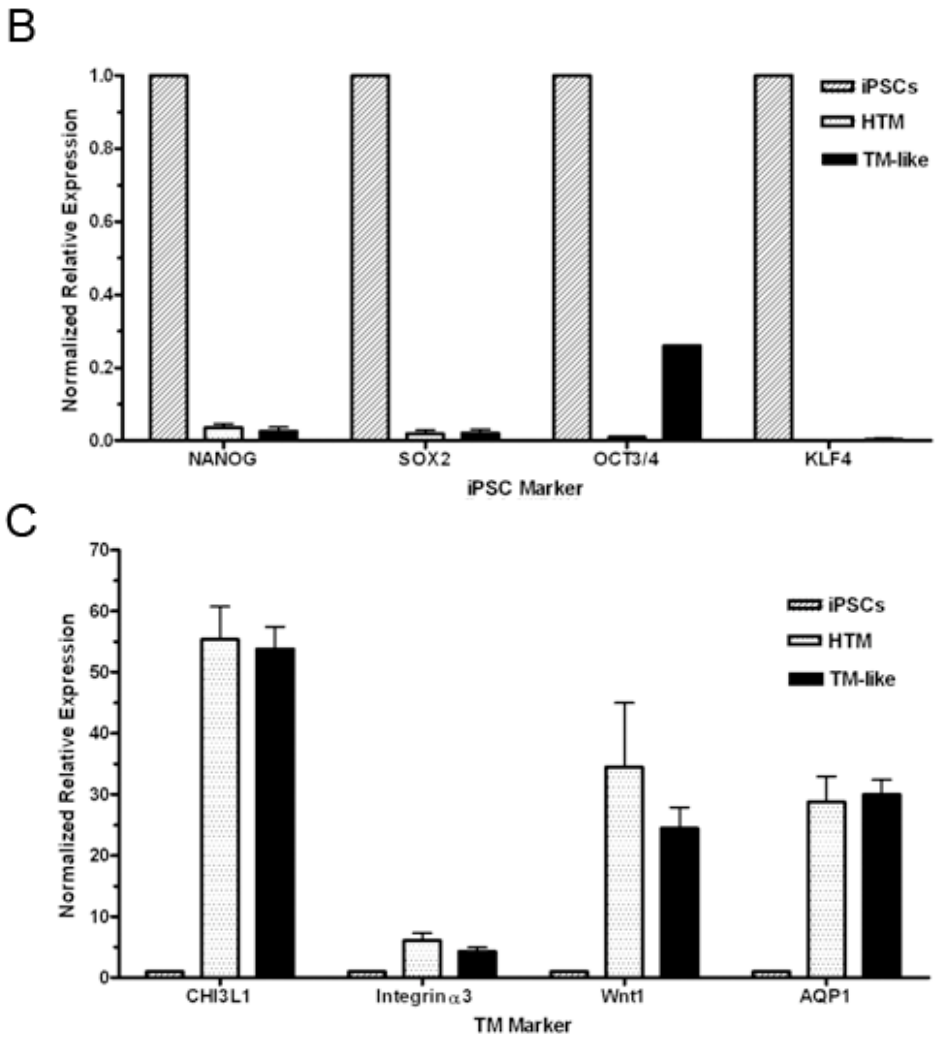

Figure 3.3: TM-like iPSCs express TM markers and diminish the expression of iPS markers. Human TM cells, human iPS cells and TM-like iPSCs were grown on 6 well plates and the crude cell lysate was collected. **(A)** The disappearance of iPS cell markers and the appearance of TM cell markers were confirmed by Western immunoblotting. α-Tubulin was used as a loading control. **(B) and (C)** Quantification of the bands in **(A)** was done using ImageJ software and relative amounts to those quantified in iPSCs were normalized to α-Tubulin to compensate for the loading differences. Error bars represent the standard error of the mean and n=3.

A

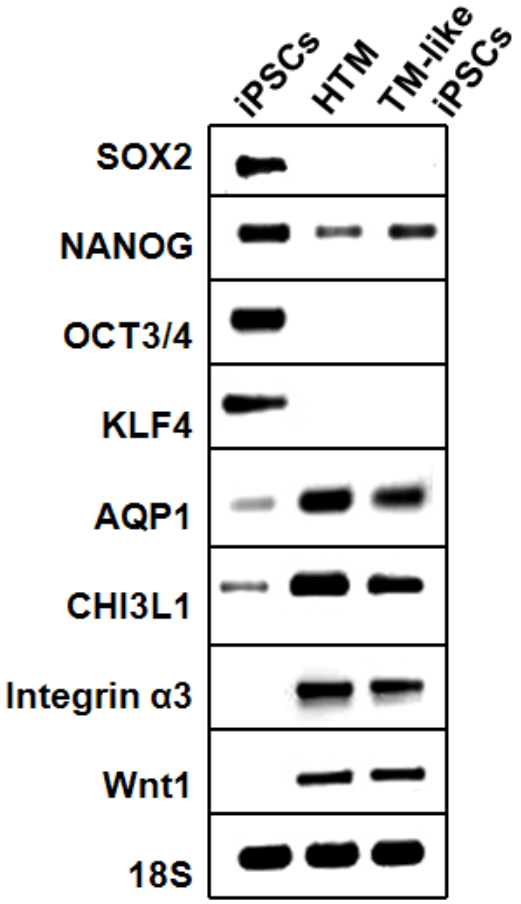
iPSCs
HTM
TM-like iPSCs
SOX2
NANOG
OCT3/4
KLF4
AQP1
CHI3L1
Integrin α3
Wnt1
18S

B

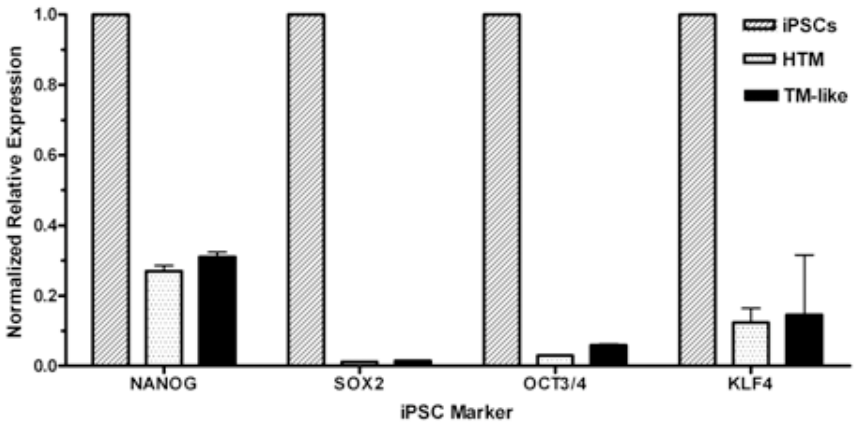

C

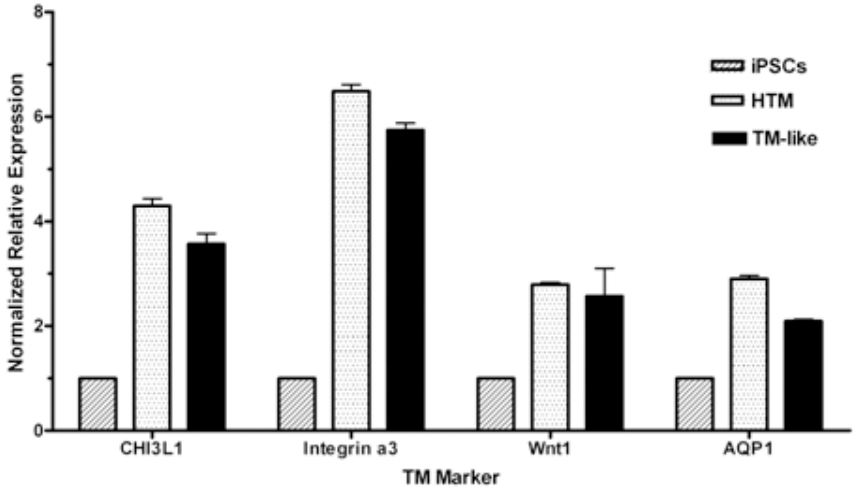

Figure 3.4: PCR mRNA marker levels of TM and iPS in TM-like iPSCs were **compared to mRNA levels in iPS and HTM**. RNA was extracted from TM, iPS and TM-like iPSC cells, then reverse-transcribed into cDNA. **(A)** TM-like iPSCs express mRNAs like HTM cells but inhibited the expression of RNAs typically expressed by iPS cells. The RT-PCR reactions were run in triplicates for each gene and the average normalized relative expression of each is represented by the columns in **(B) and (C).** Error bars represent the standard error of the mean.

3.4.3 TM-like iPSCs attached to the TM beams and integrated into the TM after transplantation into depleted anterior segments.

The TM-like iPSCs were transplanted into the partially saponin-denuded human anterior segments to replace lost TM cells. Using the cell depletion model that we developed earlier (*manuscript in review*), treatment of perfused human anterior segments with saponin at 0.01% concentration for 7 minutes depleted TM cell density by approximately 30%. This simulates the average cellular loss detected in glaucomatous eyes [98]. This cellular loss also severely compromises the ability of these anterior segments to produce an IOP homeostatic response (paper in chapter 2) When we added 300,000 QDot-labeled TM-like iPSCs, many attached and became integrated into the TM. Frontal sections (Fig. 3.5B, 3.5C, S3.2) show that the cells integrated throughout the TM, including deep within the juxtacanalicular region near Schlemm's canal, where the outflow resistance is thought to reside [98, 198].

3.4.4 Transplanted TM-like iPSCs can rescue the IOP homeostatic response.

Since the whole objective of TM cell replacement is to restore IOP regulation, we evaluated whether the transplanted TM-like iPSCs were able to rescue the regulatory IOP homeostatic response. In the saponin model (paper in chapter 2) loss of approximately 30% of TM cells is sufficient to compromise the ability of the outflow pathway to trigger the IOP homeostatic response. The IOP homeostatic response is defined here as the ability of the outflow pathway to sense a doubling of perfusion pressure and to respond over several days by reducing the outflow resistance in an attempt to restore IOP to normal [57, 98, 207].

After flow rates had stabilized at 1x perfusion pressure, saponin was added (0.01% for 7 minutes) and then washed out. Flow was resumed at 1x pressure for 24

hours and no change in basal flow rate was observed (Fig 3.5D). When subjected to a 2x pressure challenge, the flow rate doubled immediately, but no homeostatic resistance change was achieved by approximately 50 hours. In a normal perfused anterior segment, the outflow resistance would have been gradually reduced in response to this pressure challenge by the TM cells over this time, allowing a gradual increase in the flow rate. Next, 300,000 TM-like iPSCs were flowed in at 0.5x perfusion pressure and then the flow was stopped to allow them to attach to the denuded portions of the outflow pathway. Perfusion was resumed at 1x perfusion pressure. After baseline stabilization, the system was then subjected to a second 2x pressure challenge (at approximately 100 hours; Fig. 3.5D). This time, the repopulated outflow pathway was able to mount an IOP homeostatic response by slowly reducing the outflow resistance. The flow rate then gradually increased from 100 hours to 200 hours (Fig. 3.5D).

Transplantation of dermal fibroblasts did not restore the IOP homeostatic response (Fig. 3.5E, 3.S3) nor did the addition of EBs that had been differentiated with 5% AH alone (Fig. 3.5F). Those cells no longer expressed the pluripotency factors, but did not express TM markers in a similar pattern and amount to TM cells (see supplemental data Fig. 3.S1). Since the trabecular beams are covered with endothelial cells in the TM, HUVEC cells were transplanted. HUVEC cells also did not restore the IOP homeostatic response (Fig 3.5G). Additionally, a control, saponin-treated but without cells transplanted, was also included in this set of experiments (Fig. 3.5H), and did not restore the IOP homeostatic response either.

A

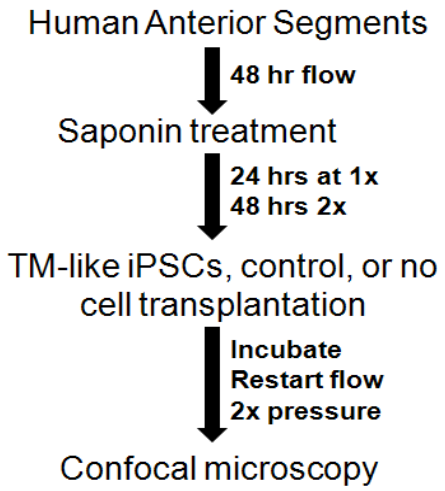
Human Anterior Segments
48 hr flow
Saponin treatment
24 hrs at 1x
48 hrs 2x
TM-like iPSCs, control, or no cell transplantation
Incubate
Restart flow
2x pressure
Confocal microscopy

B

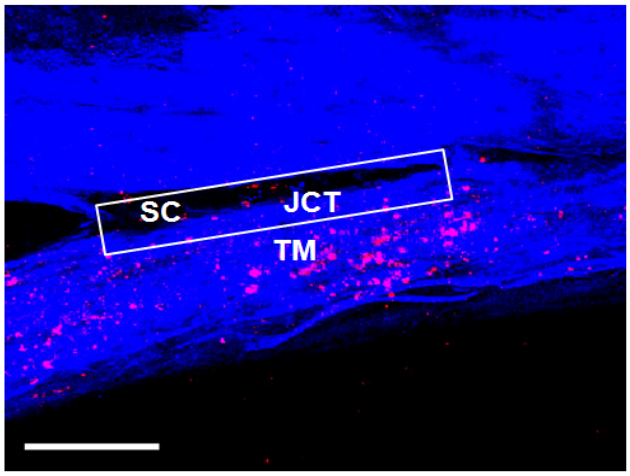
SC
JCT
TM

C

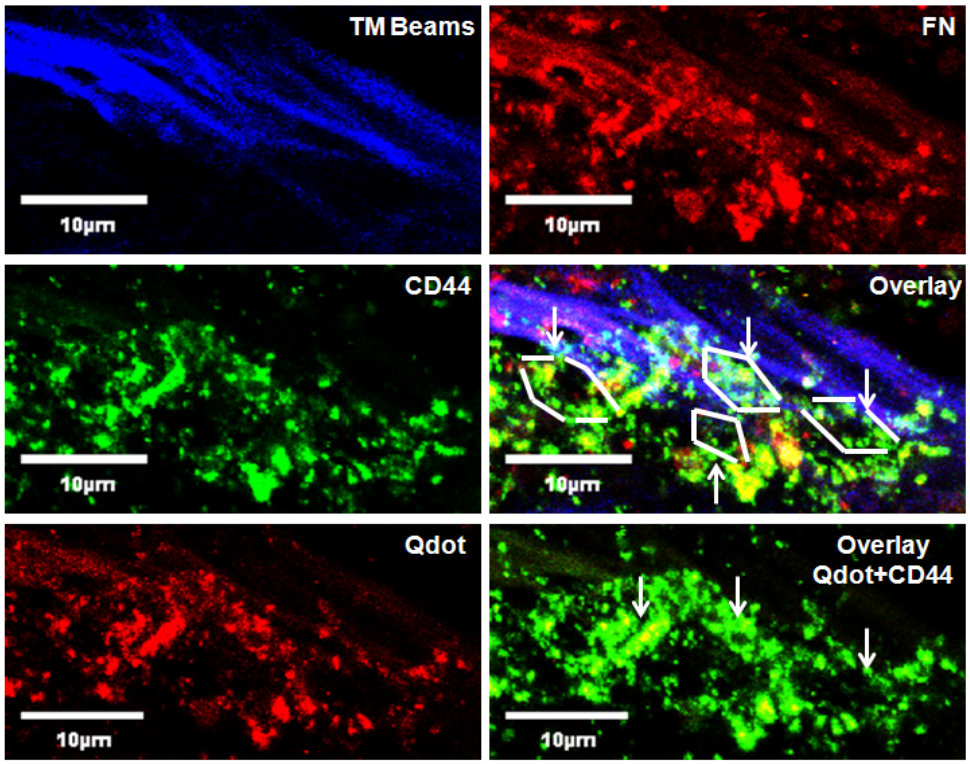
TM Beams
FN
CD44
Overlay
Qdot
Overlay
Qdot+CD44
10µm

D

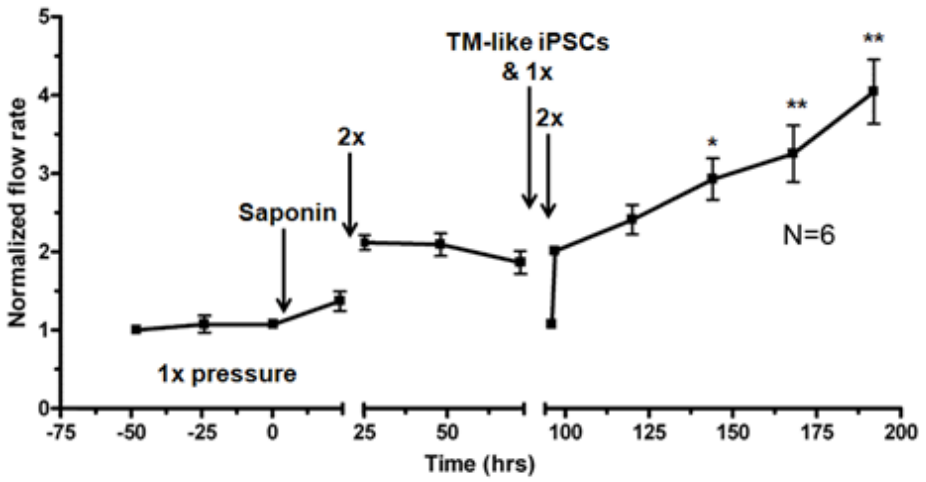
TM-like iPSCs
& 1x
2x
2x
Saponin
1x pressure
N=6
Normalized flow rate
Time (hrs)

E

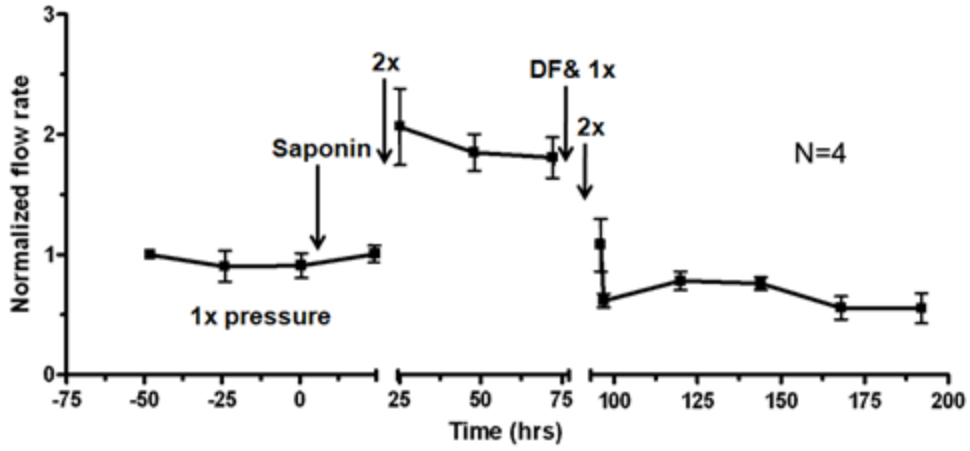
2x
DF& 1x
2x
Saponin
1x pressure
N=4
Normalized flow rate
Time (hrs)

F

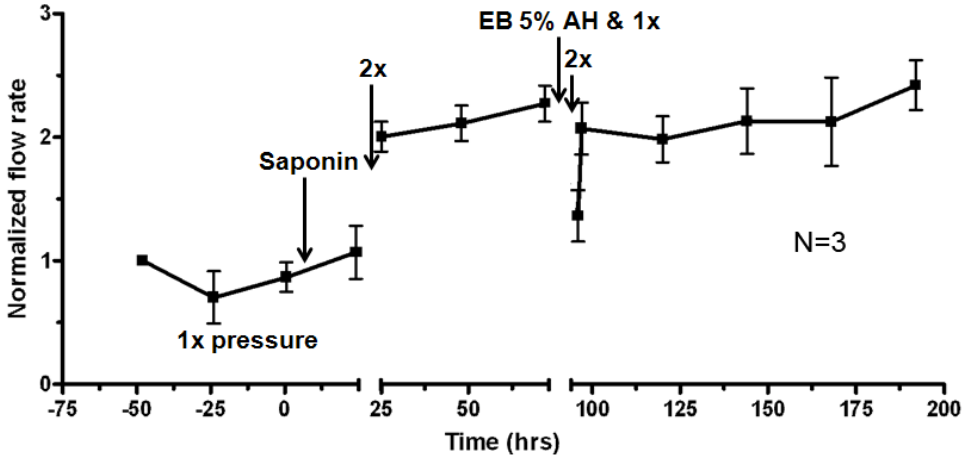
EB 5% AH & 1x
2x
2x
Saponin
1x pressure
N=3
Normalized flow rate
Time (hrs)

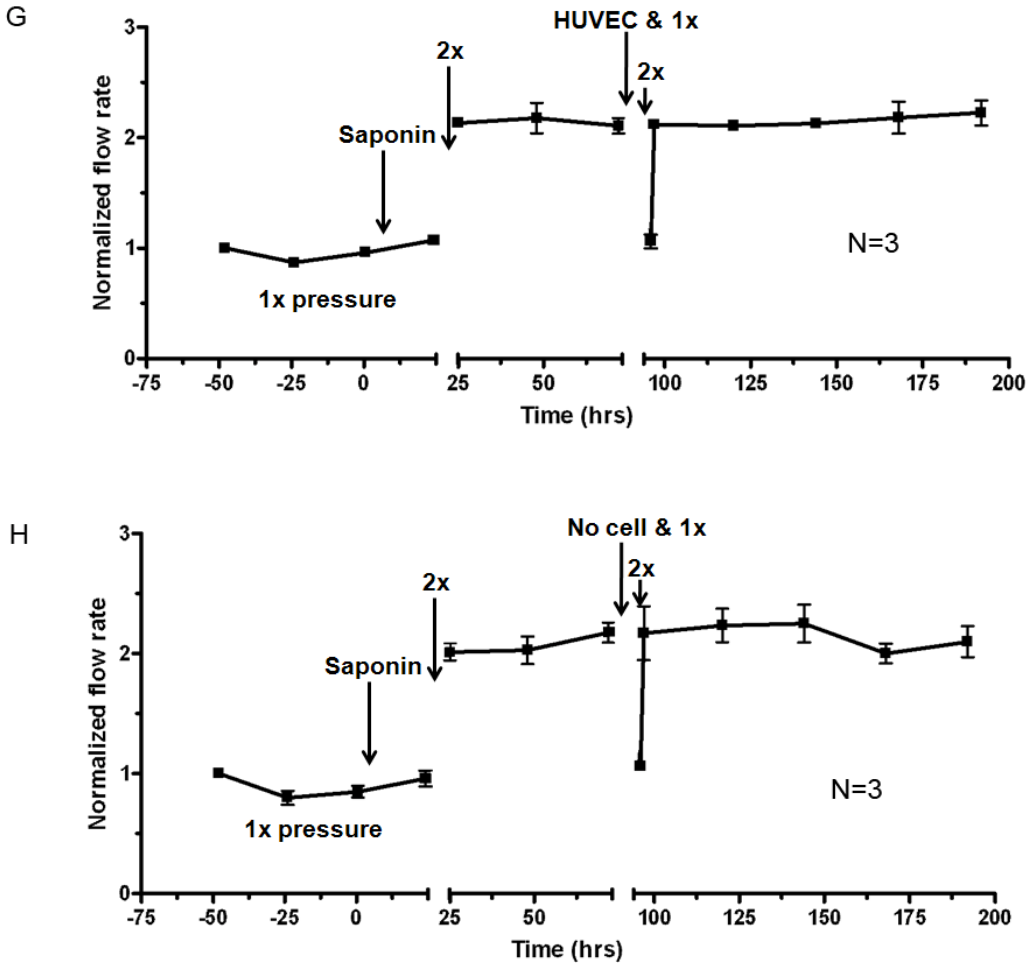

Figure 3.5: replacement TM-like iPSCs integrate into the TM and restore the IOP homeostatic response. (A) The experimental scheme to test the integration of TM-like iPSCs into TM structure and the restoration of IOP homeostasis. **(B)** The transplanted TM-like iPSCs integrated into the TM beam structure. Frontal sections were generated after nanoparticle (Q-dot) labeled TM-like iPSCs were transplanted into the TM. The replacement cells, labeled by red nanoparticles, were detected in all regions of the TM even reaching the innermost JCT region and to SC (as shown in the white square). Scale bar represents 100 μm. **(C)** The transplanted TM-like cells labeled with Q-dots were stained for CD44 to mark their outline (green, dashed line) and fibronectin (FN)

(red) was stained as a component of the ECM that covers the TM beams. The TM-like iPS cells (green) integrated into the TM tissue and attached to the TM beam surface (blue autofluorecence). In **(C)** scale bar represent 10 μm**. (D)** Human eyes were perfused for 48 hrs under normal pressure (1x) followed by saponin treatment. After saponin was rinsed out, the flow was restarted at 1x for 24 hrs then at 2x for 48hrs to test if cell density triggers the IOP homeostatic response. Afterwards, the TM-like iPSCs were transplanted and pushed into the TM at 0.5x for 2 hours, and then the flow was stopped and the TM-like iPSCs were incubated overnight with the flow chamber of the model system in an upside-down position. The flow was resumed the next day at 1x pressure for 24hrs then increased to 2x pressure for 96hrs. Transplanted TM-like iPSCs restored the IOP homeostatic response by increasing the flow rate and decreasing the resistance with time after the pressure was doubled for several days. In contrast, **(E)** Dermal fibroblasts did not restore the IOP homeostatic response and plugged the pathway between TM beams so that even at the basic rate at 1x pressure for 24 hrs, the fluid cannot pass. **(F)** EBs that were differentiated in the presence of 5% AH only, without CM or ECM, were transplanted as a control but they cannot restore the homeostatic response. These cells stopped the expression of pluripotency markers, but they did not express TM markers in comparable amounts and patterns to TM cells. **(G)** Since TM cells are endothelial-like cells, HUVEC cells were transplanted as a control for this experiment. As observed with the other cell types tested, they also did not restore the IOP homestatic response. **(H)** In this set of anterior segments, no cells were transplanted to the TM, and the IOP homeostatic response was not restored. Error bars represent the standard error of the mean.

3.4.5 TM-like iPSCs can perform phagocytosis.

TM cells are very active in phagocytosis of cellular debris that is present in the AH before it reaches the juxtacanalicular region which is very susceptible to clogging [191]. However, iPSCs are ineffectual at phagocytosis. Hence, we examined whether or not the differentiated TM-like cells had acquired the ability to perform phagocytosis in a manner similar to endogenous TM cells. TM-like iPSCs were cultured with zymosan particles and stained afterwards for the lyosomal marker LAMP1. The co-localization of the particles with LAMP1 indicates their engulfment into the lysosomes of both HTM and TM-like iPSCs but not iPS cells (Fig. 3.6A-B).

A

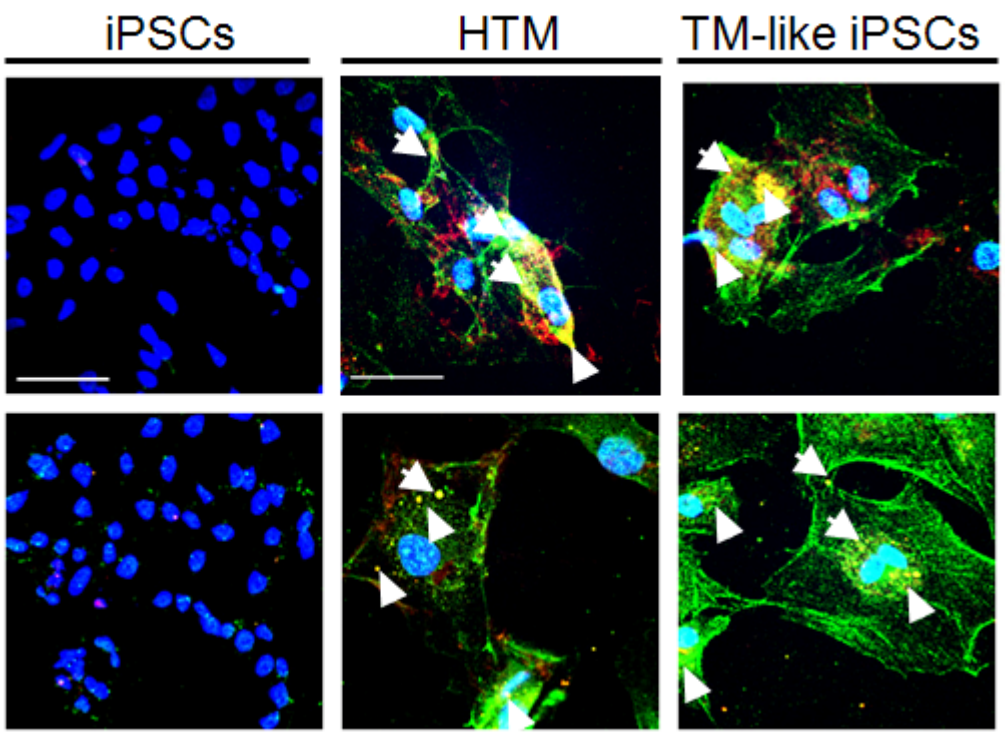
iPSCs
HTM
TM-like iPSCs

B

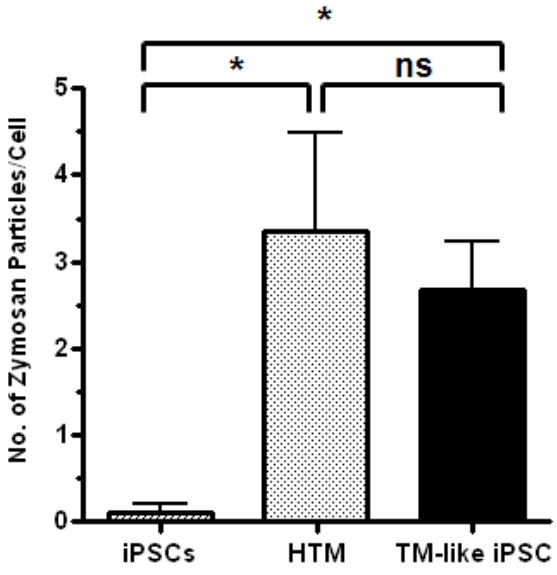
*
*
ns
No. of Zymosan Particles/Cell
0
1
2
3
4
5
iPSCs
HTM
TM-like iPSC

Figure 3.6: TM-like iPSCs can perform phagocytosis. **(A)** TM-like iPSCs, HTM and iPSCs cultured on chamber slides were incubated with zymosan particles (green) for an hour. They were then fixed and stained with LAMP1 lysosomal marker (red). The co-localization of zymosan particles with LAMP1 (yellow spots) indicates the phagocytosis of the particles into the lysosomes (white arrow heads). Both HTM and TM-like iPSCs phagocytosed the particles but iPSCs did not. Nuclei were demarcated by DAPI staining (blue). Scale bar represents 100 μm. **(B)** The number of zymosan particles that co-localize with LAMP1 was counted and the total number was divided by total number of cells in the field. P value is less than 0.05 and ns = not significant.

3.5 Discussion

The purpose of these studies was to generate and transplant TM-like cells that can perform the two major functions of the TM, phagocytosis of debris [1, 3, 4, 42, 57, 67, 94, 156, and 198] and IOP homeostasis [43, 202]. The iPSCs in this study were derived from de-differentiated dermal fibroblasts and manipulated by suspension to EBs, which subsequently were re-differentiated to TM-like cells. Although the reprogramming to a different cell type is often done by using specific, often intricate protocols for various germ layers, the TM is thought to develop embryologically from both ectoderm (neural crest origin) and mesodermal (paraxial mesenchyme) components, which complicates matters [55, 57, 199, 200, and 201]. We hypothesized that separate elements of the TM niche might contribute to reprogramming iPSCs to a TM cell type. We used combinations of TM cell CM and growth medium with the cells maintained on TM cell ECM in culture. We found a combination that effectively differentiate EBs to TM-like iPSCs *(manuscript in preparation*) and used these conditions herein.

Although there are no specific biomarkers for TM, we established a panel of markers, based upon our own comparisons with iPSCs and the literature that provided easily discernable differences and similarities between iPSCs, TM, and differentiated TM-like iPSCs [185, 186, 203, 204, 205, and 206]. This study shows that iPSCs can be induced to differentiate into TM-like cells presenting a similar morphology, and expressing the cell markers typically noted in normal TM cells, while no longer expressing typical iPSC markers. In addition, we evaluated the ability of these cell types to phagocytose debris, an important TM cell function necessary to maintain a pathway for AH outflow. TM cells and TM-like iPSCs but not undifferentiated iPSCs were able to phagocytose small zymosan particles (Fig. 3.6) [75, 77, 156, 180, and 181]. The co-

localization of zymosan with a lysosomal marker, LAMP1, on confocal microscopy showed that both TM-like iPSCs and HTM cells had internalized the zymosan particles, but that iPSCs could not.

To demonstrate the clinical potential for future transplantation into human eyes, we used a model for cellular depletion that we had previously developed, the saponin model, (*paper in chapter 2*). This experimental model simulates the cell loss detected in POAG at a more standardized level than that obtained from donor glaucomatous eyes. Since these eyes are in different stages of the disease and tissue damage and have been exposed to diverse medical therapies, the use of our saponin model in normal eyes to mimic cellular loss in glaucoma avoids many of these disadvantages. We then transplanted the labeled TM-like iPSCs into perfused anterior segment organ culture for functional testing. A transplanted stem cell to correct a disease is only valuable if it can revitalize the structure or organ by causing a return to a more normal, healthier state; in other words, it must restore normal functioning. Figure 3.5A shows the sequence of events in determining if the TM-like iPSCs could restore function to TM explants that had been partially denuded and compromised by saponin. The labeled transplanted cells were found to attach tightly at all levels of TM, including the proposed sites of the resistance to outflow, the juxtacanalicular region and the inner wall of Schlemm's canal. These TM-like cells were not dislodged by flow (Fig. 3.5B). When we used our saponin model to partially denude the normal explants of TM cells and then doubled the pressure (Fig. 3.5C arrow-2x), the flow rate doubled, but did not increase over time, showing that there was no IOP homeostasis. Upon adding TM-like iPSCs to these saponin treated explants, the system was again subjected to a 2x pressure increase. In this case, after the flow rate doubled immediately, it continued to increase slowly for 100 hours, showing

that the transplanted saponin treated anterior segment was able to decrease the resistance, producing an IOP homeostatic response. Several other types of cells were unable to restore the IOP homeostatic response.

Thus, these iPSCs differentiated into TM-like cells may hold the potential to restore normal IOP homeostatic and phagocytic function to glaucomatous eyes exhibiting reduced TM cellularity. That the iPSCs could be autologous, derived from the glaucoma patient, alleviates potential immunologic rejection concerns. Although glaucoma is caused by numerous genetic and probably environmental issues, the reduced cellularity is a common feature and restoration of TM cell function should ameliorate loss of IOP regulation in many cases.

3.6 Acknowledgments

The authors thank Ruth Phinney (Lions Vision Gift, Portland, Oregon) for facilitating the procurement of human donor eyes.

Supported by NIH grants EY021800 (MJK), EY003279 (TSA), EY008247 (TSA), and EY010572 (TSA), an unrestricted grant to the Casey Eye Institute from Research to Prevent Blindness, New York, New York, and the University of Jordan.

Disclosure: **D. W. Abu-Hassan**, None; **X. Li**, None; **E. Ryan**, None; **T.S. Acott**, None; **M.J. Kelley**, None

(This page was intentionally left blank)

Chapter 4

Conclusions and Future Directions

"Wisdom is the goal of the faithful, his wherever he finds it." -**Prophet Mohammad-peace be upon him.**

"Research is to see what everybody else has seen, and to think what nobody else has thought." -**Albert Szent**

"Somewhere, something incredible is waiting to be known."-**Carl Sagan**

"Research is what I'm doing when I don't know what I'm doing."- **Werner von Braun**

5.1 Overview

The major findings and investigations of this dissertation are (i) development of the saponin-induced partial denudation glaucoma model, (ii) experimental verification that reduced TM cellularity impacts outflow function, (iii) differentiation of iPS cells into TM-like cells, (iv) characterization of the differentiated TM-like cells, and (v) verification of the functionality of those cells. In the next sections of this chapter, a synopsis of the major findings and contributions is outlined along with some important aspects and directions for future research in this field.

5.2 Conclusions

Glaucoma is a leading cause of blindness especially in the elderly population. It affects millions of people worldwide. In the United States, the clinical management of glaucoma costs billions of dollars yearly. Nevertheless, with the available treatment options, glaucoma patients either have recurrence of disease, failure of treatment, the inconvenience due to daily medication schedules, or ocular deprivation of normal AH functional roles supporting eye health. The irreversible blindness that glaucoma causes is preventable if we can fix the pathological changes of the TM and retain its functionality.

Many studies investigate stem cells for treating glaucoma but they mainly target repairing the damage in the optic nerve or retina, the posterior structures in the eye. However, very few research groups utilize stem cells in the TM. The novelty of the studies performed in this thesis project lies behind investigating a preventive treatment strategy of glaucoma by using stem cells in the trabecular meshwork.

Before we began our proposed studies, we had to provide an appropriate model for cell loss in the TM as it is the main principle we rely on in our experiments. Most of

the cadaver human eyes available for research come from senior donors. Furthermore, cadaver eyes with glaucoma are scarce and even if available; they were exposed to different treatments and display various histopathological stages of the disease. As a result, glaucomatous eyes may behave differently in response to treatments.

The gradual loss of TM cells that perform critical roles in maintenance of IOP homeostasis and filter the AH may have serious implications. Although a cause-effect relationship between TM cell loss and the etiology of glaucoma has not been established, this substantial loss may have serious implications that affect IOP regulation. In the studies described in chapter 2, we circumvented the previously mentioned problems by developing the cellular depletion saponin model. In this model, saponin dosage was optimized to achieve a partial induction of death, simulating the partial cell loss detected in glaucoma. Our model provides a useful tool for transplantation studies since the saponin treatment partially induces death of TM cells. Moreover, it enables the use of cadaver human eyes instead of other animal models that differ in their anatomical and physiological features from human eyes. In addition to the effect of saponin on cells, it may affect the structural integrity and the architectural organization of TM. Consequently, implementation of this saponin model can help determine the potential role structure plays in preservation of normal and healthy TM function. However, our model has limitations that were previously discussed in Chapter 2. The feasibility of using cadaver cell transplantation as an option was evaluated prior to pursuing experiments with stem cells (Chapter 2). Clinically, however, using human cadaver TM cells as replacement cells is impractical as the potential immunorejection consequences, overall health, and senescence of extracted cadaver cells is unknown.

The studies described in this manuscript were focused on the differentiation of iPSCs into TM-like cells. The iPSCs were induced to differentiate into TM-like cells by the presence of an extracellular matrix of porcine TM cells and conditioned media from human TM cell culture. Since the exact mechanism and molecular components of TM cell differentiation remain unknown, we proposed that the ECM and CM would contain the necessary and essential factors to signal and direct the differentiation of iPSCs into TM-like cells. We did not co-culture iPSCs with TM cells to avoid the necessary separation steps later on since TM cells do not have specific markers and labeling of one cell type to distinguish it from the other does not last long enough to finish experiments. Although co-culture of iPSCs with TM cells would have been used, if necessary, CM was effective so it was not utilized. We also excluded aqueous humor from being a major contribution for differentiation as it begins circulating through the TM tissue after it has already developed. In addition, neither AH nor co-culture is optimum from a logistics perspective. See future directions section of this chapter for more details about studying the differentiation process of TM cells.

The studies discussed in the final section of this manuscript have investigated replacing the lost cells in the TM of glaucomatous eyes by TM-like cells derived from iPSCs. In addition, the two major functional roles that the TM cells perform were replicated by the transplanted TM-like cells.

5.3 Future Directions

Our initial feasibility investigations assessed the future potential of using patient-specific iPSCs as a replacement for dead or damaged TM cells in glaucomatous eyes. Further investigation and fine-tuning of stem cell transplantation as a prospective treatment strategy remains to be performed. Determining the dosage or the transplanted cell number should be investigated for optimal clinical results. Comprehensive examination of the longevity and vitality of transplanted cells *in vivo* and the frequency of cell injection are also essential. In fact, tumor formation after TM-like cell transplantation has to be tested in the available glaucoma animal models *in vivo*, prior to clinical trials.

The differentiation of the ocular drainage structures, including the TM and SC, is not completely understood. Identification of the specific factor/s in the conditioned media that is/are necessary for efficient differentiation is one of our long-term goals. We will fractionate the conditioned media into several fractions using size exclusion chromatography. Each fraction will be used in conjunction with the TM-ECM to drive differentiation of iPSCs. The resulting cells will be characterized and compared to human TM cells. The expression of iPSC as well as TM markers will be compared and quantified in each cell type. Functionally, the different resulting cells will be transplanted individually into saponin-denuded human eyes and their ability to restore the homeostatic response when they are challenged with high pressure will be examined. To test the other essential function of the TM cells, phagocytosis, each cell type will be incubated with zymosan particles and then the co-localization of the particles with Lamp1 lysosomal marker will be examined by confocal microscopy. After we determine the fraction that contains the necessary factor/s for differentiation, indicated by inducing TM differentiation, we will analyze its content using mass spectrometry. We will then add

the potential candidate/s to the differentiation media to verify the necessity of this factor for driving differentiation properly.

Since our former experiments showed that ECM is essential for TM cell differentiation, we will determine which component/s is/are the driving factor/s. We will coat differentiation plates with one or more ECM component/s and differentiate the iPSCs on them in the presence of conditioned media. ECM constituents such as fibronectin, laminin, collagen I, III and IV, tenascin, vitronectin, versican, syndecan, hyaluronic acid or hyaluronan, chondroitin, dermatan sulfate, keratan sulfate and heparan sulfate will be used individually and in combinations to coat differentiation plates.

TM cells respond to changes in pressure by remodeling the ECM and inducing expression of some genes to modify resistance and allow higher flow rate. We will investigate the mechanism by which the TM-like iPSCs can restore the homeostatic response and bring the IOP down to normal values. We will stretch the TM-like iPSCs for 24, 48 and 72 hrs, then perform immunohistochemistry and Western blotting to check the expression of certain proteins such as, versican, integrins, collagens, TGF-β, etc. In addition, the mRNA levels of the previous proteins will be measured by real time PCR. We will determine whether TM-like iPSCs simulate the action of TM cells.

Studies discussed in this manuscript have investigated the novel idea of replacing the lost cells in glaucomatous eyes by iPSCs. However, other cell types might replace TM cells as well, such as mesenchymal stem cells. Although they are a reasonable autologous source for stem cells, the surgical procedure to attain them is relatively invasive especially in aged individuals. In addition, they are multipotent with a restricted guided fate. Preliminary data from our lab suggests they restore the IOP

homeostatic response when transplanted into anterior segment explants treated with saponin (data not shown). We also used cadaver human eyes to extract TM cells and transplant them back into saponin treated eyes. Nonetheless, the health of these cells is questionable since they are derived from aged, usually medically-compromised, individual eyes. Moreover, immune rejection is still possible.

In this manuscript, we established for the first time a connection between the loss of cellularity and disturbances of IOP homeostasis. Additionally, we developed the partial cell depletion saponin model that can be implemented in other studies such as determining the role that structural integrity plays in maintaining normal function of the TM. Moreover, we performed the initial studies that test the feasibility of stem cell differentiation and transplantation as a promising alternative and preventive treatment modality for POAG.

(This page was intentionally left blank)

References

1. Quigley HA, Broman AT. The number of people with glaucoma worldwide in 2010 and 2020. *Br. J. Ophthalmol*. 2006; 90(3):262–267.

2. Thylefors B and Negrel AD. The global impact of glaucoma. *Bull World Health Organ*. 1994; 72: 323-326.

3. Quigley HA. Number of people with glaucoma worldwide. *Br. J. Ophthalmol.* 1996; 80: 389-393.

4. Quigley HA. Open-angle glaucoma. *N Engl J Med.* 1993 Apr 15;328(15):1097-1106.

5. Quigley HA, Vitale S. Models of open-angle glaucoma prevalence and incidence in the United States. *Invest Ophthalmol Vis Sci.* 1997 Jan;38(1):83-91.

6. Traverso CE, Walt JG, Kelly SP, et al. Direct costs of glaucoma and severity of the disease: a multinational longterm study of resource utilization in Europe*. Br J Ophthalmol*. 2005; 89:1245–1249.

7. Kobelt-Nguyen G, Gerdtham UG, Alm A. Costs of treating primary open-angle glaucoma and ocular hypertension: a retrospective, observational two-year chart review of newly diagnosed patients in Sweden and the United States. *J Glaucoma*. 1998 Apr; 7(2):95-104.

8. Gould DB, Smith RS, and John SWM. Anterior segment development relevant to glaucoma. *Int. J. Dev. Biol.* 2004; 48: 000-000.

9. Sowden JC. Molecular and developmental mechanisms of anterior segment dysgenesis. *Eye*. 2007; 21: 1310–1318.

10. Hamanaka T, Bill A, Ichinohasama R. and Ishida T. Aspects of the development of Schlemm's canal. *Exp. Eye Res*. 1992; 55: 479-488.

11. Smith RS, Zabaleta A, Savinova OV and John SW. The mouse anterior chamber angle and trabecular meshwork develop without cell death. *BMC Dev Biol*. 2001; 1: 3.

12. Noden DM. An analysis of migratory behavior of avian cephalic neural crest cells. *Dev. Biol*. 1975; 42: 106-130.

13. Johnston MC, Noden DM, Hazelton RD, Coulombre JL and Coulombre AJ. Origins of avian ocular and periocular tissues. *Exp. Eye Res*. 1979; 29: 27-43.

14. Trainor PA, and Tam PP. Cranial paraxial mesoderm and neural crest cells of the mouse embryo: co-distribution in the craniofacial mesenchyme but distinct segregation in branchial arches. *Development.* 1995; 121: 2569-2582.

15. Wulle KG. The development of the productive and draining system of the aqueous humor in the human eye. *Adv. Ophthalmol*. 1972; 26, 296-355.

16. Tamm ER. The trabecular meshwork outflow pathways: Structural and functional aspects. *Exp. Eye Res*. 2009; 88: 648–655.

17. Reme C, and Epinay SL. Periods of development of the normal human chamber angle. *Doc. Ophthalmol*. 1981; 51:241-268.

18. Baulmann DC, Ohlmann A, Flugel-Koch C, Goswami S, Cvekl A and Tamm ER. Pax6 heterozygous eyes show defects in chamber angle differentiation that are associated with a wide spectrum of other anterior eye segment abnormalities. *Mech. Dev*. 2002; 118: 3-17.

19. Van Buskirk EM. Clinical Atlas of Glaucoma. Philadelphia: WB Saunders 1986.

20. Flocks M. The anatomy of the trabecular meshwork as seen in tangential section. *AMA Arch Ophthalmol*. 1956; 56(5): 708-718.

21. Cvekl A, and Tamm ER. Anterior eye development and ocular mesenchyme: new insights from mouse models and human diseases. *BioEssays*. 2004; 26:374–386.

22. Mao M, Hedberg-Buenz A, Koehn D, John S. W. M, and Anderson MG. Anterior Segment Dysgenesis and Early-Onset Glaucoma in nee Mice with Mutation of Sh3pxd2b. *Invest. Ophthalmol. Vis. Sci.*, April 2011; 52(5): 2679-2688.

23. Epstein D, Anderson P, 1984. The biochemistry of outflow mechanisms. In: Drance, S. (Ed.), Glaucoma: Applied Pharmacology in Medical Treatment. Grune & Stratton, New York, pp. 135-150.

24. Epstein DL, Rohen JW. Morphology of the trabecular meshwork and inner-wall endothelium after cationized ferritin perfusion in the monkey eye. *Invest. Ophthalmol. Vis. Sci.* 1991; 32: 160-171.

25. Ethier CR. The inner wall of Schlemm's canal. *Exp. Eye Res*. 2002; 74: 161-172.

26. Ethier CR, Kamm RD, et al. Calculations of flow resistance in the juxtacanalicular meshwork. *Invest. Ophthalmol. Vis. Sci.* 1986; 27: 1741-1750.

27. Ethier CR, Read AT, et al. Biomechanics of Schlemm's canal endothelial cells: influence on F-actin architecture. *Biophys. J.* 2004; 87: 2828-2837.

28. Fautsch MP, Johnson DH. Aqueous humor outflow: what do we know? Where will it lead us? *Invest. Ophthalmol. Vis. Sci.* 2006; 47: 4181-4187.

29. Ellingsen BA, Grant WM. Trabeculotomy and sinusotomy in enucleated human eyes. *Invest. Ophthalmol. Vis. Sci.* 1972; 11: 21-28.

30. Johnson M, Shapiro A, et al. Modulation of outflow resistance by the pores of the inner wall endothelium*. Invest. Ophthalmol. Vis. Sci*. 1992; 33: 1670-1675.

31. Sabanay I, Gabelt B, et al. H-7 effects on the structure and fluid conductance of monkey trabecular meshwork. *Arch. Ophthalmol*. 2000; 118: 955-962.

32. Rosenquist R, Epstein D, et al. Outflow resistance of enucleated human eyes at two different perfusion pressures and different extents of trabeculotomy. *Curr. Eye Res.* 1989; 8: 1233-1240.

33. Tawara A, Varner HH, Hollyfield JG. Distribution and characterization of sulfated proteoglycans in the human trabecular tissue. *Invest Ophthalmol Vis Sci*. 1989 Oct; 30(10): 2215-2231.

34. Lütjen-Drecoll E, Schenholm M, Tamm E, Tengblad A. Visualization of hyaluronic acid in the anterior segment of rabbit and monkey eyes. *Exp Eye Res.* 1990 Jul; 51(1): 55-63.

35. Gong H, Freddo TF, Johnson M. Age-related changes of sulfated proteoglycans in the normal human trabecular meshwork. *Exp Eye Res.* 1992 Nov; 55(5): 691-709.

36. Fine BS. Structure of the trabecular meshwork and the canal of Schlemm. *Trans Am Acad Ophthalmol Otolaryngol*. 1966; 70(5): 777-790.

37. Fine BS. Observations on the drainage angle in man and rhesus monkey: a concept of the pathogenesis of chronic simple glaucoma. a light and electron microscopic study. *Invest Ophthalmol*.1964; 3: 609-646.

38. Gong H, Overby D, et al. Human outflow pathway viewed by quick freeze deep etch. *Invest. Ophthalmol. Vis. Sci*. 2001; 42: S749.

39. Grant WM. Facility of flow through the trabecular meshwork. *Arch. Ophthalmol.* 1956; 54: 245-248.

40. Grierson I, Lee WR, et al. Associations between the cells of the walls of Schlemm's canal. *Albrecht Von Graefes Arch. Klin. Exp. Ophthalmol.* 1978; 208: 33-47.

41. Hann CR, Johnson DH, 2007. Trabecular meshwork pigmentation and collector channels - areas of higher flow? *Invest. Ophthalmol. Vis. Sci.* ARVO e-Abstracts, #2053.

42. Hogan MJ, Alvarado JA, et al., 1971. Histology of the Human Eye. An Atlas and Textbook. W.B. Saunders Company, Philadelphia, PA.

43. Johnson M, Erickson K, 2000. Mechanisms and routes of aqueous humor drainage. In: Albert, D., Jakobie, F. (Eds.), Principles and Practice of Ophthalmology. W.B. Saunders Company, Philadelphia, PA, pp. 2577-2595.

44. Johnstone MA. The aqueous outflow system as a mechanical pump: evidence from examination of tissue and aqueous movement in human and non-human primates. *J. Glaucoma*. 2004; 13: 421-438.

45. Lütjen-Drecoll E. Functional morphology of the trabecular meshwork in primate eyes. *Prog. Retin. Eye Res*. 1999; 18: 91-119.

46. Lütjen-Drecoll E, Rohen JW, 1994. Anatomy of aqueous humor formation and drainage. In: Podos, S.M., Yanoff, M. (Eds.), Textbook of Ophthalmology, 7. Mosby, London, pp. 1.1-1.16.

47. Rohen JW, Lütjen-Drecoll E, 1982. Biology of the Trabecular Meshwork. F.K. Schattauer Verlag, Stuttgart.

48. Rohen JW, Schachtschabel DO, et al. Histoautoradiographic and biochemical studies on human and monkey trabecular meshwork and ciliary body in short-term explant culture. *Albrecht Von Graefes Arch. Klin. Exp. Ophthalmol.* 1984; 221: 199-206.

49. Rohen JW, Lütjen-Drecoll E, et al. Ultrastructure of the trabecular meshwork in untreated cases of primary open-angle glaucoma (POAG). *Exp. Eye Res.* 1993; 56: 683-692.

50. Tamm E, Flugel C, et al. Contractile cells in the human scleral spur. *Exp. Eye Res.* 1992; 54: 531-543.

51. Tamm E, Flugel C, et al. Immunocytochemical and ultrastructural studies of human scleral spur. Characterization of a contractile cell population. *Ophthalmologe*. 1993; 90: 66-72.

52. Tripathi RC. Mechanism of the aqueous outflow across the trabecular wall of Schlemm's canal. *Exp. Eye Res.* 1971; 11: 116-121.

53. Tripathi RC. The functional morphology of the outflow systems of ocular and cerebrospinal fluids. *Exp. Eye Res.* 1977; 25 (Suppl.): 65-116.

54. Weinreb RN. Uveoscleral outflow: the other outflow pathway. *J. Glaucoma.* 2000; 9: 343-345.

55. Gordon MO, Beiser JA, Brandt JD, Heuer D, Higginbotham EJ, Johnson CA, Keltner JL, Miller JP, Parrish 2nd RK, Wilson MR, Kass MA. The ocular hypertension treatment

study: baseline factors that predict the onset of primary open-angle glaucoma. *Arch. Ophthalmol*. 2002; 120: 714–720. discussion 829–830.

56.Grant WM. Experimental aqueous perfusion in enucleated human eyes. *Arch Ophthalmol.* 1963; 69:783-801.

57. Johnson M. What controls aqueous humour outflow resistance? *Exp. Eye Res.* 2006; 82: 545–557.

58. McEwen W. Application of Poiseuilles law to aqueous outflow. *Arch Ophthalmol.* 1958; 60:290-304.

59. Lütjen-Drecoll E, Rohen JW. 1996. Morphology of aqueous outflow pathways in normal and glaucomatous eyes. In: Ritch, R, Shields, M. B, Krupin, T. (Eds.), The Glaucomas. I. Mosby-Year Book, Inc., St. Louis, MO, pp. 89-124.

60. Acott TS, 1994a. Biochemistry of aqueous humor outflow. In: Kaufman, P.L., Mittag, T.W. (Eds.), Textbook of Ophthalmology, 7. Mosby, London, pp. 1.47-1.78.

61. Acott TS, Wirtz MK., 1996. Biochemistry of aqueous outflow. In: Ritch, R., Shields, M.B., Krupin, T. (Eds.), The Glaucomas. I. Mosby, St Louis, MO, pp. 281-305.

62. Bahler CK, Hann CR, et al. Pharmacologic disruption of Schlemm's canal cells and outflow facility in anterior segments of human eyes. *Invest. Ophthalmol. Vis. Sci*. 2004; 45: 2246-2254.

63. Bárány E. In vitro studies of the resistance to flow through the angle of the anterior chamber. *Acta Soc. Med. Uppsala*. 1953; 59: 260-276.

64. Brubaker RF. Flow of aqueous humor in humans. *Invest. Ophthalmol. Vis. Sci*. 1991; 32: 3145-3166.

65. Buller C, Johnson D. Segmental variability of the trabecular meshwork in normal and glaucomatous eyes. *Invest. Ophthalmol. Vis. Sci*. 1994; 35: 3841-3851.

66. Gong, H, Ruberti, J, et al. A new view of the human trabecular meshwork using quick-freeze, deep-etch electron microscopy. *Exp. Eye Res.* 2002; 75: 347-358

67. Morrison JC, Acott TS, 2003. Anatomy and physiology of aqueous humor outflow. In: Morrison, J.C., Pollack, I.P. (Eds.), Glaucoma: Science and Practice Thieme, New York, pp. 34-41

68. Lütjen-Drecoll E, Futa R, et al. Ultrahistochemical studies on tangential sections of the trabecular meshwork in normal and glaucomatous eyes. *Invest. Ophthalmol. Vis. Sci.* 1981; 21: 563-573.

69. Gong H, Trinkaus-Randall V, et al. Ultrastructural immunocytochemical localization of elastin in normal human trabecular meshwork. *Curr.Eye Res.* 1989; 8: 1071-1082.

70. Bron AM, Garcher CP, Sirbat D, Allaire CM, Lablache-Combier MJ, Trinquand CJ. Comparison of two fixed beta-blocker-pilocarpine combinations. The Carteolol-Pilocarpine Study Group. *Eur J Ophthalmol.* 1997 Oct-Dec; 7(4): 351-356.

71. Lütjen-Drecoll E, Rohen JW, 2001. Functional morphology of the trabecular meshwork. In: Tasman, W., Jaeger, E.A. (Eds.), Duane's Foundations of Clinical Ophthalmology. J.B. Lippincott Company, Philadelphia, PA, pp. 1-30.

72. Marshall GE, Konstas AG, Lee WR. Immunogold ultrastructural localization of collagens in the aged human outflow system. *Ophthalmology*. 1991; 98: 692–700.

73. Murphy CG, Yun AJ, et al. Localization of extracellular proteins of the human trabecular meshwork by indirect immunofluorescence. *Am. J. Ophthalmol.* 1987; 104: 33-43.

74. Marshall GE, Konstas AG, et al. Immunogold localization of type IV collagen and laminin in the aging human outflow system. *Exp. Eye Res*. 1990; 51: 691-699.

75. Bradley JMB, Vranka JA, et al. Effects of matrix metalloproteinase activity on outflow in perfused human organ culture. *Invest. Ophthalmol. Vis. Sci.* 1998; 39: 2649-2658.

76. Bill A. Blood circulation and fluid dynamics in the eye. *Physiol Rev.* 1975; 55: 383-417.

77. Bradley JMB, Kelley MJ, et al. Effects of mechanical stretching on trabecular matrix metalloproteinases. *Invest. Ophthalmol. Vis. Sci*. 2001; 42: 1505-1513.

78. Borras T, Rowlette LL, et al. Effects of elevated intraocular pressure on outflow facility and TIGR/MYOC expression in perfused human anterior segments. *Invest. Ophthalmol. Vis. Sci*. 2002; 43: 33-40.

79. Parks W, Mecham R. (Eds.), 1998. Matrix Metalloproteinases. Academic Press, San Diego, CA.

80. Acott TS., 1992. Trabecular extracellular matrix regulation. In: Drance, S.M., Van Buskirk, E.M., Neufeld, A.H. (Eds.), Pharmacology of Glaucoma. Williams & Wilkins, Baltimore, MD, pp. 125-157.

81. Vittal V, Rose A, et al. Changes in gene expression by trabecular meshwork cells in response to mechanical stretching. *Invest. Ophthalmol. Vis. Sci.* 2005; 46: 2857-2868.

82. Gonzalez P, Epstein DL, et al. Genes upregulated in the human trabecular meshwork in response to elevated intraocular pressure. *Invest. Ophthalmol. Vis. Sci*. 2000; 41: 352-361.

83. Bradley JMB, Kelley MJ, et al. Effects of mechanical stretching on trabecular matrix metalloproteinases. *Invest. Ophthalmol. Vis. Sci.* 2001; 42: 1505-1513.

84. Bárány EH, Scotchbrook S. Influence of testicular hyaluronidase on the resistance to flow through the angle of the anterior chamber. *Acta Physiol. Scand.* 1954; 30: 240-248.

85. Bárány EH, Woodin AM. Hyaluronic acid and hyaluronidase in the aqueous humour and the angle of the anterior chamber. *Acta Physiol. Scand*. 1954; 33: 257-290.

86. Bill A, Svedbergh B. Scanning electron microscopic studies of the trabecular meshwork and the canal of Schlemm-an attempt to localize the main resistance to outflow of aqueous humor in man. *Acta Ophthalmol (Copenh).* 1972; 50(3): 295-320.

87. Ethier CR, Coloma FM, Sit AJ, Johnson M. Two pore types in the inner-wall endothelium of Schlemm's canal. *Invest Ophthalmol Vis Sci.* 1998 Oct; 39(11): 2041-2048.

88. Stamer WD, Acott TS. Current understanding of conventional outflow dysfunction in glaucoma. *Curr Opin Ophthalmol.* 2012; 23(2):135-143.

89. Ye W, Gong H, Sit A, Johnson M, Freddo TF. Interendothelial junctions in normal human Schlemm's canal respond to changes in pressure. *Invest Ophthalmol Vis Sci.* 1997 Nov; 38(12): 2460-2468.

90. Johnson DH, Bradley JM, Acott TS. The effect of dexamethasone on glycosaminoglycans of human trabecular meshwork in perfusion organ culture. *Invest Ophthalmol Vis Sci.* 1990 Dec; 31(12): 2568-2571.

91. Inomata H, Bill,A, et al. Aqueous humor pathways through the trabecular meshwork and into Schlemm’s canal in the cynomolgus monkey (Macaca irus): an electron microscopic study. *Am. J. Ophthalmol.* 1972; 73: 760.

92. Bill A, Maepea O, 1994. Mechanisms and routes of aqueous humor drainage. In: Albert, D.M., Jakotiec, F.A. (Eds.), Principles and Practices of Ophthalmology. WB Saunders, Philadelphia, PA, pp. 206-226.

93. Tamm ER, Lütjen-Drecoll E. Ciliary body. *Microsc Res Tech.* 1996 Apr 1; 33(5):390-439.

94. Leske MC, Heijl A, Hussein M, Bengtsson B, Hyman L, Komaroff E. Factors for glaucoma progression and the effect of treatment: the early manifest glaucoma trial. *Arch. Ophthalmol*. 2003; 121: 48–56.

95. Rohen JW, Witmer R. Electron microscopic studies on the trabecular meshwork in glaucoma simplex. *Albrecht Von Graefes Arch Klin Exp Ophthalmol*. 1972; 183: 251-66.

96. Rohen JW. Why is intraocular pressure elevated in chronic simple glaucoma? *Ophthalmology* 1983; 90: 758-765.

97. Rohen JW, Lutjen-Drecoll E, 1981. Ageing- and Non-ageing Processes within the Connective Tissues of the Anterior Segment of the Eye. Steiner Verlag, Weisbaden.

98. Alvarado J, Murphy C, Juster R, Trabecular meshwork cellularity in primary open-angle glaucoma and nonglaucomatous normals. *Ophthalmology*. 1984; 91(6):564-79.

99. Alvarado J, Murphy C, Polansky J, Juster R. Age-related changes in trabecular meshwork cellularity. *Invest Ophthalmol Vis Sci.* 1981; 21:714-27.

100. Samuelson D, Plummer C, Lewis P, Gelatt K. Schwalbe line's cell in the normal and glaucomatous dog. *Vet Ophthalmol.* 2001 Mar; 4(1):47-53.

101. Oertel MF, May CA, Bloemendal H, Lütjen-Drecoll E. Alpha-B-crystallin expression in tissues derived from different species in different age groups. *Ophthalmologica*. 2000 Jan-Feb; 214(1):13-23.

102. Gonzalez P, Epstein DL, Luna C, Liton PB. Characterization of free-floating spheres from human trabecular meshwork (HTM) cell culture in vitro. *Exp Eye Res.* 2006 Jun; 82(6): 959-967.

103. Acott TS, Samples JR, Bradley JM, Bacon DR, Bylsma SS, Van Buskirk EM. Trabecular repopulation by anterior trabecular meshwork cells after laser trabeculoplasty. *Am J Ophthalmol.* 1989 Jan 15; 107(1): 1-6.

104. Lütgen-Drecoll E, Rohen JW. Morphology of aqueous outflow pathways in normal and glaucomatous eyes. In: Ritch R, Shields MB, Krupin T, Eds. The glaucomas. St. Louis: Mosby 1989.

105. Bhattacharya SK, Annangudi SP, Salomon RG, Kuchtey RW, Peachey NS, Crabb JW. Cochlin deposits in the trabecular meshwork of the glaucomatous DBA/2J mouse. *Exp Eye Res 2005*; 80(5): 741-744.

106. Bhattacharya SK, Rockwood EJ, Smith SD, et al. Proteomics reveal Cochlin deposits associated with glaucomatous trabecular meshwork. *J Biol Chem.* 2005; 280(7): 6080-6084.

107. Gottanka J, Johnson DH, Martus P, Lütjen-Drecoll E. Severity of optic nerve damage in eyes with POAG is correlated with changes in the trabecular meshwork. *J Glaucoma.* 1997 Apr; 6(2): 123-132.

108. Lepple-Wienhues A, Stahl F, Wiederholt M. Differential smooth muscle-like contractile properties of trabecular meshwork and ciliary muscle. *Exp Eye Res*. 1991; 53: 33-38.

109. Stumpff F, Wiederholt M. Regulation of trabecular meshwork contractility. *Ophthalmologica.* 2000; 214: 33-53.

110. Ingber DE. The architecture of life. *Sci Am*. 1998; 278: 48-57.

111. Differences in the amount of 'plaque-material' in the outflow system of eyes with chronic simple and exfoliation glaucoma. In: Lütjen-Drecoll E, Tamm E. (Eds.), Glaucoma Update III. Springer-Verlag, Berlin, Heidelberg.

112. Lütjen-Drecoll E, Shimizu T, et al. Quantitative analysis of ''plaque material'' in the inner- and outer wall of Schlemm's canal in normal and glaucomatous eyes. *Exp. Eye Res.* 1986; 42: 443-455.

113. Tian B, Kaufman PL, et al. H-7 disrupts the actin cytoskeleton and increases outflow facility. *Arch. Ophthalmol*. 1998; 116: 633-643.

114. Meller K, Theiss C. Atomic force microscopy and confocal laser scanning microscopy on the cytoskeleton of permeabilized and embedded cells. *Ultramicroscopy*. 2006; 106: 320-325.

115. Clark, A.F., Miggans, S.T., et al. Cytoskeletal changes in cultured human glaucoma trabecular meshwork cells. *J. Glaucoma,* 1995a; 4: 183-188.

116. Yoneda A, Couchman JR. Regulation of cytoskeletal organization by syndecan transmembrane proteoglycans. *Matrix Biol.* 2003; 22: 25-33.

117. Tumminia SJ, Mitton KP, et al. Mechanical stretch alters the actin cytoskeletal network and signal transduction in human trabecular meshwork cells. *Invest. Ophthalmol. Vis. Sci.* 1998; 39: 1361-1371

118. Sanka K, Maddala R, et al. Influence of actin cytoskeletal integrity on matrix metalloproteinase-2 activation in cultured human trabecular meshwork cells. *Invest. Ophthalmol. Vis. Sci.* 2007; 48: 2105-2114.

119. Clark AF, Wilson K, McCartney MD, Miggans ST, Kunkle M, Howe W. Glucocorticoid-induced formation of cross-linked actin networks in cultured human trabecular meshwork cells. *Invest Ophthalmol Vis Sci.* 1994 Jan; 35(1): 281-94.

120. Johnson D, Gottanka J, et al. Ultrastructural changes in the trabecular meshwork of human eyes treated with corticosteroids. *Arch. Ophthalmol*. 1997; 115: 375-383.

121. Wilson K, McCartney MD, Miggans ST, Clark AF. Dexamethasone induced ultrastructural changes in cultured human trabecular meshwork cells. *Curr Eye Res.* 1993 Sep; 12(9): 783-93.

122. Zhuo YH, He Y, Leung KW, Hou F, Li YQ, Chai F, Ge J. Dexamethasone disrupts intercellular junction formation and cytoskeleton organization in human trabecular meshwork cells. *Molecular Vision.* 2010; 16: 61-71.

123. Clark AF, Wilson K, et al. Dexamethasone-induced ocular hypertension in perfusion-cultured human eyes. *Invest. Ophthalmol. Vis. Sci.* 1995b; 36: 478-489.

124. Clark AF, Brotchie D, et al. Dexamethasone alters F-actin architecture and promotes cross-linked actin network formation in human trabecular meshwork tissue. *Cell Motil. Cytoskeleton*. 2005; 60: 83-95.

125. Grierson I, Lee WR. Junctions between the cells of the trabecular meshwork. *Albrecht Von Graefes Arch. Klin. Exp. Ophthalmol*. 1974; 192: 89-104.

126. Raviola G, Raviola E. Paracellular route of aqueous outflow in the trabecular meshwork and canal of Schlemm. A freeze-fracture study of the endothelial junctions in the sclerocorneal angel of the macaque monkey eye. *Invest. Ophthalmol. Vis. Sci*. 1981; 21: 52-72.

127. Bhatt K, Gong H, et al. Freeze-fracture studies of interendothelial junctions in the angle of the human eye. *Invest. Ophthalmol. Vis. Sci*. 1995; 36: 1379-1389.

128. Fuchshofer R, Welge-Lussen U, et al. Biochemical and morphological analysis of basement membrane component expression in corneoscleral and cribriform human trabecular meshwork cells. *Invest. Ophthalmol. Vis. Sci.* 2006; 47: 794-801.

129. Vittitow J, Borras T. Genes expressed in the human trabecular meshwork during pressure-induced homeostatic response. *J. Cell Physiol.* 2004; 201: 126-137.

130. Wang N, Chintala SK, et al. Activation of a tissue-specific stress response in the aqueous outflow pathway of the eye defines the glaucoma disease phenotype. *Nat. Med.* 2001; 7: 304-309.

131. Wordinger RJ, Fleenor DL, et al. Effects of TGF-beta2, BMP-4, and gremlin in the trabecular meshwork: implications for glaucoma. *Invest. Ophthalmol. Vis. Sci.* 2007; 48: 1191-1200.

132. Xue W, Comes N, et al. Presence of an established calcification marker in trabecular meshwork tissue of glaucoma donors. *Invest. Ophthalmol. Vis. Sci*. 2007; 48: 3184-3194.

133. Yue BYJT. The extracellular matrix and its modulation in the trabecular meshwork. *Surv. Ophthalmol*. 1996; 40: 379-390.

134. Zhou LL, Zhang SR, et al. Adhesion of human trabecular meshwork cells to extracellular matrix proteins: roles and distribution of integrin receptors. *Invest. Ophthalmol. Vis. Sci.* 1996; 37: 104-113.

135. Zhou L, Li Y, et al. Glucocorticoid effects on extracellular matrix proteins and integrins in bovine trabecular meshwork cells in relation to glaucoma. *Int. J. Mol. Med.* 1998b; 1: 339-346.

136. Zhou L, Li Y, et al. Alteration of cytoskeletal structure, integrin distribution, and migratory activity by phagocytic challenge in cells from an ocular tissue--the trabecular meshwork. *In Vitro Cell Dev. Biol. Anim.* 1999a; 35: 144-149.

137. Zhou L, Li Y, et al. Oxidative stress affects cytoskeletal structure and cell-matrix interactions in cells from an ocular tissue: the trabecular meshwork. *J. Cell Physiol.* 1999b; 180: 182-189.

138. Zhou L, Maruyama I, et al. Expression of integrin receptors in the human trabecular meshwork. *Curr. Eye Res*. 1999c; 19: 395-402.

139. Tschumper RC, Johnson DH, et al. Glycosaminoglycans of human trabecular meshwork in perfusion organ culture. *Curr. Eye Res*. 1990; 9: 363-369.

140. Tripathi RC, Li J, et al. Aqueous humor in glaucomatous eyes contains an increased level of TGF-beta 2. *Exp. Eye Res.* 1994; 59: 723-727.

141. Tripathi BJ, Hansen M, et al. Identification of type VI collagen in the trabecular meshwork and expression of its mRNA by trabecular cells. *Exp. Eye Res*. 1994; 58: 181-187.

142. Samples JR, Alexander JP, et al. Regulation of the levels of human trabecular matrix metalloproteinases and inhibitor by interleukin-1 and dexamethasone. *Invest. Ophthalmol. Vis. Sci.* 1993*;* 34: 3386-3395.

143. Rose AY, Bradley JM, et al. Integrin responses to mechanical stretching in trabecular meshwork cells. *Invest. Ophthalmol. Vis. Sci. 2002;* 43: 1021.

144. Reale E, Groos S, et al. In the mammalian eye type VI collagen tetramers form three morphologically different aggregates. *Matrix Biol*. 2001; 20: 37-51.

145. Parshley DE, Bradley JMB, et al. Early changes in matrix metalloproteinases and inhibitors after in vivo laser treatment to the trabecular meshwork. *Curr. Eye Res*. 1995; 14: 537-544.

146. Lütjen-Drecoll E, Rittig M, et al. Immunomicroscopical study of type VI collagen in the trabecular meshwork of normal and glaucomatous eyes. *Exp. Eye Res.* 1989; 48: 139-147.

147. Fuchshofer R, Yu AH, et al. Bone morphogenetic protein-7 is an antagonist of transforming growth factor-beta2 in human trabecular meshwork cells. *Invest. Ophthalmol. Vis. Sci.* 2007; 48: 715-726.

148. Fleenor DL, Shepard AR, et al. TGFbeta2-induced changes in human trabecular meshwork: implications for intraocular pressure. *Invest. Ophthalmol. Vis. Sci.* 2006; 47: 226-234.

149. Bahler CK, Howell KG, Hann CR, Fautsch MP, Johnson DH. Prostaglandins increase trabecular meshwork outflow facility in cultured human anterior segments. *Am J Ophthalmol.* 2008 Jan; 145(1): 114-119.

150. Cracknell KP, Grierson I. Prostaglandin analogues in the anterior eye: their pressure lowering action and side effects. *Exp Eye Res.* 2009 Apr; 88(4): 786-791.

151. Clark AF, Wordinger RJ. The role of steroids in outflow resistance. *Exp Eye Res.* 2009 Apr; 88(4): 752-759.

152. Tektas OY, Lütjen-Drecoll E. Structural changes of the trabecular meshwork in different kinds of glaucoma. *Exp Eye Res.* 2009 Apr;88(4): 769-775.

153. Knupp C, Pinali C, et al. Structural correlation between collagen VI microfibrils and collagen VI banded aggregates. *J. Struct. Biol.* 2006; 154: 312-326.

154. Parc C, Johnson D, et al. Giant vacuoles are found preferentially near collector channels. *Invest. Ophthalmol. Vis. Sci*. 2000; 41: 2984-2990.

155. Knepper PA, Goossens W, et al. Glycosaminoglycan stratification of the juxtacanalicular tissue in normal and primary open-angle glaucoma. *Invest. Ophthalmol. Vis. Sci.* 1996b; 37: 2414-2425.

156. Quigley HA. Glaucoma. *Lancet*. 2011; 377: 1367-1377.

157. Llobet A, Gasull X, and Gual A. Understanding Trabecular Meshwork Physiology: A Key to the Control of Intraocular Pressure? *Physiology.* 2003; 18: 205-209.

158. Bill A, and Philips CT. Uveoscleral drainage of aqueous humor in human eye. *Exp. Eye Res.* 1971;12: 275-81.

159. Brubaker RF. The effect of intraocular pressure on conventional outflow resistance in the enucleated human eye. *Invest Ophthalmol Vis Sci.* 1975;14: 286–292.

160. Tschumper RC and Johnson DH. Trabecular Meshwork Cellularity, Differences Between Fellow Eyes. *Invest Ophthalmol Vis Sci.* 1990, 31(7): 1327-1331.

161. Grierson I. What is open angle glaucoma? *Eye*. 1987; 1: 15-28.13.

162. Grierson I, Howes RC. Age-related depletion of the cell population in the human trabecular meshwork. *Eye*. 1987; 1: 204-10.

163. Grierson I, Wang Q, McMenamin PG and Lee WR: The effects of age and antiglaucoma drugs on the meshwork cell population. *Res Clin Forums.* 1982; 4: 69-92.

164. Grierson I, Calthorpe CM, 1989. Characteristics of meshwork cells and age changes in the outflow system of the eye: their relevance to primary open angle glaucoma. In: Mills, K.B. (Ed.), Glaucoma. Proceedings of the Fourth International Symposium of the Northern Eye Institute. Pergamon Press, Oxford, pp. 12-31.

165. Johnson M and Erickson K. Aqueous humor and the dynamics of its flow. In: Principles and practice of ophthalmology, edited by Albert DM and Jakobiec FA. Philadelphia: Saunders, 2000, p. 2577-2595.

166. Rohen JW, Futa R, and Lutjen-Drecoll E. The fine structure of the cribriform meshwork in normal and glaucomatous eyes as seen in tangential sections. *Invest Ophthalmol Vis Sci* .1981; 21: 574-585.

167. Kelley MJ, Rose AY, Keller KE, Hessle H, Samples JR, Acott TS. Stem cells in the trabecular meshwork: present and future promises. *Exp Eye Res*. 2009 Apr; 88 (4): 747-51.

168. Ching-An Wu and Ya-Wun Yang. Induction of Cell Death by Saponin and Antigen. Delivery. *Pharmaceutical Res.* 2004; 21: 271-277.

169. Arabski M, We˛gierek-Ciuk A, Czerwonka G, Lankoff A and Kaca W. Effects of Saponins against Clinical E. coli Strains and Eukaryotic Cell Line. *J of Biomed and Biotech.* 2011:2012:1-6.

170. Mitchell CH, Fleischhauer JC, Stamer DW, Peterson-Yantorno K, and Civan MM. Human trabecular meshwork cell volume regulation. *Am J Physiol Cell Physiol*. 2002; 283: C315-C326.

171. McMenamin PG, Lee WR, Aitken DAN: Age related changes in the human outflow apparatus. *Ophthalmology*. 1986; 93: 194-209.

172. Miyazaki M, Segawa K, Urakawa Y. Age-related changes in the trabecular meshwork of the normal human eye. *Jpn J Ophthalmol*. 1987; 31(4):558-569.

173. Alexander JP, Acott TS. Involvement of protein kinase C in TNF regulation of trabecular matrix metalloproteinases and TIMPs. *Inves Ophthalmol Vis Sci.* 2001; 42: 2831-2838.

174. Alexander JP, Acott TS. Involvement of Erk-MAP kinase pathway in TNF-regulation of trabecular metalloproteinases and TIMPs. *Invest Ophthalmol Vis Sci*. 2003; 44: 164–169.

175. Alexander JP, Samples JR, Van Buskirk EM, Acott TS. Expression of matrix metalloproteinases and inhibitor by human trabecular meshwork. *Invest Ophthalmol Vis Sci.* 1991; 32: 172–180.

176. Polansky JR, Weinreb R, Alvarado JA. Studies on human trabecular cells propagated in vitro. *Vision Res.* 1981; 21: 155–160.

177. Polansky JR, Weinreb RN, Baxter JD, Alvarado J. Human trabecular cells. I. Establishment in tissue culture and growth characteristics. *Invest Ophthalmol Vis Sci.* 1979; 18: 1043–1049.

178. Stamer WD, Seftor RE, Williams SK, Samaha HA, Snyder RW. Isolation and culture of human trabecular meshwork cells by extracellular matrix digestion. *Curr Eye Res.* 1995; 14: 611–617.

179. Bradley JMB, Anderssohn AM, Colvis CM, et al. Mediation of laser trabeculoplasty-induced matrix metalloproteinase expression by IL-1 and TNF. *Invest Ophthalmol Vis Sci.* 2000; 41: 422–430.

180. Johnson DH, Tschumper RC. The effect of organ culture on human trabecular meshwork. *Exp Eye Res.* 1989; 49: 113–127.

181. Johnson DH, Tschumper RC. Human trabecular meshwork organ culture. *Invest Ophthalmol Vis Sci.* 1987; 28: 945–953.

182. Bachmann B, Birke M, Kook D, Eichhorn M, Lütjen-Drecoll E. Ultrastructural and biochemical evaluation of the porcine anterior chamber perfusion model. *Invest Ophthalmol Vis Sci.* 2006; 47: 2011–2020.

183. Takahashi K, Tanabe K, Ohnuki M, Narita M, Ichisaka T, Tomoda K, and Yamanaka S. Induction of Pluripotent Stem Cells from Adult Human Fibroblasts by Defined Factors. *Cell*. 2007; 131: 861-872.

184. Okita K, Nakagawa M, Hyenjong H, Ichisaka T, Yamanaka S. Generation of mouse induced pluripotent stem cells without viral vectors. *Science.* 2008; 3227: 949-953.

185. Stamer WD, Snyder RW, Smith BL, Agre P, Regan JW. Localization of aquaporin CHIP in the human eye: implications in the pathogenesis of glaucoma and other disorders of ocular fluid balance. *Invest Ophthalmol Vis Sci.* 1994; 35: 3867–3872.

186. Stamer WD, Peppel K, O'Donnell ME, Roberts BC, Wu F, and Epstein DL. Expression of aquaporin-1 in human trabecular meshwork cells: role in resting cell volume. *Invest Ophthalmol Vis Sci*. 2001; 42: 1803-1811.

187. Du Y, Roh DS, Mann MM, Funderburgh ML, Funderburgh JL, and Schuman JS. Multipotent Stem Cells from Trabecular Meshwork Become Phagocytic TM Cells. *Invest Ophthalmol Vis Sci.* 2012; 53:1566-1575.

188. Johnson DH, Richardson TM, Epstein DL. Trabecular meshwork recovery after phagocytic challenge. *Curr Eye Res*. 1989 Nov;8(11):1121-1130.

189. Rojas B, Ramirez A, De-Hoz R, Salazar JJ, Ramirez JM, Trivino A. Structural changes of the anterior chamber angle in primary congenital glaucoma with respect to normal development. *Arch Soc Esp Oftalmol*. 81:65-72 (2006)

190. Zhao T, Zhang Z-N, Rong Z, Xu Y. Immunogenicity of induced pluripotent stem cells. *Nature*. 42011; 74: 212-216.

191. Duller C, Johnson DH, and Tschumper RC. Human Trabecular Meshwork Phagocytosis Observations in on Organ Culture System*. Invest Ophthalmol Vis Sci. 1990;* 31: 2156-2163.

192. Johnstone MA, Grant WM. Microsurgery of Schlemm's canal and the human aqueous outflow system. *Am J Ophthalmol. 1*973 Dec; 76(6): 906-917.

193. Morrison SJ, Shah NM, et al. Regulatory mechanisms in stem cell biology. *Cell*.1997; 88: 287–298.

194. Thomson JA, Itskovitz-Eldor J, et al. Embryonic stem cell lines derived from human blastocysts. Science 1998; 282: 1145–1147.

195. Yuasa S, Fukada K. Recent advances in cardiovascular regenerative medicine: the induced pluripotent stem cell era. *Expert Rev. Cardiovascul. Ther*. 2008; 6: 803–810

196. Acott TS, Kingsley PD, Samples JR, Van Buskirk EM. Human trabecular meshwork organ culture: Morphology and glycosaminoglycan synthesis. *Invest Ophthalmol Vis Sci*. 1988; 29: 90-100.

197. Bill A. Aqueous humor dynamics in monkeys (Macaca irus and Cercopithecus ethiops). *Exp Eye Res.* 1971; 11: 195-206.

198. Acott TS, Kelley MJ. Extracellular matrix in the trabecular meshwork (Review). *Exp Eye Res.* 2008; 86: 543-561.

199. Kass MA, Heuer DK, Higginbotham EJ, et al. The Ocular Hypertension Treatment Study: a randomized trial determines that topical ocular hypotensive medication delays or prevents the onset of primary open-angle glaucoma. *Arch Ophthalmo.l* 2002; 120: 701-713; discussion 829-730.

200. Artes PH, Chauhan BC, Keltner JL, et al. Longitudinal and cross-sectional analyses of visual field progression in participants of the Ocular Hypertension Treatment Study. *Arch Ophthalmol.* 2010; 128: 1528-1532.

201. Allingham RR, Liu Y, Rhee DJ. The genetics of primary open-angle glaucoma: a review. *Exp Eye Res.* 2009; 88: 837-844.

202. Morrison JC, Pollack IP (eds). *Glaucoma: Science and Practice*. New York: Thieme; 2003.

203. Liton PB, Luna C, Challa P, Epstein DL, Gonzalez P. Genome-wide expression profile of human trabecular meshwork cultured cells, nonglaucomatous and primary open angle glaucoma tissue. *Mol Vis.* 2006 Jul 12;12: 774-790.

204. Gonzalez P, Caballero M, Liton PB, Stamer WD, Epstein DL. Expression analysis of the matrix GLA protein and VE-cadherin gene promoters in the outflow pathway*. Invest Ophthalmol Vis Sci.* 2004 May; 45(5):1389-1395.

205. Liton PB, Liu X, Stamer WD, Challa P, Epstein DL, Gonzalez P. Specific targeting of gene expression to a subset of human trabecular meshwork cells using the chitinase 3-like 1 promoter. *Invest Ophthalmol Vis Sci.* 2005 Jan; 46(1): 183-190.

206. Luna C, Li G, Liton PB, Epstein DL, Gonzalez P. Alterations in gene expression induced by cyclic mechanical stress in trabecular meshwork cells. *Mol Vis.* 2009; 15: 534-544.

207. Acott TS, Kelley MJ, Keller KE, Vranka JA, Abu-Hassan DW, Li X, Aga M, and Bradley J. IOP. Homeostasis - Maintaining Balance in a High Pressure Environment. *Ocul Pharmacol Ther. In Press.*

Appendix

Curriculum Vitae

Curriculum Vitae

Diala W. Abu-Hassan

Department of Biochemistry & Molecular Biology

School of Medicine

Oregon Health & Science University

3181 Sam Jackson Park Road, L-224

Portland, OR 97239

Phone: (503) 888-9408

Electronic contact information: e-mail: abuhassa@ohsu.edu, d.abuhassan@gmail.com

---

Education:

2008-2013 **Ph.D.** Biochemistry and Molecular Biology
OHSU, Portland, Oregon

Dissertation: "TRANSPLANTATION OF DIFFERENETIATED IPSCs AS A TREATMENT STRATEGY FOR GLAUCOMA."

2000-2005 **D.D.S** Doctor of Dental Surgery, University of Jordan, Amman, Jordan.

Experience:

Research:

- Graduate Student at OHSU (2008-2013)

Department of Biochemistry and Molecular Biology.

Advisors: Ted Acott/Mary Kelley (August 2011- September 2013)

Peter Rotwein laboratory (July 2009-July 2011)

Research Rotations at OHSU:

Rotation Graduate Student at Peter Rotwein laboratory (April 2009 June 2009).

Rotation Graduate Student at Michael Chapman laboratory (January 2009-March 2009).

Rotation Graduate Student at Larry David laboratory (October 2008-December 2008).

Teaching:

- Teaching Assistant at the Department of Biochemistry and Physiology School of Medicine, University of Jordan, Amman, Jordan (October 2006- September 2008).

Clinical Practice:

- General Dental Practitioner at the private sector, Amman, Jordan (January 2006-October 2006).

- Dental Intern at Jordan University Hospital (July 2005-January 2006).

Volunteer / Public Service:

-Member of the Conjoint Curriculum Committee (CCC), 01/2010-present
Revising and improving the first year conjoint classes in the Program of Molecular and Cellular Biosciences (PMCB).

-2010 Member of the Student Retreat Committee-Planning the retreat for the upcoming graduate students-Fall 2010.

-Annual Biomedical Research Conference for Minority Students (ABRCMS), November 2012 San Jose, CA. OHSU Student Exhibitor, Volunteer Poster Judge (biochemistry).

-Annual Biomedical Research Conference for Minority Students (ABRCMS), November 2011 St Louis, MI. OHSU Student Exhibitor, Volunteer Poster Judge (cell biology).

-Oregon Food Bank -OHSU volunteer.

-Life makers volunteer.

-Student Dental Volunteer Days Participant – March 2004 – North Jordan.

-Dental Volunteer Days Participant – October 2005 – Tafila - Jordan.

Honors and Awards:

-2001 Outstanding academic accomplishment scholarship - Competitive year-long scholarship for dental students with the best academic accomplishment - University of Jordan, Amman, Jordan.

-2002 Outstanding academic accomplishment scholarship - Competitive year-long scholarship for dental students with the best academic accomplishment - University of Jordan, Amman, Jordan

---

Professional Organizations:

- Association for Research in Vision and Ophthalmology (ARVO), since 2012

- American Association for the Advancement of Science (AAAS), since 2009

- Jordan Dental Association (JDA), since 2005

Meetings attended:

- Association for Research in Vision and Ophthalmology (ARVO) annual meeting, May 2013, Seattle, WA

- Annual Biomedical Research Conference for Minority Students (ABRCMS), November 2012, San Jose, CA

- Association for Research in Vision and Ophthalmology (ARVO) annual meeting, May 2012, Fort Lauderdale, FL

- Annual Biomedical Research Conference for Minority Students (ABRCMS), November 2011, St Louis, MO

Publications:

In Press:

-Acott, T.S, Kelley, M.J, Keller K.E, Vranka J.A, **Abu-Hassan, D.W**, Li, X, Aga, M, and Bradley, J. IOP Homeostasis - Maintaining Balance in a High Pressure Environment. Journal of Ocular Pharmacology and Therapeutics.

In preparation:

1. **Abu-Hassan, D.W**, Li, X, Ryan, E, Kelley, M.J, and Acott, T.S. A Novel Cell Loss Model for Primary Open Angle Glaucoma.

2. **Abu-Hassan, D.W**, Li, X, Kelley, M.J, and Acott, T.S. Use of iPS Cells to Restore Intraocular Pressure Homeostasis in a Human Model for Glaucoma.

Abstracts:

- Kelley, M.J**, Abu-Hassan, D.W**, Li, X, Ryan, E, and Acott, T.S. "A Novel Cell Loss Model for Primary Open Angle Glaucoma". The Trabecular Meshwork Society, New Orleans, LA, December 13-14, 2013.

- Acott, T.S, Kelley, M.J, Keller K.E, Vranka J.A, **Abu-Hassan, D.W**, Li, X, Aga M, and Bradley, J. "IOP Homeostasis & Segmental Outflow". The Trabecular Meshwork Society, New Orleans, LA, December 13-14, 2013.

- Kelley, M.J, Li, X, **Abu-Hassan, D.W**, Ryan, E, Rose, A, Bradley, J, and Acott, T.S. "Restoration of Trabecular Meshwork by stem cells", The Annual Trabecular Meshwork & Angle Closure Study Club, San Fransisco, CA, December 15, 2012.

- **Abu-Hassan, D.W**, Li, X, Ryan, E, Acott, T.S and Kelley, M.J. "A Novel Model for Primary Open Angle Glaucoma", The Annual Biomedical Research Conference for Minority Students, San Jose, CA, November 7-10 2012.

- Li, X, **Abu-Hassan, D.W**, Vranka, J.A, Acott, T.S and Kelley, M.J. "Cell-Matrix and Cell-Cell Interactions And The Aqueous Humor Outflow In Trabecular Meshwork (TM) Cells", The Association For Research In Vision and Opthalmology, Fort Lauderdale, FL, May 6-10 2012.

- Kelley, M.J, Li, X, **Abu-Hassan, D.W**, Vranka, J.A, Hayashi, L., and Acott, T.S. "Relationship between Type VI Collagen, Integrin, and Non-Integrin Receptors in Trabecular Meshwork" ,The Annual Trabecular Meshwork & Angle Closure Study Club, Denver, AR, 2011.

-**Abu-Hassan, D.W** and Rotwein, P, “AKT role in skeletal muscle differentiation”, Student Research Forum, Oregon Health and Science University, Portland, OR, May 2011.

The work presented in this dissertation was performed entirely by the author except where noted.

All the work was performed between 2011-2013 in Portland, Oregon at Oregon Health & Science University.